



ΠΟΛΥΤΕΧΝΕΙΟ ΚΡΗΤΗΣ
TECHNICAL UNIVERSITY OF CRETE

SCHOOL OF PRODUCTION ENGINEERING & MANAGEMENT

DIPLOMA THESIS by Antonis Marakakis

Supervisor: Prof. Michail Konsolakis

**“Catalytic hydrogenation of carbon dioxide (CO₂) to
methane (CH₄): Current status and perspectives”**

CHANIA

APRIL 2023

Antonis Marakakis

“Catalytic hydrogenation of carbon dioxide (CO₂) to methane (CH₄): Current status and perspectives”

Supervisor

Konsolakis

Michail

Professor

School of Production
Engineering and
Management Technical
University of
Crete

Member 1

Papaefthimiou

Spyridon

Professor

School of Production
Engineering and
Management Technical
University of
Crete

Member 2

Ipsakis

Dimitrios

Assistant Professor
School of Production
Engineering and
Management Technical
University of
Crete

SCHOOL OF PRODUCTION ENGINEERING & MANAGEMENT

TECHNICAL UNIVERSITY OF CRETE

CHANIA

APRIL 2023

Contents

Acknowledgments	5
Περίληψη	6
Abstract.....	7
1. Introduction.....	8
2. Reaction analysis.....	10
2.1 Brief history of the reaction.....	10
2.2 Thermodynamics.....	10
2.2.1 Reactions and thermodynamic parameters	11
2.2.2 Effect of pressure and temperature.....	13
2.2.3 Effect of reactants concentrations	14
2.2.4 Products and other gases effect	15
3 Carbon Dioxide Capture	16
3.1 Capture technologies	16
3.2 Separation technologies.....	17
3.3 CO ₂ transportation	20
4 Hydrogen.....	22
4.1 Water-based hydrogen production.....	23
4.1.1 Electrolysis	23
4.1.2 Thermochemical cycles.....	29
4.1.3 Photolysis and photo-electrolysis	36
4.2 Biomass.....	37
4.3 Bio-based	38
4.3.1 Direct and indirect bio-photolysis	38
4.3.2 Dark fermentation.....	39
4.3.3 Photo fermentation.....	39
4.4 Hydrogen from fossil fuels.....	40
4.5 Hydrogen pallet.....	42
4.6 Hydrogen storage and transportation.....	43
5 CO ₂ catalytic hydrogenation to CH ₄	46
5.1 Methanation methods	46
5.2 CO ₂ thermal methanation.....	47
5.3 Active metals	47
5.3.1 Noble metals.....	49

5.3.1.1	Ruthenium	49
5.3.1.2	Rhodium.....	49
5.3.1.3	Palladium	49
5.3.2	Non-noble metals.....	50
5.3.2.1	Nickel	50
5.3.2.2	Molybdenum.....	50
5.3.2.3	Iron	51
5.3.2.4	Cobalt.....	51
5.4	Bimetallic	51
5.5	Reactor design	52
5.6	Support materials.....	56
5.6.1	Metal oxides.....	57
5.6.2	Metal organic frameworks.....	57
5.6.3	Zeolites	58
5.6.4	Carbon	58
5.7	Promoters	59
5.8	Catalysts summary	60
5.9	Catalyst preparation methods	64
5.10	Catalyst deactivation.....	65
6	Opportunities and challenges.....	67
6.1	Life cycle assessment	67
6.2	Cost estimations and Techno-economic analyses	71
6.3	Existing plants	76
6.4	Sociopolitical aspect.....	81
7	Conclusions.....	83
	References.....	84

Acknowledgments

Coming to the end of my studies, I could not be more grateful for my supervising professor Dr. Michail Konsolakis for the preparation of this present thesis. His contribution was invaluable. Moreover, I would also like to thank my family for supporting me throughout my studies and setting the foundations, in order to make sure I could pursue my dream of becoming an engineer.

Περίληψη

Η αλόγιστη χρήση των ορυκτών καυσίμων έχει οδηγήσει σε μια άνευ προηγουμένου αύξηση της συγκέντρωσης του διοξειδίου του άνθρακα (CO₂) στην ατμόσφαιρα. Αυτή η αύξηση παίζει τον σημαντικότερο ρόλο για την επίταση του φαινομένου του θερμοκηπίου και την επικείμενη κλιματική αλλαγή. Με τις επιπτώσεις της κλιματικής αλλαγής να γίνονται όλο και πιο φανερές, η ανάγκη μιας βιώσιμης λύσης βρίσκεται στην κορυφή των επιστημονικών και πολιτικών προτεραιοτήτων. Πολλές από τις προτεινόμενες λύσεις, συνεπάγονται με την αντικατάσταση των συμβατικών μορφών ενέργειας και την αναζήτηση περιβαλλοντικά φιλικών και ενεργειακά αποδοτικών νέων τεχνολογιών. Ανάμεσα στις λύσεις βρίσκεται και η μετατροπή του CO₂ σε χρήσιμα χημικά προϊόντα ή/και καύσιμα όπως το μεθάνιο (CH₄) ή αλκοόλες.

Η παρούσα Διπλωματική Εργασία (ΔΕ) εστιάζει στη καταλυτική μεθανοποίηση του CO₂ ως μία εναλλακτική λύση. Ο σκοπός αυτής της έρευνας είναι να αναλύσει την αποδοτικότητα της διεργασίας χρησιμοποιώντας χαμηλού κόστους υλικά και υψηλής δραστηριότητας καταλύτες. Σε αυτό το πλαίσιο, οι παράμετροι που επηρεάζουν την απόδοση της αντίδρασης του Sabatier εξετάζονται. Έπειτα, η συλλογή CO₂ και παραγωγή H₂ αξιολογούνται, με έμφαση στις τεχνολογίες που δεν απαιτούν χρήση ορυκτών καυσίμων. Σε αυτήν την εργασία εξετάζεται επίσης η απόδοση της αντίδρασης για διάφορα καταλυτικά υλικά, καθώς και το περιβαλλοντικό της αντίκτυπο και η οικονομική της βιωσιμότητα. Τα ευρήματα αυτής της έρευνας παρέχουν πολύτιμες πληροφορίες για τις δυνατότητες της καταλυτικής μεθανοποίησης του CO₂ ως μια βιώσιμη λύση για την μείωση των εκπομπών CO₂ και στην άμβλυση των επιδράσεων της κλιματικής αλλαγής.

Abstract

The excessive use of fossil fuels has led to an unprecedented increase in the concentration of CO₂ in the atmosphere. This increase plays the most important role in exacerbating the greenhouse effect and contributing to imminent climate change. As the irreversible effects of climate change become increasingly apparent, the need for a sustainable solution is now at the forefront of both scientific and political agendas. Many of the solutions suggested, entail the substitution of conventional energy sources and the development of environmentally friendly and energy-efficient technologies. Among these solutions is the idea of converting CO₂ into useful chemical products and/or fuels, such as methane (CH₄) or alcohols.

This diploma thesis focuses on CO₂ catalytic methanation as an alternative solution. The objective of this research is to analyze the efficiency of the process using low-cost materials and highly active catalysts. Within this context, the parameters that affect the efficiency of the Sabatier reaction are examined. Then, CO₂ capture and H₂ production are reviewed, by focusing on technologies that are not powered by fossil fuels. The study also examines the performance of the reaction over various catalytic materials, as well as its environmental impact and financial sustainability. The findings of this research provide valuable insight into the potential of CO₂ catalytic methanation as a sustainable solution to reduce CO₂ emissions and mitigate the effects of climate change.

1. Introduction

Last decades, the intensification of industrial activities, urbanism and increase in human population have led to a surge of energy demand around the globe. Since the dawn of the first industrial revolution, humans have developed the exploitation of fossil fuels in order to cover our energy demands, as even in modern times they make up to 80% of global energy production. The consumption of fossil fuels however is the driving force for greenhouse gas (GHG) emissions in the atmosphere, mostly CO₂, triggering a domino effect of consequences. GHG effect is responsible for global temperature rise, leading to climate change, influencing ecosystems and the varieties of plants, animal species and seasonal events timing in them, affecting human health and economy through extreme weather conditions.

To get a better grip of the surge of CO₂ emissions in the atmosphere, in 1960 the annual emissions were 11 billion tons [1], where in 2022 reached 36.8 billion tons [2]. Future projections are pessimistic as they estimate an increase to 43.08 billion tons of CO₂ emissions in 2050 [3], as for energy consumption, a 50% increase in global demand is projected, with industrial consumption reaching 305 quadrillion Btu [3].

With the GHG effects becoming more remarkable as the years go by, the Paris Agreement, which came into effect in 2016, is binding 196 parties to face climate change. More precisely, the main objective of the agreement is to maintain global temperature increase below 2°C from pre-industrial levels, setting the limit at 1.5°C. This agreement has motivated researchers to focus on carbon capture and utilization (CCU) technologies that aim to recycle CO₂ and potentially produce energy.

With these into perspective, production of alternative fuels from CO₂, have been in the spotlight. CO₂ methanation have quickly gained ground as potential solution, producing CH₄, which has one of the highest calorific values among fuels (50-55 kJ/kg[4]), in a process capable of being powered solely by renewable energy sources (RES) and the product can potentially be injected into the natural gas (NG) grid, using the existing infrastructures for storage and transportation [5].

Over the last years, several studies investigate the means and the opportunities of this process. Multiple catalytic systems have been assessed, regarding their capability of enhancing methane production. Alongside the catalysts, the thermodynamic conditions, side reactions, components concentrations and reactors play a significant role in the process outcome, leading to extensive literature reviews. Beside the maturity of the technology through research, the environmental impact of the process, the economics of such facilities and their socio-political impact must be reviewed in order for the technology to capture the attention of energy production industry.

In this thesis, CO₂ catalytic methanation is reviewed, with refers to the latest advances, limitations and potential. Section 2 is mainly focused on the thermodynamics of the reaction, combined with a brief reference to the timeline of the process. Section 3 and 4 analyze the CO₂ capture and hydrogen production respectively, followed by a detailed breakdown of the CO₂ catalytic methanation process in section 5. Lastly, section 6 takes a look beyond the process, reviewing Life Cycle Assessment (LCA) results, techno-economic analyses and sociopolitical reports.

2. Reaction analysis

2.1 Brief history of the reaction

In 1902, the French novelist Paul Sabatier and the chemist Jean-Baptiste Senderens were the first to document CO and CO₂ methanation. Using hydrogen and the oxides of carbon as reactants, combined with reduced nickel at 250 degrees Celsius, methane and water were formed.

These methanation techniques have seen numerous applications the past century. The first and most significant application was to eliminate traces of CO and CO₂ from production of gases like ammonia. Later in the 20th century, due to the oil crisis in the 1970's, these techniques were resurfaced, focusing on the production of synthetic natural gas (SNG) from coal and biomass [6]. In the early stages of this process, there were experiments regarding CO₂ methanation, using coke oven gas or blast furnace gas. However, only a few of these concepts found application.

As the environmental awareness grew in late 20th century, with the effects of CO₂ emissions from fossil fuels usage in the spotlight, institutes reinstated their interest to its methanation, thus reviving the most recent discoveries. In this context, Hashimoto proposed the groundbreaking concept of reforming CO₂ to CH₄, with hydrogen extracted from seawater, as a measure to prevent global warming [7].

With no viable large-scale option to prevent the accumulation of CO₂ in the atmosphere up to this day, accompanied by the need of storing energy surplus, the carbon oxides methanation techniques are lately examined as a solution for converting energy surplus from renewable sources into gas, named Power-to-Gas (PtG).

Recently, the application of these methods is also examined for long-term extraterrestrial explorations in order to provide energy and water in manned missions [8] and eliminating CO emissions from proton exchange membrane (PEM) fuel cells, making them a possible source of clean and efficient power [9].

2.2 Thermodynamics

Carbon oxides methanation is a complex process, with many reactions taking place simultaneously. Studying the thermodynamic aspect of these reactions can hint an easier path for specific products, making reactions stand out depending on their

parameters. Moreover, readjusting reaction conditions such as pressure, temperature and components ratio can lead to a thermodynamic equilibrium of the chemical system, which achieves higher concentrations of specific products [10]–[16].

From experimental thermodynamic analyses conducted, regarding this reaction [10]–[13], [16], the optimal conditions for the reaction, are determined by the analysis of the chemical system in thermodynamic equilibrium. The estimation of the systems composition was measured with the Gibbs free energy minimization, a method based on the principle that minimum value of Gibbs free energy is achieved when the system reaches equilibrium [13].

2.2.1 Reactions and thermodynamic parameters

In this process several reactions take place simultaneously (Table 2.1), each defined by different thermodynamic parameters. In order to meticulously study these reactions, besides Gibbs free energy change (ΔG), the natural logarithm of the equilibrium constant ($\ln(K)$), alongside with the enthalpy (ΔH) and the entropy (ΔS) change are taken into consideration. These parameters interact with each other through the second law of thermodynamics and the thermodynamic equilibrium formula.

$$\Delta H = \Delta G + T\Delta S \quad (1)$$

$$K = \exp \left[\frac{\Delta G}{RT} \right] \quad (2)$$

Table 2.1: Reactions involved in CO₂ methanation, thermodynamically studied at T=25°C and P = 0.1 MPa [13]

No.	Reactions	Reaction description	ΔH	ΔS	ΔG	$\ln(K)$
1	$\text{CO}_2(\text{g}) + 4\text{H}_2(\text{g}) \rightleftharpoons \text{CH}_4(\text{g}) + 2\text{H}_2\text{O}(\text{g})$	CO ₂ methanation	-164.747	-214.497	-141.932	24.868
2	$\text{CO}_2(\text{g}) + 2\text{H}_2(\text{g}) \rightleftharpoons \text{C} + 2\text{H}_2\text{O}(\text{g})$	CO ₂ reduction	-90.147	-91.722	-62.800	11.003
3	$2\text{CO}_2(\text{g}) + 3\text{H}_2(\text{g}) \rightleftharpoons \text{CH}_3\text{OH}(\text{g}) + 4\text{H}_2\text{O}(\text{g})$	CO ₂ hydrogenation to CH ₃ OH	-49.321	-177.109	3.484	-0.61
4	$\text{CO}_2(\text{g}) + 2\text{H}_2(\text{g}) \rightleftharpoons \text{CO}(\text{g}) + \text{H}_2\text{O}(\text{g})$	Reverse water gas shift	41.138	42.045	28.602	-5.011
5	$2\text{CO}_2(\text{g}) + 7\text{H}_2(\text{g}) \rightleftharpoons \text{C}_2\text{H}_6(\text{g}) + 4\text{H}_2\text{O}(\text{g})$	CO ₂ hydrogenation to C ₂ H ₆	-264.978	-357.361	-158.43	27.759

6	$\text{CO}_2(\text{g}) + \text{CH}_4(\text{g}) \rightleftharpoons 2\text{CO}(\text{g}) + 2\text{H}_2(\text{g})$	Dry reforming of CH_4	247.023	256.542	170.535	-29.879
7	$2\text{CO}(\text{g}) \rightleftharpoons \text{C} + \text{CO}_2(\text{g})$	Boudouard reaction	-172.423	-175.812	-120.004	21.026
8	$\text{CH}_4(\text{g}) \rightleftharpoons \text{C} + 2\text{H}_2(\text{g})$	CH_4 cracking	74.6	80.73	50.53	-8.853
9	$\text{CO}(\text{g}) + 3\text{H}_2(\text{g}) \rightleftharpoons \text{CH}_4(\text{g}) + \text{H}_2\text{O}(\text{g})$	CO methanation	206	-172.452	-113.330	19.857
10	$\text{CO}(\text{g}) + 2\text{H}_2(\text{g}) \rightleftharpoons \text{CH}_3\text{OH}(\text{g})$	CO hydrogenation to CH_3OH	-90.459	-219.153	-25.118	4.401
11	$\text{CO}(\text{g}) + \text{H}_2(\text{g}) \rightleftharpoons \text{C} + \text{H}_2\text{O}(\text{g})$	CO reduction	-131.285	-133.767	-91.402	16.015
12	$2\text{CO}(\text{g}) + 5\text{H}_2(\text{g}) \rightleftharpoons \text{C}_2\text{H}_6(\text{g}) + 2\text{H}_2\text{O}(\text{g})$	CO hydrogenation to C_2H_6	347.254	-441.45	-215.635	37.782

According to Figure 2.1, combined with the results of the parameters that are shown at the Table 2.1, it is obvious that different groups of reactions are feasible and dominate the mixture in different temperatures. CO_2 methanation (1), CO_2 reduction (2), Boudouard reaction (7), CO methanation (9), CO reduction (11) are reactions with high $\ln(K)$ values, highly spontaneous due to negative ΔG values and besides reaction (9) are exothermic (negative ΔH values). Consequently, these reactions are feasible and most likely to dominate during the methanation process. On the contrary, Reverse water gas shift (4), Dry reforming of CH_4 (6), CH_4 cracking (8) are endothermic reactions (positive ΔH) with positive $\ln(K)$ values, evincing their infeasibility. From temperatures between 450 and 500°C CO_2 and CO hydrogenation to C_2H_6 (5,12) are becoming feasible, with them becoming infeasible again after 500°C. CO_2 and CO hydrogenation to CH_3OH (10,3) are favored from lower temperatures.

In order to assess the performance of the reaction, in different conditions and with different catalysts, the following performance parameters will be examined.

$$\text{CO}_2 \text{ conversion: } X_{\text{CO}_2} = \left(1 - \frac{I_{\text{CO}_2}^{\text{out}}}{I_{\text{CO}_2}^{\text{out}} + I_{\text{CH}_4}^{\text{out}} + I_{\text{CO}}^{\text{out}}} \right) \times 100\% \quad (3)$$

$$\text{CH}_4 \text{ yeild: } Y_{\text{CH}_4} = \frac{I_{\text{CH}_4}^{\text{out}}}{I_{\text{CO}_2}^{\text{out}} + I_{\text{CH}_4}^{\text{out}} + I_{\text{CO}}^{\text{out}}} \times 100\% \quad (4)$$

$$\text{CH}_4 \text{ selectivity: } S_{\text{CH}_4} = \frac{Y_{\text{CH}_4}}{X_{\text{CO}_2}} \times 100\% \quad (5)$$

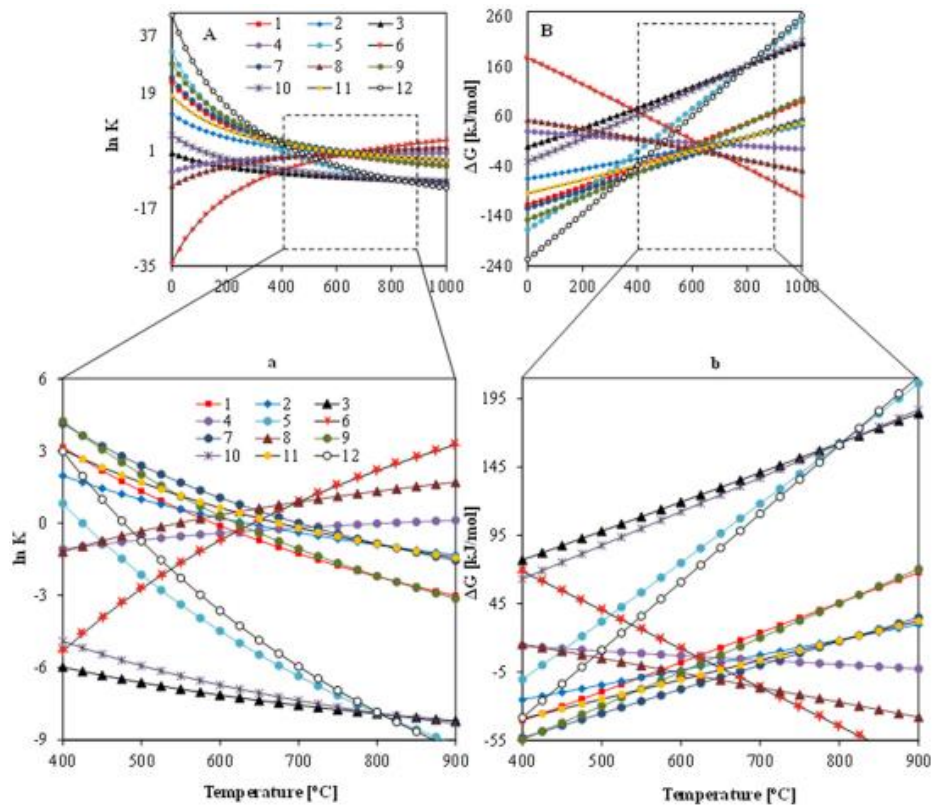


Figure 2.1 Equilibrium constant (A,a) and Gibbs free energy (B,b) graphs for different temperature values [13]

2.2.2 Effect of pressure and temperature

Despite the parameters mentioned above, pressure and temperature play a significant role in the concentrations that form the mixture. By increasing the pressure of a mixture that contains at least one gas reactant, it simultaneously increases the molecular concentration of the reactant, with more particle collisions taking place, accelerating the reaction. Studies prove that higher pressure favors CO_2 conversion and CH_4 selectivity, with pressure values up to 100 bar standing out the most [10], [12], [17], [18]. On the contrary, CO selectivity decreased with the increasing pressure. By modifying the temperature with certain pressure applied, the CH_4 yield, and selectivity and CO_2 conversion are decreasing dramatically, while CO selectivity increases with reaction 4 dominating as an endothermic reaction. Meng et al. [16] studied the carbon yield produced from reactions 2,7,8 and 11, with reaction 7 account for the largest amount of carbon deposition, due to higher value of $\ln(K)$. Additionally, for 1 bar and around 575°C the carbon yield reaches the maximum value of 23%. All in all, as Hussain et al. [13] mention, carbon oxides methanation is optimized in low temperature and high pressure, where in industrial scale high temperature and low pressure is favored due to precautionary reasons. Thus, the

temperature of 300- 500°C and pressure of 3 to 10 bar are ideal for commercial application of carbon oxide hydration to CH₄.

2.2.3 Effect of reactants concentrations

Besides temperature and pressure, the ratio of H₂ to CO₂ strongly influence on the product concentrations. Figure 2.2 depicted by Miguel et al. [12] prove the correlation of H₂/CO₂ feed ratio with temperature and pressure, in influencing CO₂ conversion, CH₄ selectivity, as CH₄ and C yield as well. As it is shown, for H₂/ CO₂ ratio of 4, CO₂ is the favored reaction, as the ratio obeys the reaction stoichiometry, with H₂O molar flow being double compared to CH₄. However, for feed ratio mentioned, for temperatures higher than 300°C and for pressure lower than 5 bar CO₂ selectivity and CH₄ yield drops with a small fraction of CO forming (yield of CO < 1%) through reaction 4. With ratios decreasing, so does CO₂ conversion, CH₄ yield and selectivity percentages. This derives from surplus of unconverted CO₂, since H₂ is less than required from the stoichiometry of the reaction. Moreover, for the feed ratios of 2 and 3, methane yield peaks around 200-250°C, with CO₂ selectivity decreasing for lower pressure and higher temperature, while CH₄ selectivity increases with higher temperature. The most interesting observation is that for the feed ratios of 2 and 3, coke formation is notably increased, with the smaller ratio leading to C yield around 55% for 150°C.

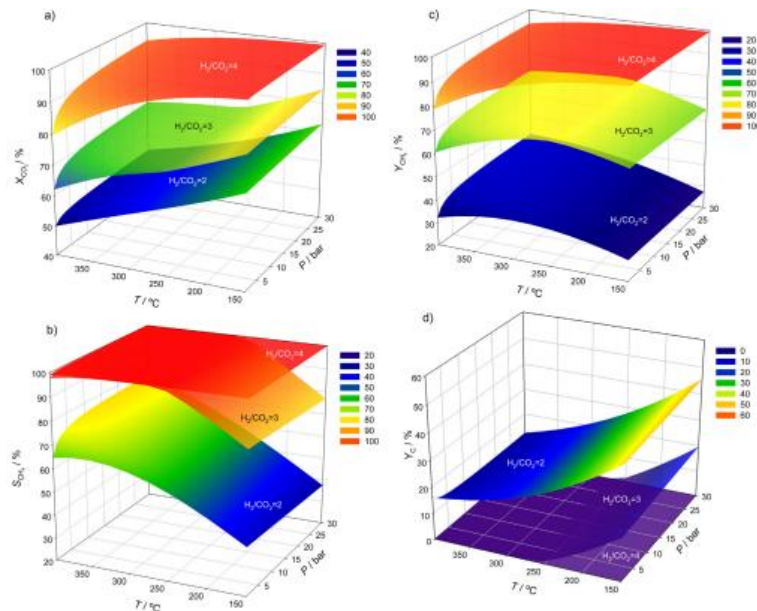


Figure 2.2 Contour graph of temperature, pressure and H₂/CO₂ ratio effect on a) CO₂ conversion, b) CH₄ selectivity, c) CH₄ yield, d) Carbon yield [12].

2.2.4 Products and other gases effect

Studies also examine the effects of individual and conjoint content of H₂O and O₂ in the reaction. Steam with absent O₂, as a product of CO₂ methanation decreases the CO₂ conversion, as it is one of the products of reaction 1. For the H₂/CO₂ ratio of 4, CO₂ selectivity decrease is not as noticeable as for the ratio of 3, while CH₄ selectivity reaches almost 100% for H₂/CO₂ ratios examined. According to Miguel et al. [12] the existence of water decreases coke formation at temperatures below 250°C, alongside with the ability of controlling the heat produced of the exothermic reaction of methanation. Small concentration of oxygen is found in coal gasification and emanating flue gas. O₂ has the ability of reacting with H₂ and CH₄, leading to a decay in CO₂ and CO conversion especially in temperatures higher than 500°C. Similar results found for CH₄ selectivity as for pressure equal to 1 bar, selectivity plummeted for increasing temperature and O₂ concentration values, while for pressure set at 30 bar CH₄ selectivity dropped steadily for the same modifications. As O₂ reacts with H₂ and CH₄ forming H₂O, having O₂ and H₂O simultaneously in the feed leads to further decay in carbon oxides conversion, with temperatures above 300°C in atmospheric pressure a slight CO is noted (CO yield <1%), which can be avoided with an increase of pressure.

3 Carbon Dioxide Capture

3.1 Capture technologies

Carbon dioxide is crucial for methane production, as the only carbon containing reactant. Its production is mostly associated with fossil fuel combustion, providing energy for human activities throughout the centuries. However, it is mostly contained in a mixture of gases and usually released to the atmosphere. Thus, CO₂ must be collected from either an emitting source or from the atmosphere. Such technologies have been under the academic and the industrial microscope the last decades, with numerous plants operating globally. CCU and Carbon Capture and storage (CCS) technologies include a plethora of methods for CO₂ capture, separation and transportation [17]. However, the high cost of these technologies and the CO₂ produced to meet the energy demands of such facilities, referred as energy penalty, are the most challenging parameters.

CO₂ formed as a result of combustion and in order to efficiently extract it, a different removal process is being implemented for every type of combustion process. There are many available technologies, but they usually make up 70-80% of the total CCS project cost, with the majority of studies focusing on the reduction of the overall operating cost [18]. There main CO₂ technologies are the options associated with combustion processes (post-combustion, pre-combustion, oxyfuel).

Post-combustion process, is usually applied to already existing power plants, removing CO₂ from flue gasses after combustion has taken place. The CO₂ concentration in combustion flue gas is scarce (for coal-fired plant is 7-14% v/v, while for gas-fired boilers is as low as 7-8% and for gas-fired turbines is 2-4%), leading to limited CO₂ capture efficiency while capturing large quantities of dust and impurities, combined with a high energy penalty and operational cost. However, this technology can extract high purity CO₂ from enhanced oil recovery, urea production and food/beverage plants, with the largest operating unit capable of recovering up to 800t/day. Kanniche et al. [19] reported an estimated 32% increase in electricity cost for gas fired plants and 65% increase in coal fired plants.

In pre-combustion process, the fuel in use, usually coal or NG is pre-treated before the combustion. In this process, the fuel is being converted into syngas. For NG, CH₄ is reformed (Eq.6) with H₂O, producing CO and H₂, while coal is being gasified (Eq.7) under low oxygen level. Then syngas is taking part in the water gas shift reaction (Eq.8), reacting with steam and producing CO₂ and H₂.



The flue gas produced contains a CO₂ concentration greater than 20% v/v, the absence of N₂ provides a clean CO₂ source, while the gas mixture is under pressure making the process more energy and consequently financially efficient [19]. After CO₂ separation, H₂ is burnt, reacting with O₂ and producing H₂O, generating energy for the plant. Studies prove the high efficiency of this process, with an efficiency loss of 7-8% for its application to Integrated Gasification Combined Cycle (IGCC) coal power plant, while pre-combustion application on advanced combined cycle gas turbine plants, operating with NG achieved 80% CO₂ capture efficiency [20].

In oxyfuel combustion, cryogenic air separation provides the system with pure oxygen mixed with flue gases, eliminating nitrogen products generated from combustion with air, producing CO₂ with higher partial pressure in coal combustion. The products are primarily CO₂, H₂O, with particulates and SO₂ often found in the flue gases, which are eliminated through electrostatic precipitation and desulphurization methods respectively. Then CO₂ and H₂O are being separated after water condensation leading to 98% CO₂ purity which then is transported in supercritical state. On the downside, air separation is increasing the energy demands and the operational cost of the plant, leading to an energy penalty potentially over 7%, compared to a plant without CCS, as leftover impurities in the CO₂ streamline may cause vibrations and shock loads in the pipe, which can be avoided with further dehydration [20], [21].

After sidetracking the flue gas from the plant, and capturing a rich CO₂ gas mixture, a separation process takes places, producing pure CO₂. The technologies developed are primarily studied are absorption, adsorption, cryogenic distillation, membrane separation, hydrate-based separation and chemical looping combustion.

3.2 Separation technologies

In absorption process, an amine liquid sorbent or solid matrix is used to separate CO₂ from the product gas. This process relies on absorbing only CO₂, which later can be obtained from the solution and the sorbent residue is recycled to absorb CO₂ from newly produced flue gas. Monoethanolamine (MEA), Diethanolamine (DEA), Diglycolamine (DGA), Methyl diethanolamine (MDEA), Piperazine (PZ), K₂CO₃ or mixture of amines are typically used [22], with MEA being the most favored solvent for this process, as it is efficient and economic. Moreover, MEA finds applications in the chemical industry for over 60 years, with extensively studied properties and easy regeneration process. However, oxygen and sulfuric acid leftovers can corrode the infrastructure and lead to limited solvent regeneration, while high temperatures can degrade the solvents, forming nitrosamines and nitramines, posing a threat to human health and the environment. Consequently, alternative solvents are being studied, with aqueous ammonia posing as the most efficient solution in matters of energy and cost [17], [20], [23].

In the adsorption process, a heterogeneous process captures gas CO₂ molecules from flue gases, as they get trapped by a solid sorbent or physi-sorbed [23]. Flue gases, consists of multiple nitrogen, carbon and sulfur gases, in varying concentrations. Multiple materials have proven ability of selectively adsorbing CO₂ in cracks, pores or on their surface, under specific thermodynamic conditions.

In order to determine the optimum sorbent, which is characterized with high selectivity, low cost, capability to regenerate, combined with mechanical and chemical strength, countless materials have been tested. Recent studies focus on activated carbon (AC), activated carbon fiber (ACF), carbon nanotubes (CNT), organic polymers, molecular sieves, zeolites, metal organic frameworks (MOFs), microporous coordination polymers (MCPs), zeolitic imidazolate frameworks (ZIFs), metal oxides and graphene and graphene-based materials [24]. However, every material has parameters limiting their large-scale application, with surface modifications necessary for process optimization.

Multiple adsorption methods have been studied with pressure swing adsorption (PSA), temperature swing adsorption (TSA) and electrical swing adsorption (ESA). In TSA the solvent column is cooled during the adsorption process, favoring CO₂ adsorption as flue gas flows through the adsorbent pores, followed by a raise in temperature, purging the adsorbed CO₂ [25], with studies calculating obtained CO₂ purity of 96.22%, recovery of 86.5% and productivity of 0.279 kg/hour [26]. PSA takes place in constant temperature, with adsorption being carried out at typically 10-40 bar, with desorption taking place with pressure slightly above atmospheric and as a sequence the solvent is being regenerated. This method on average achieves 79.8-99.4% CO₂ purity and 94-97.7% recovery rate. ESA is similar to TSA, with the honeycomb solvent column being regenerated through Joule effect application, as electricity passes through a conductor, lowering desorption time [27]. The application of this method offers 89.8% overall CO₂ purity.

Adsorption methods stand out for their simplicity and low capital needs. The sorbents can be reused multiple times, providing a financially sustainable solution for multiple industries, with operational circumstances are not characterized as dangerous, with pressure and temperature fluctuating in controllable ranges. On the contrary, large amounts of CO₂ cannot be easily handled with this method. Moreover, the solvents pores usually adsorb amounts of N₂ leading to product impurities [23].

In cryogenic distillation, CO₂ is distilled from feed gas, which is assumed that consists of CO₂ and N₂ with the prior liquified under extreme conditions. After combustion, flue gas produced is filtered, with CO₂ and N₂ remaining, sent into a chamber where high pressure and temperatures lower than -73.3°C lead to CO₂ liquification (triple point of CO₂ is -56.6°C) with N₂ escaping as a gas, leading to CO₂ purity higher 99.95%.

Cryogenic distillation has multiple advantages and disadvantages. First and foremost, this method is capable of handling CO₂ concentrations higher than 50% v/v. Moreover, it leads to a liquid product which can be transported easier, while it does not require

chemical additives throughout the process. These advantages however, come with a high capital cost due the high energy requirement in order to achieve low temperatures. Additionally, a further removal of potentially freezing components must take place, for the process to be efficient [28], [29]. CO₂ is distilled from feed gas, which is assumed that consists of CO₂ and N₂ with the prior liquified under extreme conditions. After combustion, flue gas produced is filtered, with CO₂ and N₂ remaining, sent into a chamber where high pressure and temperatures lower than -73.3°C lead to CO₂ liquification (triple point of CO₂ is -56.6°C) with N₂ escaping as a gas, leading to CO₂ purity higher 99.95%.

Membranes can act as sieves, concentrating CO₂, excluding other components from flue gases. Membranes used for these applications can be distinguished in two layers, a thin reactive layer responsible for CO₂ selectivity, made of composite polymer, metal or ceramics and a thicker neutral layer that offers mechanical support [30].

As combustion takes places, product gas enters a chamber, which is separated by a membrane, which can have four potential methods of separating CO₂ from glue gas. The first is solution-diffusion mechanism where flue gas is absorbed by the membrane, diffused and CO₂ gets desorbed downstream. Another mechanism is the facilitated transport, with biological membranes interacting with CO₂ molecules, transporting them through the membrane. The most common concept is the mechanical sieving, where porous membranes are applied filtering CO₂ molecules from other gases with larger molecules. At last, preferential adsorption-monomolecular surface diffusion mechanism has also been examined, as membranes with pores walls covered with a material which attracts and absorbs only CO₂ molecules through[31] After separation takes place, or before flue gas enters the chamber nitrogen and sulfur oxides are removed improving CO₂ purity.

Different reactive types of polymer membranes have emerged, with ether oxygen-rich polymers, polymeric ionic liquids, perfluoropolymers, thermally rearranged polymers, iptycene-containing polymers, facilitated transport membranes (FTMs) containing amine or other carriers, at the epicenter of academic reviews [30]. The selective layer plays essential role to the process with its dimensions varying for every mechanism and material used, typically range between 0.1-10 μm [32].

Membrane separation is the simplest concept in terms of equipment, with limited energy needs compared to other methods. However, CO₂ selectivity of the membranes, the poison of the selective layer from SO_x and NO_x, combined with clogging of the pores from vapor or other gases are commonly encountered problems.

Hydrate application is also a considerable option. Gas hydrates are ice like structures called clathrates, formed from gas molecules, which are getting trapped within cavities of hydrogen bonded water molecules [33]. Small nonpolar carbon gases like CO₂ are favored occupants of this method, forming hydrates in contact with water and possibly cyclopentane, when temperature is lower than equilibrium temperature and pressure higher than equilibrium pressure. The optimum mole fraction of this method

is 0.148 with weight fraction of 0.31 gCO₂/H₂O, as 8 CO₂ molecules can be caged by 46 H₂O molecules under optimal conditions [34] with hydrates having at least four times greater CO₂ concentration compared to its gas phase [33].

Shifeng Li et al. [35] mention the increased density of hydrate state of a gas, provide this mechanism with the ability to store large amounts of gas with more than 99% CO₂ collected from flue gas, after a three-stage hydration process. The first step is the formation of solid hydrates under high pressure and low temperature, capturing CO₂, followed by leftover gas and hydrate slurry separation. Then the hydrates are dissociated releasing high purity CO₂ for further processing.

Hydrate process leading to a hydrate product rich with CO₂, with high density, offering an efficient transportation option. On the other hand, in order to form CO₂ hydrates the extreme conditions of approximately 89 bar and 0°C are required, with Tajima et al [36] conducting a study on a hydrate-based carbon capture 100 MW thermal power plant, with 7000 m³ reactor reaching the energy penalty of 15.8% and other methods reaching as high as 35% [23]. Moreover, this method demand for increased efficiency for CO₂ capture as 35.29% of CO₂ entering the chamber is in hydrate state for water cyclopentane emulsion [35].

Chemical looping combustion is a promising process, which substitutes pure oxygen with a metal oxide, in oxyfuel combustion. During combustion, CO₂ and water vapor is produced, which can be easily removed through condensation, providing pure CO₂ without energy consumption of separation.

Multiple metal oxides find application in this process. Fe₂O₃, NiO, CuO, Mn₂O₃ and CoO are some of the metal oxides reviewed [37], [38]. After combustion, the reduced metal, enters an air chamber, regenerating metal oxide for further CO₂ capture, with product released in the atmosphere as the concentrations of the pollutants produced can be disregarded [39]

The limited energy needs of this process, decreasing the operational costs, combined with high efficiency CO₂ capture make this process stand out. Another notable advantage is the low toxicity of the products, while being biodegradable. On the other hand, the continuous recycle of the metal impracticable, due to components degradation. Another effect of the metal oxidation taking place, is the potential corrosion to the equipment.

3.3 CO₂ transportation

As CO₂ is captured and separated from the flue gases, a sufficient CO₂ transportation method to storage or industrial utilization is required. The most crucial parameters for a reliable CO₂ transportation system, are safety and cost. Depending on the volume of the gas and the type of transportation (onshore, offshore), various methods have been developed, ranging from pipeline transportation to road tanker and ships [20].

Pipeline transportation is the most used medium. Carbon dioxide is similar to NG in terms of transportation form, while it is non-toxic and non-flammable. NG pipeline transportation is an already mature process, with some modifications required to transport CO₂. Another characteristic is the efficiency, with large volumes being transported with low cost. Moreover, CO₂ leakage does not pose a threat of explosion, but it bears a toll to plants humans and marine ecosystem, thus monitoring is required [40]

This method has some obstacles to overcome regarding its application. It requires temperature and pressure monitoring, reassuring CO₂ maintains the same phase throughout the process (liquid, gas, dense-phase, supercritical), leading to a well-tempered transportation, as phase transition in the pipeline may lead to clogging [41]. Moreover, impurities must also be monitored, in order to avoid corrosion or damage to the equipment. Regarding capital investment, the volume of initial cost to construct the pipeline facilities, is momentous, making these methods available to limited industries.

The optimal CO₂ phase for pipeline transportation is either liquid or supercritical. Johnsen et al. [42] studied the optimal conditions, with supercritical phase standing out, leading to operational temperature of 32.1°C and 74 bar, with typical pipeline conditions varying from 13-44°C and 85-150 bar reassuring single-state CO₂ flow [20] with compressors placed periodically maintaining a constant pressure value. Pantoleonatos et al. [43] conducted a transportation and cost optimization analysis, of a 34,000 km pipeline facility, connecting 17 plants from central Europe, with 16 utilization facilities in the Mediterranean coastline based on solar energy. The operational cost estimated reached 9 billion euros/year, with approximately 2 billion dedicated to the 93 Mt CO₂ transported yearly.

Other options for smaller and scattered CO₂ sources are marine, motor and railway transportation, usually connecting storage tanks to a pipeline system. Marine transportation consists of a liquefaction facility, stored in tanks and transferred with a ship and with CO₂ being loaded to storage tanks in a new location. Already existent LPG marine transportation ship can be utilized with CO₂ capturing 60% of its total capacity [44]. This method is already established for various industrial purposes, has a high operational cost but a low capital cost, and an approved marine environment alteration. Motor and railway transportation are onshore options, not preferred due to limited capacity, incapability of transferring efficiently large amounts of CO₂.

4 Hydrogen

Besides CO_2 , H_2 is the other reactant of Sabatier reaction (Table 2.1, reaction 1). Consequently, obtaining H_2 is a crucial part of the methanation process chain. Throughout the years, multiple hydrogen production processes have been developed and have been classified according to the energy source used, the emissions and costs. Different colors have been used to distinguish every class, with green, blue and grey hydrogen predominantly studied, while purple and yellow can also be found in scientific literature [45]. In addition, Yu et al. [46] reviewed a subterranean method of hydrogen production, developed by University of Calgary and Proton Technologies [47], [48], classified as aqua hydrogen. The color separation regarding energy sources powering hydrogen production is depicted in Figure 4.1.

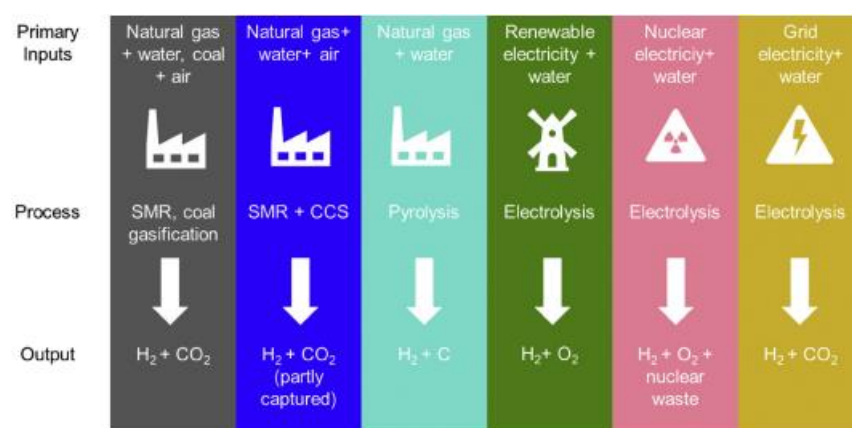


Figure 4.1 Hydrogen production colors [45]

Hydrogen is a versatile element with multiple applications in industry, electricity, transportation and other fields. The hydrogen production consists of upstream hydrogen production, followed by midstream storage and transportation and lastly the downstream applications [45], [49]–[52]. Some hydrogen production methods are quite mature, while others are still under research. Hydrogen production based on fossil fuels, using NG, coal, oil or biomass, as a source, produces H_2 through steam methane reforming (SMR) or gasification, emitting CO_2 which can potentially be captured and stored (CCS) or utilized (CCU). Other developed methods are methane pyrolysis, based on methane thermal cracking (Table 2.1, reaction 8) leading to pure carbon by-products [53] with potential substitution of methane with biomass.

Another well-established method is water electrolysis with industrial applications before the 20th century reported. This method is environmentally sustainable, producing H_2 and O_2 . Additionally, electrolysis can potentially lead to a zero-carbon H_2 production, powered by renewable energy sources (RES), while nuclear energy can be an alternative, mostly overlooked due to its notoriety, with only a handful of countries examining it. Furthermore, water electrolysis can be powered by a low-carbon option,

or using energy produced from the grid. This method however cannot be considered green, since the electrical power is mostly produced by a mixture of sources, with fossil fuels being the primary energy source for electricity production, making up to 63.3% of global electricity production in 2019 [54].

4.1 Water-based hydrogen production

Water is the most common hydrogen containing element on the surface of Earth, making it an inexhaustible source of hydrogen, with the application of certain processes. There are three processes developed for water dissociation, with electrolysis being the most well-established, as thermolysis and photo-electrolysis techniques emerging. According to Martinez-Burgos et al. [55] from 2000 until 2019, 199 patents have been filed, where 3% are referring to thermolysis, 27% to photolysis and 70% electrolysis, with electrolysis being the only process applied to industrial scale.

4.1.1 Electrolysis

Electrolysis is a process, in which H_2O surrounds an electrolyzer, which circulates in direct current, splitting H_2O to H_2 and O_2 . The electrolyzer consists of the anode and the cathode operating two half reactions, which are responsible for oxygen evolution reaction and hydrogen evolution reaction respectively [39]. Electrolyzer module types are divided between monopolar and bipolar. Monopolar modules are being characterized by robustness, simpleness and considerable size, while bipolar modules are more complex, yet have a more compact structure [56]. In general, industrial electrolyzers usually consist of bipolar electrolyzers, with multiple cells connected in series, generating the desired H_2 amount. In addition, a separating layer is placed between the electrodes. Depending on the electrolyzer operating principle there are three main types of electrolysis: Alkaline Water Electrolysis (AEL), Proton Exchange Membrane (PEM) and Solid Oxide Electrolysis (SOEL) [39], [57].

AEL is the electrolysis technology with the most applications globally, invented in the 19th century and by 1902 more than 400 electrolyzers were providing hydrogen commercially [58]. In this method, an aqueous solution, containing 30%wt of diluted potassium hydrate (KOH) or sodium hydroxide (NaOH) leading to increased ionic conductivity. The operating temperatures vary between 60-100°C as the conductivity of the solutions in use, peaks in this range of concentration and temperature [59], with pressure typically in the range of 1-30 bar, where some models reach even 448 bar [57].

Electrolysis cells, consists of two porous electrodes, made from low-carbon steel with or without nickel-coating. The cell is divided by a diaphragm, made typically from asbestos, with an electrode in each tank. As direct current flows in the electrodes, it forms the negatively charged cathode and the positively charged anode, which are reacting with water according to Eq.9 and Eq.10 respectively. In the cathode water is reduced, releasing H_2 gas and hydroxide anions, which circulate the diaphragm to the anode, where the anions recombine, forming O_2 gas bubbles as two electrons are closing the circuit [57]. A detailed AEL electrolyzer can be seen in Figure 4.3.

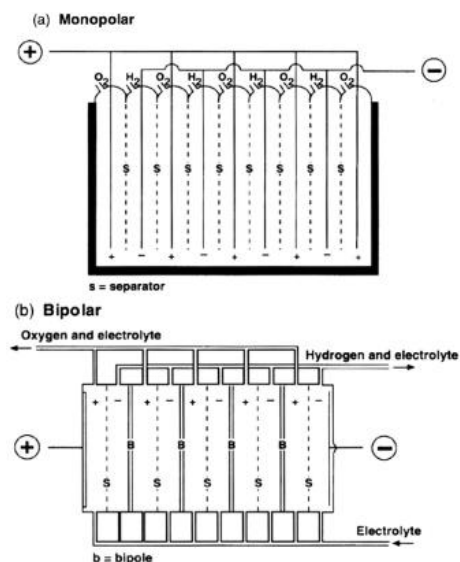


Figure 3.2 Alkaline electrolysis cell module a) monopolar b) bipolar [56]

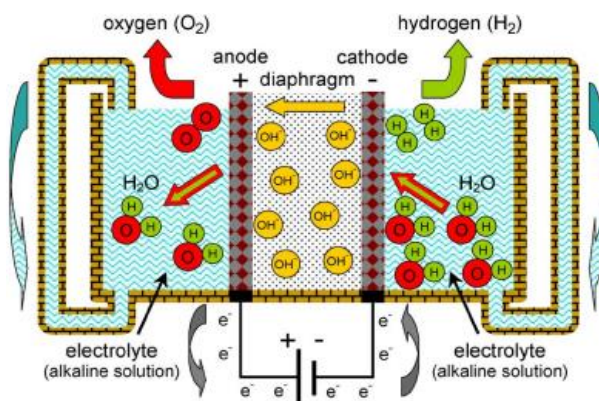


Figure 4.3 Design and operating principle of an AEL electrolyzer [57]

The efficiency of an AEL electrolyzer depends on multiple parameters. The design of the electrodes plays a significant role, as they are responsible for the evolution of the gas products. An efficient electrolyzer design, contains electrodes with maximized interfacial contact with the solution [57]. Besides that, as cathode consumes water and the anode reforms water from anions, the recirculation of the electrolyte is crucial, maintaining a constant concentration of electrolytes in the solution, leading to uncontaminated product gases. Moreover, the proper concentration reassurance, under constant control is crucial, as gas contamination can lead to flammable mixtures, especially when part load is low [60]. Lastly, ohmic losses occur as gas bubbles develop on the electrode surface, as their sizes correlates directly with an increase on the electrical resistance of the system, insulating the electrodes from the solution. Recent studies focus on the addition of substances, preventing the gas from being attached to the electrode [61], [62].

High purity is characterizing the gas products. Hydrogen purity percentage can reach 99.9% and oxygen 99.7% without further purification process applied [57]. The AEL applications are based on freshwater, as seawater electrolysis is being studied extensively, leading to an inexhaustible source of water as only 0.5% of global water reservoirs is available fresh water, while 97% of global water is found in oceans [63].

The development of PEM for ion exchange is a nearly commercialized technology, developed in 1960s by General Electric [64]. This technology is based on a proton exchange membrane, also referred as solid polymer electrolyte (SPE). In general, polyfluorosulfonic, a highly acidic material (mostly Nafion[®], a DuPont trademark [65]) with width between 50-250 μ m[66]), separating two electrodes made from primary noble metals like platinum or iridium. The application of noble metals is preferred, as the acidic environment would dissolve non-noble metals [66], [67]. The cell consists of a bipolar module, with the electrodes attached to the membrane, forming the so-called MEA (membrane electrode assembly) [39]. The anode oxidizes water, with protons closing the circuit as they move through the membrane to the cathode, reducing to hydrogen bubbles. The PEM electrolyzer configuration is depicted in Figure 4.4. The reactions of the anode and the cathode are written in detail below:



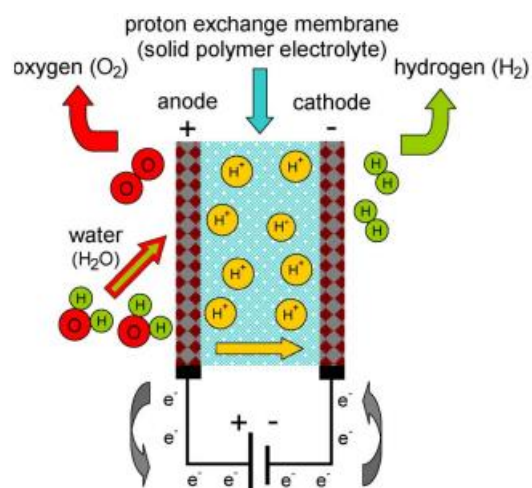


Figure 4.4 Design and operating principle of an PEM electrolyzer [57]

PEM electrolysis finds low-scale application for the time, as indicated in Table 4.1 below. The cells are operating below 80°C, as ambient operating pressure is common, the pressure value ranges up to 20-30 bar and in some instances to 85 bar [57]. The optimal operating temperature increases proportionally with the current density, following an analytically solvable function as Scheepers et al. [68] proved. The modules operating this type of electrolysis are characterized by a compact design, with the ability of handling different pressure values on each side of the MEA configuration, producing gases in different pressures.

Table 4.1 Leading manufactures of PEM electrolyzers [69]

Manufacturer	Series and Operating pressure	Hydrogen Flow Rate (Nm ³ ·h ⁻¹)	Energy Consumption (kWh·Nm ⁻³ ·H ₂)	Load Range (%)	Electrolyte	Power
Proton OnSite	S Series 13.8 bar	0.265–1.05	6.7	0–100	SPE	No details
Proton OnSite	H Series 15–30 bar	2–6	6.8–7.3	0–100	SPE	No details
H-TEC Systems	H-TEC Series-S	0.22–1.1	No details	No details	SPE	1–5 kW
H-TEC Systems	ME unpressurised 30 bar	13–210	4.9	No details	SPE	225 kW–1 MW
Areva H ₂ gen	E series Up to 35 bar	10–200	4.7–5.3	No details	SPE	80–1600 kVA
Hydrogenics	HyLYZER 0–7.9 bar	1–2	6.7	0–100	SPE	No details

ITM Power	HPac, HCore, HBox, HFuel 15 bar	0.6–35	4.8–5.0 (system)	No details	SPE	2 MW
Siemens	SILYZER 35 bar	200	225	No details	No details SPE	1.25 MW
Green Hydrogen	P-series/ 50 bar	15–	1	No details	25– 100	SPE 4.95 kW
NEL	M Series bar	30	103–413	4.53	0–100	SPE 0.5–2 mW

A PEM cell bare the ability of producing high purity gases. In most cases hydrogen produced from these technologies, has purity above 99.99%, without further filtration, due its wide load range. Additionally, the membrane structural characteristics make it almost impenetrable from gases, thus eliminating the risk of forming flammable mixtures [57]. Moreover, PEM electrolyzers are capable of handling fluctuating power feed.

The study of solid oxides for electrolysis first appeared in Germany at Brookhaven National Laboratory and in General Electric laboratories [70]. The principal of solid oxides application in quite complicated, with the academic community studying its properties the last 15 years. The increased temperature, usually between 700 and 1000°C, increases the hydrogen production efficiency as the division of water molecules is thermodynamically and kinetically favored. The operating principle is groundbreaking, with the reactant now in gas state, mixed with hydrogen, reacting with the cathode with more hydrogen generated (Eq. (13)). Oxide anions are attracted to the anode where they deposit the electron surplus forming oxygen (Eq. (14)) [39], [71].



A common cell design, consist of two electrodes, separated by a dense ionic conductivity electrolyte, with the total thickness of the cell varying from 200-300 μm. There are two basic SOEL electrolyzer designs, the electrolyte-supported cell (ESC) and the cathode-supported cell (CSC). The first concept is based on a thick electrolyte layer where thin anode and cathode mounted to each side. On the contrary, in the second design, both a thin electrolyte and a thin anode are based on a thick cathode. The difference in the architecture of the cell, leads to different properties and efficiency rates for every cell type [71]. A typical ESC electrolyzer is shown below in Figure 4.5.

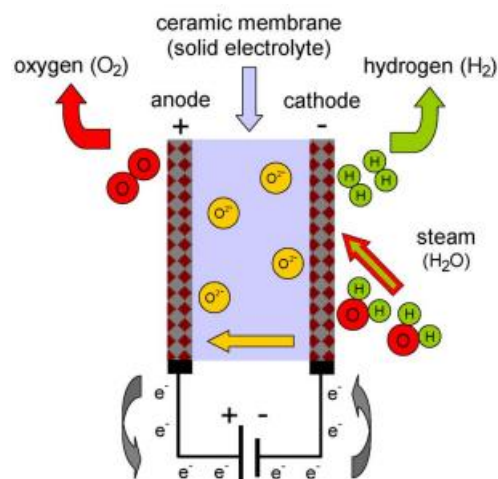


Figure 4.5 Design and operating principle of an SOEL electrolyzer [57]

The evolution of the product gases takes place on an electrode reacting with steam, making the gas separation and the maximization of the reacting surface area of the electrode the most valuable parameter. In general, the electrode materials have to be good electricity conductors with high ionic conductivity and adequate porosity in order to efficiently react with the products and the reactants. They typically are coated by multiple yttria(Y_2O_3)-stabilized zirconia (YSZ), with the cathode usually consisting of ceramic YSZ and nickel and the anode consisting of YSZ and perovskites like $LaMnO_3$, $LaFeO_3$, $LaCoO_3$ [57]. The electrode materials are being intensively studied, in order to maximize the efficiency of SOEL and become industrially feasible [72].

SOEL technology is considered to outpace the well-established AEL technologies soon. The power efficiency of this technology, in elevated temperatures is noteworthy, as the ability of producing multiple gas mixtures from co-electrolysis (e.g., syngas) [71], [73] or even generate electricity, operating in reverse [74]. This great potential however is restricted by the short lifespan of the cells, compared to other methods.

The typical characteristics and a brief comparison of the three electrolysis technologies available, are listed in Table 4.2 below.

Table 4.2 Comparison of electrolysis methods [57], [71], [75]–[78]

Technology	AEL	PEM	SOEL
Operating conditions	60-100°C 1-20 bar	>80°C 20-30 bar	700-1000 °C Ambient pressure
Cathode material	Ni alloys	Pt/Pb Carbon black Carbon multiwalled nanotubes	Ni-YSZ Perovskites

Anode material	Ni>Co>Fe oxides Perovskites	IrO ₂ , RuO ₂ Supports: TiO ₂ , ITO, TiC	Ir _x Ru _{1-x} O ₂ , La _x Sr _{1-x} MnO ₃ + Y-Stabilized ZrO ₃
Lifespan (years)	20-30	10-20	2-3
Efficiency	59-70%	62-82%	≤100%
Electricity demand (kWh/kg(H ₂))	51.8	54	42.3
Production size (kg(H ₂)/h)	19.3	18.5	23.6
Applicability	Commercial	Near-term commercialization	Demonstration
Advantages	Well-established. Non-noble catalysts. Low cost/Cost effective. Long lifespan.	Compact design. Good partial load range. High gas purity. Dynamic operation.	Efficiency up to 100%. Non-noble catalysts Enhanced. thermodynamics and kinetics. Low energy demands. Low costs
Disadvantages	Gas products contamination. Restricted dynamics. Corrosive liquid electrolyte. Low pressure.	High cost Highly corrosive, low pH (~2) environment. Iridium is scarce.	Not mature yet. Susceptible to leaking. Bulky design. Not extensive cost information for commercial scale.
Challenges	Improve durability. Improve kinetics with electrolyte additives/catalysts. Gas bubble management.	Reduce cost. Reduce/substitute noble materials. Improve membrane characteristics.	Multiple stream management. Cell operation optimization. Minimize electrode rapid degradation.

4.1.2 Thermochemical cycles

The process known as water thermolysis or thermochemical water splitting, is a hydrogen producing process with water as raw material. This process is divided in two techniques, the one-step process where water is heated in a temperature high enough

(pressure up to 1 bar and temperature over 2500°C [79], [80]) for water molecules to split, while in the thermochemical cycles process, water reacts with different additives, which are then exposed to high temperature, where they dissociate to H₂ and O₂ gases with the substances added recycled. In thermochemical cycles the temperature for the dissociation of these elements is significantly lower than the temperature in one-step thermolysis, leading to decreased energy demands and increase in the overall efficiency [81], [82].

One-step thermolysis is based on a simple principal. Water is exposed to an enormous amount of heat, which thermodynamically leads to water molecule schism, producing hydrogen and oxygen (Eq. (15)) [82]. Although in order to fully separate water molecules, temperature must exceed 4,000°C, which consequently leads to excessive energy demands to power this process. This process can be powered by renewable, nuclear, biomass and thermal heat sources [82]. However, the management of this process is complicated, as the materials capable of enduring temperatures that high, also have a high cost. Moreover, when the temperature is high enough to decompose water, the gas product is a mixture of H₂ and O₂, tending to reform water at a gradual temperature drop [82]. Thus, due to its complications, this method is not taken into consideration for large scale applications, with the literature focusing on thermochemical multi-step cycles, in order to overcome the one-step thermolysis obstacles.



Thermochemical cycles are processes based on the principle of thermolysis. These processes consist of multiple chemical reactions, with the first reaction involving water reacting usually with metal oxides, leading to products which in their dissociation release O₂ and H₂ under high temperatures (500-2000°C), with a value notably lower than one-step thermolysis [79], [82]. The extensive research on these methods has led to the study of approximately 3000 cycles, with only a few of them capable of meeting large scale hydrogen production needs [80]. Recent studies focus on sulfur-iodine, zinc-sulfur-iodine, cooper-chlorine and magnesium-chlorine multi-step processes, as they pose as the most promising reaction chains.

Sulfur-Iodine (S-I) cycle developed in USA in 1970s, immediately capturing the interest of researchers in eastern Asia, becoming the most studied thermochemical hydrogen production process [79], [82], [83]. This thermochemical cycle consists of the 3 reactions given below.





The concept of this hydrogen production method is depicted in Figure 4.6. The first reaction, also known as Bunsen reaction, occurs as an aqueous mixture of SO_2 and excess I_2 reacts, producing heat and leading to the formation of two immiscible acids at ambient conditions. These acids are separated in two different chambers, with HI exposed to temperatures as high as 400°C and H_2SO_4 at temperatures close to 900°C , where the bonds of the acids collapse, to form H_2 and O_2 alongside with the regeneration of the reactants of the initial reaction [83]. The heat, in order Eq (16) and Eq (17) to take place, has been produced typically in High Temperature Gas-cooled Reactor (HTGR), with multiple other patents capable to cover the heat needs [84], as Modular Helium Reactor (MHR), Very High-Temperature Reactor (VHTR), Supercritical water-cooled nuclear reactor (SCWR) and others.

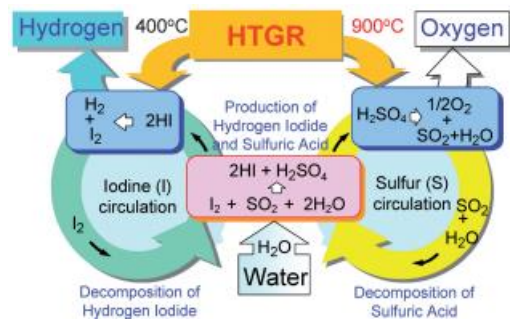


Figure 4.6 Operational principle of S-I cycle [85]

Theoretically the reactants (besides H_2O) are inexhaustible, are being regenerated along the reaction chain, however, it is possible for the Bunsen reaction products to react, forming sulfur or hydrogen sulfide, which can potentially restrict the process by clogging the equipment. Consequently, excess concentration of Iodine, with concentration even eight times greater than the stoichiometric, acts as a barrier between the acids separating them into light and heavy phases, minimizing the potential of unwanted reactions. The light phase liquids as H_2SO_4 and H_2O are separated from the heavy phase liquids as HI, I_2 and H_2O . The collected liquids are purified, reformed to the initial reactants with additional O_2 and H_2 sidetracked, consequently purifying the reactants.

The separation of the substances is not the only challenge this method is facing. The highly corrosive H_2SO_4 product, leads to demand of durable materials. Moreover, heat must be combined with the existence of a catalyst, as H_2SO_4 has restricted kinetics limiting its decomposition [82]. Additionally, HI dissociation is a reversible reaction, making the simultaneous separation of H_2 and I_2 products a necessity. As a result, the

application of a membrane able to endure the acidic environment has been studied, trapping H_2 and I_2 , increasing the production rate from the decomposition of the acid.

The development Zinc-Sulfur-Ionic (Zn-S-I) thermochemical water dissociation method, is based on the same principle with S-I cycle, with the difference of the simultaneous production of CO. This cycle consists of 6 reactions (Number 1-3), their equations are as follows.

Table 2.3: Zn-S-I cycle steps [83]

Number	Equation
1	$2H_2O + SO_2 + I_2 \rightarrow H_2SO_4 + 2H$
2	$2HI \rightleftharpoons I_2 + H_2$
3	$H_2SO_4 \rightarrow H_2O + SO_2 + \frac{1}{2} O_2$
4	$Zn + CO_2 \rightarrow ZnO + CO$
5	$2HI + ZnO \rightarrow H_2O + ZnI_2$
6	$ZnI_2 \rightarrow Zn + I_2$
7	$ZnI_2 + CO_2 \rightarrow ZnO + CO + I_2$
8	$SO_2 + 2H_2O \rightarrow H_2SO_4 + 2H^+ + 2e^-$
9	$I_2 + 2H^+ + 2e^- \rightarrow 2HI$

The Zn-S-I (Table 4.3) cycle consists of the S-I cycle, under the same condition parameters, with the addition of 3 more reactions (number 4-6) in order to recycle the initial reactants and produce CO. Zinc oxidation is the outcome when Zn is paired with CO_2 (number 4) in roughly $780^\circ C$, releasing CO as a final product and ZnO. Then, ZnO reacts spontaneously, when paired with remaining HI (number 5) in ambient conditions. The outcome of number (5) is a mixture of ZnI_2 and H_2O , which later is dehydrated forming ZnI_2 crystals, which are decomposed to approximately $740^\circ C$, closing the process cycle, reforming the initial reactants [83], [86].

As this cycle is an enhanced version of S-I cycle, the same challenges have to be encountered, where additional obstacles surface with the existence of 3 more reactions. Additional equipment is required, as more reactions and more complex processes take place. Moreover, the low yields of HI and ZnI_2 conversion, indicate the need of catalysts, primarily noble metals [86]. As a result, the overall investment capital and operating cost increases significantly. Consequently, modified cycles have been studied, as an open cycle, five-step cycle combining reactions number 4 and 6 to form 7 and lastly, electrochemical five-step cycle, which has captured the attention of the researchers as a concept [86]. An electrochemical reactor substitutes the conventional one, leading to higher production rate without the need of excessive concentrations of reactants [87]. The anode and cathode reaction are written in detail in reactions number 8 and 9 respectively.

Alongside with S-I cycle and its variants, the Cooper-Chlorine cycle (Cu-Cl) is under intense research. The reduced heat needs of this process, offers a flexibility on the potential energy sources, which can power this process. Multiple Cu-Cl pathways achieve water dissociation, with the number of steps varying from two to five [82]. As a result, the operational cost and processes complexity correlate with the number of reactions taking place in the thermochemical cycle.

Table 4.4 Cu-Cl cycles reactions [82]

Number	Equation	Temperature (K)
1	$nH_2O(l) + 4CuCl(s) \rightarrow 2Cu(s) + 2CuCl_2 \cdot nH_2O(aq)$	350
2	$H_2O(g) + 2CuCl_2 \cdot mH_2O(s) \rightarrow CuO \cdot CuCl_2(s) + HCl(g) + mH_2O(g)$	650
3	$H_2O(g) + 2CuCl_2(s) \rightarrow CuO \cdot CuCl_2(s) + 2HCl(g)$	673
4	$H_2O(g) + 2CuCl_2 \cdot nH_2O(s) \rightarrow \frac{1}{2}O_2(g) + 2HCl(g) + 2CuCl(l) + nH_2O(g)$	823
5	$H_2O(g) + Cl_2(g) \rightarrow \frac{1}{2}O_2(g) + 2HCl(g)$	1073
6	$2Cu(s) + 2HCl(g) \rightarrow H_2(g) + 2CuCl_2(l)$	723
7	$2CuCl(s) + 2HCl(aq) + nH_2O(l) \rightarrow H_2(g) + 2CuCl_2 \cdot nH_2O(aq)$	473
8	$2CuCl_2(s) \cdot nH_2O(g) \rightarrow CuO \cdot CuCl_2(s) + 2HCl(g) + (n - 1)H_2O(g)$	650
9	$CuO \cdot CuCl_2(s) \rightarrow \frac{1}{2}O_2(g) + 2CuCl_2(l)$	800
10	$2CuCl_2 \cdot nH_2O(g) \rightarrow 2CuCl_2(l) + Cl_2(g) + nH_2O(g)$	773
11	$2CuCl_2 \cdot nH_2O(aq) \rightarrow 2CuCl_2 \cdot mH_2O(s) + (n - m)H_2O(g)$	550

Table 4.5 Cu-Cl cycles [82]

Cycle	Reactions included
Two-step cycle	4-7
Three-step cycle a	4-6-1
Three-step cycle b	7-9-8
Three-step cycle c	5-7-10
Four-step cycle a	1-6-9-8
Four-step cycle b	3-7-9-11
Five-step cycle	2-6-9-1-11

The cost of the application of different thermochemical Cu-Cl cycles (Table 4.4 & Table 4.5) is relatively the same. However, studies conducted on these cycles, prove that cycles with less steps restrict solid deposition, maintaining efficient heat and mass transfer. However, higher temperature values are required, and the separation

process is complex [83]. The efficiency of the processes depends on the power source, but in general an increase in both temperature and flow rate, increases the efficiency of every cycle. Another notable aspect of these cycles is the extensive literature on this topic, proposing groundbreaking methods in order to provide enough heat for these systems, even with heat recovery from industrial systems as iron furnace [88].

Another low-temperature thermochemical hydrogen production method is the Magnesium-Chlorine cycle (Mg-Cl) shown in Table 4.6 & Table 4.7, with competitive characteristics among other thermochemical cycles. As in Cu-Cl cycle, the decreased heat demand, widens the range of the potential power sources, that this process can be paired. Multiple Mg-Cl cycles have been developed for hydrogen production, with their equations written in detail in the table below.

Table 4.6 Mg-Cl cycles reactions [83]

Number	Equation	Temperature(°C)
1	$MgCl_2(g) + H_2O(g) \rightarrow MgO(s) + HCl(aq)$	450-550
2	$MgO(s) + Cl_2(g) \rightarrow MgCl_2(s) + \frac{1}{2} O_2(g)$	450-500
3	$2HCl(aq) \rightarrow H_2(g) + Cl_2(g)(1.8V)$	70-90
4	$2HCl(g) \rightarrow H_2(g) + Cl_2(g)(1.4V)$	70
5	$2MgCl_2(g) + 2H_2O(g) \rightarrow 2MgOHCl + 2HCl(aq)$	240-300
6	$2MgOHCl + Cl_2(g) \rightarrow 2MgCl_2(s) + H_2O(g) + \frac{1}{2} O_2(g)$	450
7	$MgCl_2(g) + H_2O(g) \rightarrow MgOHCl + HCl(aq)$	280
8	$MgOHCl \rightarrow 2MgO(s) + HCl(g)$	450

Table 4.7 Mg-Cl cycles [83]

Cycle	Three-step a	Three-step b	Four-step a	Four-step b
Reactions	1-2-3	5-6-3	7-8-2-3	7-8-2-4

This process utilizes heat and electricity and water. It consists of 4 types of reactions, hydrolysis reactions (number 1 & 5 in Table 4.6), chlorination reactions (number 2 & 6 in Table 4.6), decomposition reaction (number 8 in Table 4.6) and HCl electrolysis (number 3 & 4 in Table 4.6). According to Mehrpooya et al. [83] energy and exergy efficiency ratios vary from 16.3% to 50.3% and 17.6% to 63.7% respectively. These ratios depend on the power sources and the thermodynamic cycles applied to the system (typically Rankine).

According to Ozcan et al. [89] the Mg-Cl cycle does not involve the typical problems of other thermochemical cycles. Heat requirements for this process are reduced to approximately 400-450°C from other thermochemical hydrogen production cycles. The lower heat demands of this process, leads to a plethora of potential equipment

materials, alongside with the potential utilization of nuclear waste heat to power the system, lead to a decrease in the overall cost of the system [89].

Moreover, HCl electrolysis plays a significant role in this process. Hallet Air Products had experimentally studied hydrogen production through HCl electrolysis, with exceptionally low hydrogen production yields. In Mg-Cl cycle however, the reaction mechanics of HCl electrolysis are enhanced, as the consumption of chlorine gas in O₂ production reactions (reaction number 2 & 6 in Table 4.6), pushes the electrolysis equilibrium towards HCl dissociation, preventing it from reforming. The electrolysis step is a groundbreaking factor, especially with a membrane cell application, removing anhydrous HCl (number 4) with efficiency close to 100% [89], [90].

In conclusion, hydrogen production from thermochemical cycles is a process capable of potential industrial applications. The characteristics of multiple hydrogen production cycles have been studied, with reviews evaluating the efficiency of the energy and exergy of this process, the overall cost, and the power needs of the processes. According to Mehrpooya et al. [83], variations of the S-I cycle are the highest energy and exergy efficiency, a result correlated by the greater volume of literature surrounding this method, when compared to others. However, the overall cost of the S-I cycles is competing with this of Cu-Cl, with the second cycle only providing a hundredth of the production rate of the first cycle.

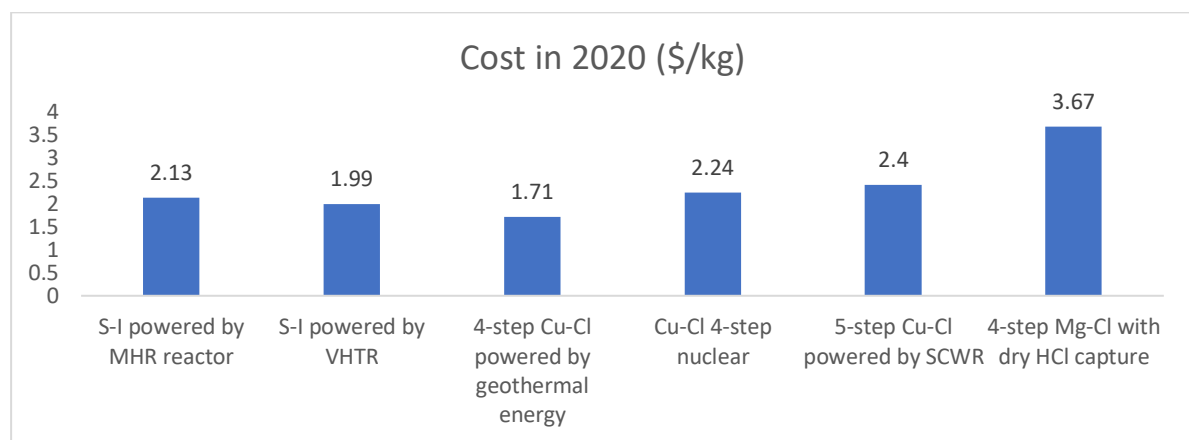


Figure 4.7 Cost comparison of different thermochemical cycles [83]

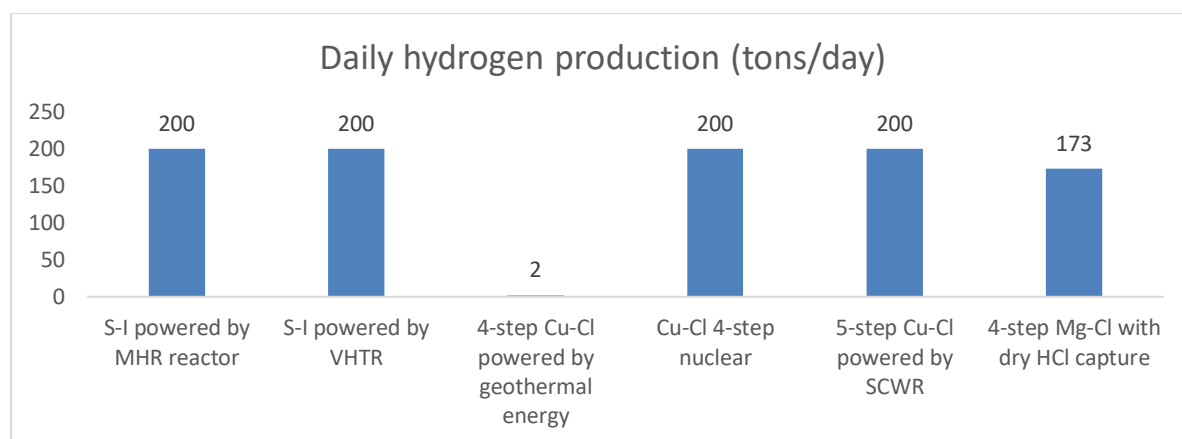


Figure 4.8 Hydrogen production rate comparison of different thermochemical cycles [83]

4.1.3 Photolysis and photo-electrolysis

Other interesting pathways for hydrogen production are those associated with solar energy. The inexhaustible solar energy found in the surface of earth can be utilized to dissociate water, producing hydrogen and oxygen, with two methods. The first one direct photolysis and the second one is photo-electrolysis.

In water photolysis or photodissociation, water molecules exposed to ultraviolet radiation, can theoretically dissociate a single water molecule, when exposed to 285.57kJ. Beside the fact that this method is direct and it only needs light, it is characterized by low efficiency, with photocatalyst, micro-organisms and dyes studied, aiming to improve the overall efficiency of the process [91].

Photo-electrolysis on the other hand is a promising renewable energy hydrogen production method, merging electrolysis operating principle with photovoltaics photon absorption. Two semiconductors are combined to form a p-n junction with a permanent electric field, which when it gets exposed to photons with a greater or equal bandgap compared to this of the material, an electron hole is formed to the junction. The deficit of electrons on the positive end, assisted by a complimentary voltage, leads to oriented electron movement, closing a circuit. When this configuration is immersed in an aqueous solution, a photon powered electrolysis takes place [81].

4.2 Biomass

Biomass is a hydrocarbon material, formed from organic wastes, which can be exploited to produce energy, with the powering of basic household needs, except electricity, being its most common application. Processes to extract hydrogen from biomass have been developed over the years, based on two different hydrogen production principles [81], [92]–[94]. The first is thermochemical processing, where biomass is exposed to high temperatures under certain conditions, releasing H₂. The second is based on biological process, utilizing enzymes.

Thermochemical hydrogen production from biomass is divided in 3 techniques. Gasification and pyrolysis are the two methods primarily studied, with biomass liquefaction mostly being overlooked, due to low hydrogen yield and operating conditions (250-330°C and 5-20 MPa in absence of ambient air) are too demanding for industrial application.

Pyrolysis of biomass takes place in temperatures ranging between 380-530°C, and pressure of 0,1-0,5 MPa without the presence of ambient air. When biomass is exposed to these conditions, is converted into oils, gases and charcoal [92]. The speed of the transition from ambient to operating conditions, combined with phase instability play a significant role on the production yields, with rapid transitions favoring the production of H₂, CH₄, CO₂ and CO gases, with restricted tar, oils and solid byproducts. Biomass is a versatile energy producing compound, with multiple potential catalysts capable of enhancing the production. With further processing hydrogen yields can overcome 90% [92].

In biomass gasification, like in pyrolysis, biomass molecules are exposed to heat, with the presence of oxygen being the main difference. Biomass of moisture percentage below 35%, is exposed to temperatures higher than 730°C, where particles are getting oxidized with the presence of oxygen, forming charcoal with is latter reduced to a mixture of gases containing H₂, CH₄, CO₂ and CO. Besides the main products however, light and heavy hydrocarbons as tar are produced, alongside with ash. These byproducts can obstruct the production of hydrogen. The formation of tar can form polymers or aerosols inside the reactor restricting hydrogen from being released. Various additives have been examined, which can eliminate its formation, or even enhance the formation of hydrogen. Ash accumulation through the process, can degrade the equipment, decreasing the efficiency of the process. When moisture content exceeds 35%, the method differs, as water at these temperatures is supercritical. The violent conditions, biomass is gasified rapidly, gases are formed rapidly, achieving gasification ratio up to 100% and hydrogen makes up to half of the total volume of the gas mixture produced [92]. The cost of the hydrogen produced cost varies between 1.77-2.5\$/kg [81].

4.3 Bio-based

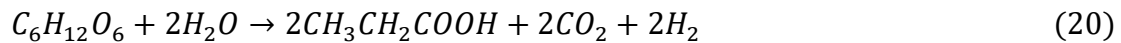
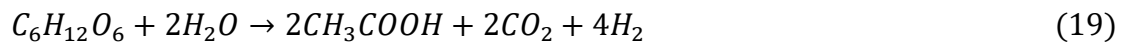
Among alternative hydrogen production methods, biological hydrogen obtained from biomass, stands out as a financially competitive and environmentally friendly technique. Microorganisms capable of splitting water and carbohydrates are applied, with hydrogenase and nitrogenase enzymes releasing hydrogen. These methods can produce H₂ via three routes: (i) direct & indirect bio-photolysis, (ii) photo-fermentation and (iii) dark-fermentation [95], [96]. These methods are complex, depend on multiple parameters, with the extensive literature available on these methods is incapable of proving their availability for large scale hydrogen production. However, the ability of utilizing waste to produce a methanation reactant is noteworthy.

4.3.1 Direct and indirect bio-photolysis

Direct and indirect bio-photolysis microorganisms are powered by light, with the only difference that direct bio-photolysis separating hydrogen molecules directly [95], when the indirect alternative cultivates organic compounds which are later converted into hydrogen, while hydrogenase and nitrogenase content of the microorganisms and anaerobic conditions are the common parameters. In direct bio-photolysis cyanobacteria and green algae are cultivated in the largest possible area, producing hydrogen and oxygen with light absorption. Oxygen production is directly correlated with the efficiency of these methods, as higher than 0.1% content of this gas inactivates the enzymes, thus restricting the hydrogen production [92]. A cost estimation per kilo of product is 2.62\$ according to Ni et al. [92], with potential substitution of oxygen with argon in order to avoid the enzyme deactivation, increasing the operating cost and consequently the product cost significantly [95]. In indirect bio-photolysis, water, light and carbon dioxide react with microorganisms to produce glucose dextrose (C₆H₁₂O₆) and oxygen, with the first is divided in hydrogen and carbon dioxide when it illuminated with the presence of water. Microalgae and cyanobacteria, which are responsible for hydrogen production are not exposed to oxygen in this method, overcoming the oxygen content obstacle. Genetically modified cells are finding application in this method, as they are modified to store more glycose, which effects positively the hydrogen yields [95]. An approximate estimation regarding the hydrogen cost is 1.31\$/kg [92]. However, this technique is not yet mature for any application, requiring further research [95]. The common disadvantage of these methods is the low efficiency of light conversion and hydrogen yield.

4.3.2 Dark fermentation

Under light and oxygen absence, heterotrophic bacteria can ferment organic wastes, producing H₂ and CO₂ gases alongside with volatile fatty acids (VFAs) [97] with the following reactions, which describe the release acetic and butyric acid, dominating the process [98].



This hydrogen production method depends on multiple parameters, with extensive literature examining and experimenting on the conditions and bacteria cultures taking place. With the chemical reactions above taking place, microorganisms reduce organic waste through oxidization, with the reactor maintaining a neutral electron load through hydrogen evolution. According to Akhalgi et al. [95] the *Clostridium* sp., *Enterobacter* sp. and *Bacillus* sp. are the most commonly implied bacteria in this process, with every bacteria culture following a different hydrogen production pathway, leading to various hydrogen yields, and byproducts. In order to exploit the most versatile waste mixtures, multiple bacteria cultures can be merged in order to maximize the hydrogen production yields and make the technology financially attractive. In terms of hydrogen yield achieved, sucrose and acetate have achieved the highest molar ratio of hydrogen to raw material, which however leads to increased operational costs. At last, minerals and trace metals can act as catalysts and enhance hydrogenases activity, while pH and temperature are crucial parameters for the process, correlated with the environment that the cultures live and thus with their efficiency. Optimal pH ranges between 5.5 and 6.5, while temperature conditions are separated to 3 categories: mesophilic (25-40°C), thermophilic (40-65°C), hyper-thermophilic (>80°C), with the first mostly implied due to restricted energy demands and the second as the most efficient in terms of hydrogen production [95], [97], [99].

4.3.3 Photo fermentation

Photo fermentation takes place in anaerobic environment with the presence of light. Photosynthetic non-sulfur bacteria (PNS) convert VFAs or carbon compounds to hydrogen and CO₂. According to Akhalgi et al. [95] *Rhodobacter* spheroids, *Rhodobacter capsulatus*, *Rhodobacter sulfidophilus*, *Rhodospseudomonas palustris* and *Rhodospirillum rubrum* are some of the PNS bacteria that can be used to photo-ferment organic waste. Through the bacteria nitrogenase and hydrogenase bacteria catalyze the process, leading to hydrogen production.

The process starts with the organic compound oxidization to CO_2 , hydrogen cations and electrons which are evolved to hydrogen through nitrogenase. Nitrogenase typically metabolizes N_2 , leading to NH_3 production and H_2 as a byproduct, with N_2 absence however, nitrogenase compliments hydrogenase, which catalyzes the formation of hydrogen in protons and electrons [95]. According to Argun et al. [97] optimal pH range is 6.8-7.5 and temperature conditions to be mesophilic (more especially ranging between 31-36°C), with light wavelengths between 400-1000 nm and with light intensity from 6 to 10 klux. The maximum theoretical photochemical light efficiency is 10%, with experiments able to achieve as high as 9.3%, while hydrogen production can reach up to 80% of the theoretical yield. Organic acids are responsible for high conversion efficiency, which leads to a preference of food industry wastes as a raw material, which also come with a low cost.

4.4 Hydrogen from fossil fuels

Current hydrogen production is based almost entirely on dissociating hydrocarbons. Almost half of hydrogen produced is a product of methane reforming, while coal gasification and partial oxidation of oil make up the rest of hydrogen production. Globally only 4% of hydrogen is derived from sources other than fossil fuels. The production of this gas from fossil fuels is highly efficient and with a luring cost for the industry. A detailed graph of the hydrogen production partition is depicted belon in Figure 4.9.

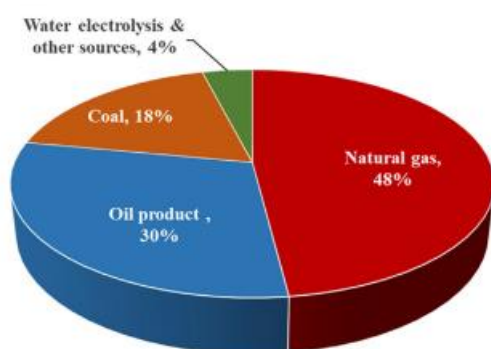


Figure 4.9 Main sources for hydrogen production [82]

The implementation of such methods on the other side, have carbon oxides as byproducts and most commonly apply Sabatier reaction in reverse. Thus, the

examination of such methods, aiming to intergrade them in a potential methanation plant is contradicting with the concept of CCU technologies. A brief analysis concerning these methods is taking place in the paragraphs below, providing a holistic view of the current state of hydrogen production, while setting the threshold of the product cost renewable sources have to comply in order to become more competitive.

As previously mentioned, NG is providing the majority of hydrogen across the globe. Methane can be reformed with steam in a highly energy consuming process, exposed to temperatures between 800-1100°C and catalyzed by Ni-based materials (reaction number 1 & 2 in Table 4.8). Moreover, it can be partially oxidized when exposed to oxygen in temperatures as high as 650-1500°C, releasing H₂ in an exothermic reaction (number 3) without a catalyst needed. These two techniques can be combined with the second providing heat loads to the first, leading to a cycle called autothermal reforming (ATR). Moreover, NG can be dissociated, releasing H₂ and solid carbon, in a reaction called methane pyrolysis, also known as methane cracking. This reaction has been studied in three different directions, the thermal and plasma pyrolysis, which are non-catalytic processes, and catalytic pyrolysis. In catalytic pyrolysis, the reaction can be triggered in temperatures lower than 500°C, however temperatures above 800°C achieve higher efficiency. In thermal pyrolysis, NG is exposed to temperatures above 700°C, with higher yields reported above 1000°C. At last plasma pyrolysis occurs at extreme conditions, above 2000°C (number 4) [53], [81], [82], [100], [101].

Besides methane, coal and oil products play a significant role in the hydrogen production industry. Coal gasification (GC) utilizes both mined coal (surface gasification) and unmined coal (underground gasification). Grinded coal is first exposed to air, releasing CO₂ (number 5) and then is exposed to steam, leading to H₂ formation (number 6). At last, oil products can be oxidized in a similar process as methane oxidation, with the only difference being the higher temperatures (1200-1500°C) their oxidization reaction (number 7) takes place [81], [82], [100], [102].

Table 4.8 Hydrogen producing reactions with fossil fuel reactants, their efficiency rates and the cost of the produced hydrogen [81], [82], [100], [102]

Process	No.	Reaction	Efficiency	Cost (\$/kg)
Steam Methane Reforming (SMR)	1	$CH_4 + H_2O \rightarrow CO + 3H_2$	70-85%	2.08-2.27
	2	$CO + H_2O \rightarrow CO_2 + H_2$		
Partial Methane Oxidation (POM)	3	$CH_4 + 0.5O_2 \rightarrow CO + 2H_2$	55-75%	1.34-1.48
Coal Gasification (CG)	4	$C + O_2 \rightarrow CO_2$	60-75%	1.63-1.34
	5	$C + H_2O \rightarrow CO + H_2$		
Partial oil product oxidation (POX)	6	$C_nH_m + 0.5nO_2 \rightarrow nCO + 2mH_2$	63-72.8%	0.84
Methane Pyrolysis	7	$CH_4 \rightarrow C + 2H_2$	14-91%	2.2

4.5 Hydrogen pallet

Traditional hydrogen production technologies are based on methane pyrolysis, oil product oxidation and coal gasification, with these technologies often referred as grey hydrogen. As mentioned in Figure 4.9, 96% of global hydrogen production comes from fossil fuels. These technologies have a heavy toll at the environment, with large amounts of carbon oxides released annually. Countries with large oil or carbon reserves, like China, meet their hydrogen needs with conventional methods. With environmental concerns, about greenhouse gases like carbon oxides, growing globally and with nations committed to neutralize their carbon footprints, H₂ has to be obtained without the burden of CO₂.

Green hydrogen principal is carbon neutral H₂ production, as the process powers typically water dissociation or biogas processes, solely from renewable energy sources. Green hydrogen can act as the trojan horse for excess energy long-term storage through Power-to-Gas (PtG) projects [103], pairing water-based hydrogen production with wind, solar, hydro, biomass and geothermal energy sources, often paired with nuclear energy [104]. However green hydrogen production correlates with an increase in demand for renewable energy production, as excess renewable energy alone, cannot substitute the energy demands for hydrogen production, which are met by fossil fuels. Replacing all grey hydrogen production globally would save annually 830 million tons of CO₂ from being released to the atmosphere, requiring 3,000 TWh/year from new renewables [105], 500TWh/year less than 2020 European power demands [106]. The assumption of a complete grey hydrogen substitution from green hydrogen in the near future is utopic, however multiple countries motivate their industry to refrain from traditional energy sources, increasing carbon tax, with the largest CO₂ producer globally, China aiming to produce 10% of their overall system energy from hydrogen, with 70% of it being produced from renewable sources. For the transition from grey to green hydrogen take places, blue hydrogen will be the crucial link between these technologies, providing a carbon-free yet sufficient production.

Blue hydrogen technologies are the evolution of grey hydrogen, as they are based on fossil fuels with integrated carbon capture utilization and storage (CCUS) technologies. The implementation of these technologies is a crucial step towards the transition to completely carbon-free methods [45]. However, a plant can be considered blue if there is a carbon capture installation, without the capturing efficiency playing a role. The efficiency rates vary from 65-85%, even 90% according to some reports [45], [107], considering however the energy consumed by the capture facility decreases the overall CO₂ captured when powered non-renewably. Blue hydrogen has attracted attention from multiple nations, with EU subsidizing CCUS with 587M euros. The toll

of CCUS application in hydrogen production, however, lead to a decrease in overall production efficiency, with SMR efficiency for example being decreased 5-14% [45].

Another option to power hydrogen production, is the overlooked nuclear energy, labeled as purple hydrogen. Nuclear energy has a notorious reputation, connected with almost clean and efficient power production alongside with tragic accidents, permanently marked in modern history. Besides its reputation, it is still a viable option for multiple nations as Russia and China, to power water electrolysis, thermochemical and thermoelectrochemical processes, or even utilize the escaping heat from the plant for fossil fuel conversion to H₂[45], [104], [108]. Nuclear energy can complement intermittent renewable sources, stabilizing the energy input to each process [104], [108].

Additional colors standing out in the hydrogen spectrum are turquoise, yellow and aqua hydrogen. Turquoise hydrogen is H₂ release from methane pyrolysis with the carbon produced as a byproduct, divided into coke (150-400 €/t), black carbon (500-1000 €/t), filaments (~1M €/t) and activated carbon (1500-1800 €/t). These products can be reapplied in industry without releasing CO₂. Yellow hydrogen is produced with energy consumed from the grid, mostly through electrolysis. This method releases CO₂, yet it is preferred from grey, in terms of overall pollution. However according to a report with research conducted on the electricity mix of 2008 in Denmark, a high operating cost was noted [109]. At last, a state-of-the-art method was developed from University of Calgary in Canada, and Proton Technologies which first was applied in February of 2021, ejecting pure oxygen to bitumen and oil reservoirs trapped underground. The in-situ gasification of bitumen is conducted under a complex system of reactions, which is triggered by an exothermic reaction caused by oxygen ejection. The heat produced separated oil from water, releases H₂ without the burden of CO₂ [46]–[48].

4.6 Hydrogen storage and transportation

For CO₂ methanation to take place, sufficient hydrogen supply and storage must be taken into consideration. The means applied can directly affect the capital investment, the operating cost and the production rate of the methanation plant.

Hydrogen storage is divided into three categories, with each category being characterized by the conditions and phases H₂ is stored. It can be stored compressed in gas phase, liquified in cryogenic conditions or stored in materials. Each method besides the different conditions that H₂ is stored, is also described by safety, storage cost, volumetric ratio and energy consumed to store hydrogen.

The most popular storage technique is compressing hydrogen in vessels. Four distinct types of vessels have been studied, with varying structures, able to store the gas under different pressure values, hence different volumetric ratios. The first and most common type of vessels is made entirely by metal, usually aluminum or steel, capable of withstanding up to 50 MPa of pressure. This design is the heaviest among compressed hydrogen storage vessels, with poor mass storage efficiency, while achieving the lowest cost. The second type of vessels consist of steel reinforced cylindrically with fiber resin, capable of maintaining immense pressure amounts, thus bearing the highest volumetric ratio. The cost of this design is increased by half, with overall weight decreased 30-40%, compared to the first type of vessels. Another type has vessels are fully constructed by fiber, typically carbon fiber, reinforced by metal. In this design, the enclosed metal relieves only 5% of the total mechanical load, with fiber substituting the majority of metal, significantly lowering the weight of the structure, weighting almost half of the previously mentioned vessel. This vessel can withstand pressure up to 45 MPa, incapable of maintain structural integrity for values greater than 70 MPa. The overall cost is elevated, being as expensive as three fully metal vessels. The last type of vessels is fully composite, as high-density polyethylene substitutes the metal skeleton of the previous design, leading to a nonporous and extremely light design and a hefty price. This composition can store hydrogen at pressure up to 1000 bar [110], [111].

Another technology developed to store H₂, is its liquefaction in cryogenic temperature of -253°C, with density of 70kg/m³ at 1 bar. Gas hydrogen gets compressed and cooled, in accordance with Linde cycle, followed by a an enthalpic Joule-Thompson expansion, becoming a liquid. The liquid is stored in a vessel bearing an insulating layer, reassuring that a certain temperature is maintained. Energy content loss equals 40%, four times as much as in compression technologies, with potential obstruction of the equipment by the extreme conditions. However, this method is safer than compression, as hydrogen can explode only upon ignition [112], [113]

Other technologies utilize materials which can chemically and physically absorb hydrogen. The solid materials used are usually found in powder form, thus must reformed so hydrogen can be embedded efficiently. The materials responsible for hydrogen storage takes up the whole tank, alongside with a heat exchanger responsible for manipulating the conditions of the chamber, whether charge or discharge of the material takes place [111], [113].

In chemical processes, hydrogen reacts with the material, thus getting intergraded in the structure. Metal hydrides display good characteristics for such applications, with liquid organic hydrogen carriers (LOHCs) also being considered by researchers, as they can carry H₂ in ambient conditions without the burden of carbon production.

However, LOHCs are incapable of carrying large amounts of H₂. The most vital parameters of these processes are cost, overall tank weight, operating temperature, charge and discharge kinetics and the presence of unwanted gases being released, adulterating hydrogen [111], [113].

Physical means of storage consist of porous materials where hydrogen adhere. These techniques show a great potential in terms of capacity and safety. Additionally, the high surface area, combined with good process kinetics, low binding energy and cost are making these methods competitive. On the other hand, thermal management issues, weight of the configuration and the density of the hydrogen stored, are some parameters that must be studied, in order for these methods to find large-scale applications. The materials with the greatest potential for physical hydrogen storage are MOFs, carbon porous materials and zeolites [111], [114].

Beside storage, the methods of transportation of this energy dense gas must be examined, in order for a methanation plant to be supplied sufficiently. Hydrogen transportation is vital for a methanation plant, influencing the operating cost of the plant directly, depending on the mean used. Different means of transportation are used, depending on the transportation network characteristics. For distances greater than 1,500 km, gas hydrogen carrying pipelines are the most effective option for terrestrial transportation [114], while seaborne transportation of liquid hydrogen can serve the intercontinental H₂ trade. Giacomazzi [115], offered tanker designs, capable of transporting liquid H₂ as early as 1989. Moreover, another onshore transportation method, is the transportation of hydrogen gas, compressed under high pressure, stored in tube trailers. Similar methods have been applied to serve mass transportation of other gases, hence there is experience considering the operating principle and safety regulations. In addition, this method has the lowest gas losses, while having the highest safety risk [113]. The options that minimize safety concerns are the methods transferring hydrogen absorbed from materials, which however come at a high cost and transfer significantly lower hydrogen quantities [111].

Table 4.9 Hydrogen transportation methods, their characteristics and costs [111], [113]

Hydrogen transportation	Pressure	Temperature	Quantity	Cost (\$/kg)
Tube trailers	200-500 bar	Ambient	420-666 kg/tube	2.86
Liquid hydrogen	Typically ambient	-253°C	0.7-4 t/tanker	1.4-2.42
Pipelines	10-20 bar	Ambient	~1000 t/day	2.73

5 CO₂ catalytic hydrogenation to CH₄

The conversion of the CO₂ released abundantly through the exploitation of fossil fuels, into higher hydrocarbons is not a new process. The documentation of the process dates back more than a century. However, the complexity of the process mechanisms has prevented it from finding commercial applications in the past. Currently, the process is being thoroughly studied, as it enables the controlled conversion of a greenhouse gas to CH₄, a useful gas which price is soaring the last years, while avoiding the risks of underground or underwater CCS. This process can be approached through different pathways, with the thermochemical process standing out. Besides that, the type of the reactor and the use of a catalysts is crucial for the efficiency of the reaction with the active metal, support material and promoter combination offering different product yields, requiring different preparation techniques and facing different limitations.

5.1 Methanation methods

The thermochemical hydration of CO₂ to CH₄ has been meticulously studied, posing as the methanation process which potentially has the most effective industrial applications. In a typical thermochemical process, CO₂ and H₂ enter a chamber, in which lies an active catalyst. The reactor is exposed to temperatures ranging between 150-500°C and pressure up to 100 bar, demanding high energy consumption in order for the reaction to be efficiently carried out. This thesis focuses on the thermochemical CO₂ hydration, with the aforementioned reaction thermodynamics revolve around it. However, the literature available expands to the study of other CO₂ methanation techniques, which are worth mentioning [116], [117].

The photosynthesis process is an alternative, capable of reforming CO₂ to CH₄ without the presence of H₂. In this technique, highly purified CO₂ enters a vacuumed reactor, alongside with a metal oxide (ZnO, TiO and others) which is typically in powder or pellet form, suspended in water. After the system is left to settle for a few hours, it gets exposed to ultraviolet, visible or infrared light. When the reaction is conducted in a normal pressure, CH₄ is the only product. The reaction principle is based on the surface excitation mechanism of the catalyst, which is triggered by the light exposure, leading to H₂O dissociation and formic acid formation, which react with hydrogen atoms, releasing CH₄ and O₂ molecules [118]–[120].

Another method that does not require H₂ is the electrochemical CO₂ hydration. In this process, CO₂ dissolves in H₂O, leading to carbonic acid formation as the aqueous CO₂ solution reaches its equilibrium. Then the solution enters the electrolysis cell, which

carries two electrodes coated with an electrocatalyst, where CO₂ adheres and the electric current forces anions and cations to migrate and form methane. This process utilizes electrical energy, is carried out in ambient conditions and is characterized as an easily controlled process [121].

In biological CO₂ hydration, microorganisms are responsible for the production of CH₄ from a CO₂ and H₂ gaseous mixture. The bio-methanation process takes place in ambient conditions and can occur either directly (Eq. (21)) or indirectly (Eq. (22) & (23)).



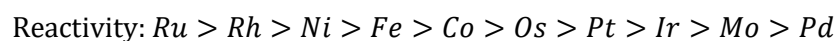
The reactions above are a result of the hydrolysis, acidogenesis and methanogenesis occurrence, which are the outcome of the synergistic action of hydrolytic-fermentative bacteria, acetogens and methanogens. These bacteria typically exist in anaerobic systems, with the reactants being fed to liquid or wet solid medium, while they are constantly stirred, improving the overall efficiency of the process [120], [122].

5.2 CO₂ thermal methanation

Over the years various methanation catalysts have been examined, with extensive literature reviewing different metals, support materials and novel catalysts combinations. The composition of a heterogeneous catalyst usually has an active metal dispersed on a metal oxide supporting material. Recently, structured catalysts and MOFs have gained popularity among the methanation research as they can be designed to deliberately enhance specific aspects of the process. W.K Fan and M. Tahir [120] have classified in detail an overview of the active metals and supports for CO₂ methanation.

5.3 Active metals

Noble and non-noble metals of groups 8-10 in the periodic table, have exhibited great ability of activating CO and CO₂ methanation, as can be seen in the reactivity and selectivity order below. Generalized reactivity and selectivity orders of the metals has been reported over several studies. However, the support materials implemented, the conditions inside the reactor, the type of the reactor and other factors play a significant role on the catalyst activity.



Selectivity: $Pd > Pt > Ir > Ni > Rh > Co > Fe > Ru > Mo$

Kuznecova et al [123] carried out a preliminary rating report, assessing some of the most applied active metals. Four parameters of the metals are assessed, with selectivity, activity and stability rating the operation performance and the cost parameter rating the economic aspect of the catalyst. The performance parameters depend also in various other parameters, however, this evaluation is not considered an authority on the catalyst activity, as it highlights the metals that have the biggest potential to form a high-performance catalyst that find industrial application. The results have Ni as the best overall option, with Fe and Ru closely following and with Co and Mo being the least favorable options.

Table 5.1 Active metals assessment [123]

Catalyst	Catalyst properties			Cost
	Selectivity	Activity	Stability	
Ru	3	5	4	1
Fe	2	4	5	5
Ni	4	3	3	4
Co	1	2	1	3
Mo	5	1	2	2

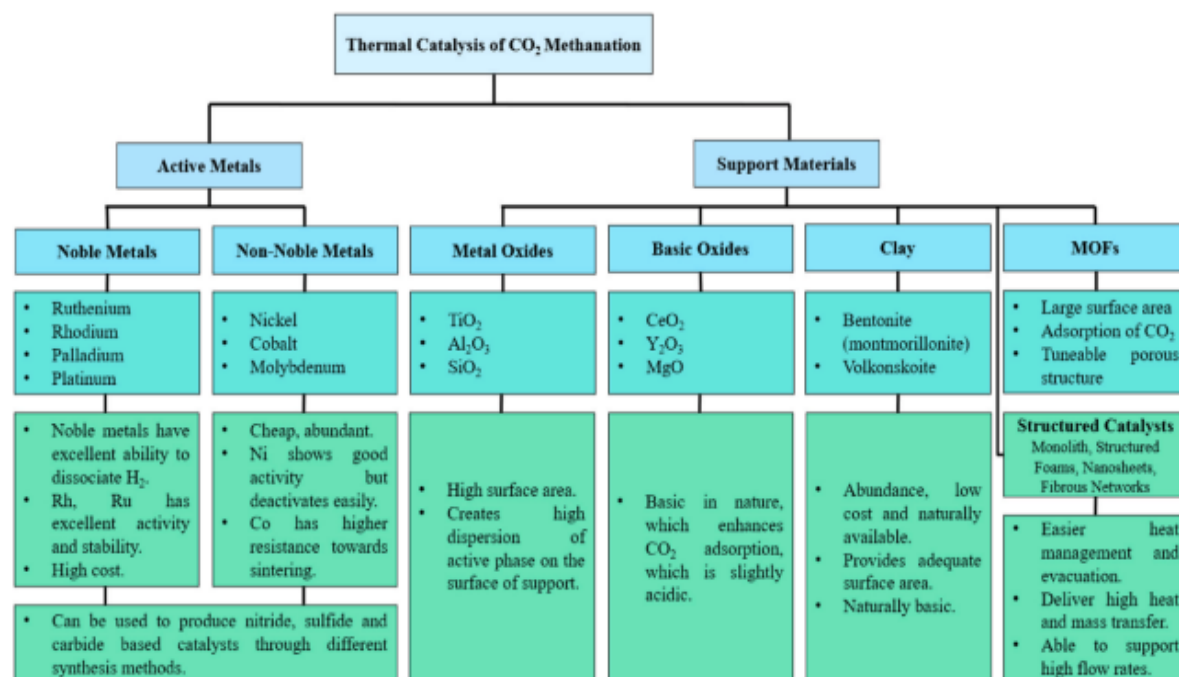


Figure 5.1 Summary of the active metals and support materials for thermal catalytic CO₂ methanation [120]

5.3.1 Noble metals

5.3.1.1 Ruthenium

Ruthenium is a noble metal that stands out as an active metal for CO₂ methanation, due to its properties. It has demonstrated an outstanding catalytic performance, with multiple ruthenium catalysts typically exhibiting the highest activity and methane selectivity, which heavily depend on the metal dispersion. Higher dispersion of ruthenium over the catalyst surface leads to improved methanation result with decreased energy demands [124]. Additionally, catalyst based on this metal show long-term thermal stability, alongside with the ability to accelerate the reaction even in low temperatures and with low loads [5]. Pressure also affects the reaction equilibrium, with a slight increase the pressure value enhancing the reaction kinetics and favoring methane production [125]. Extensive literature is available, studying the effects of ruthenium catalysts. However, the excessively high price of the metal (costs more than hundred times the cost of Nickel) has made the implementation of a Ruthenium based catalyst in commercial plants not feasible [5].

5.3.1.2 Rhodium

Rhodium is a platinum group metal, showing similar properties as ruthenium, characterized by high activity and CO₂ selectivity. Moreover, rhodium catalyst exhibit stability while being able to dissociate H₂ molecules effectively. Another noteworthy ability that rhodium catalyst bare is the product selectivity which can be tuned by the particle size, the element doping and nanoparticle environment [120]. The performance of such catalysts, however, depends on the reactor thermodynamic conditions and the feed composition. Increasing the pressure and reducing the operating temperature the methane yield is increased, a sequence derived from the exothermic nature of the reaction. As other precious metals, Rhodium is an expensive material, with its price limiting its potential for large-scale applications [126] Even though this metal can form highly active methanation catalysts, it has not attracted much attention, with limited literature around the rhodium methanation catalysts.

5.3.1.3 Palladium

Catalysts based on palladium demonstrate the ability to effectively dissociate H₂ molecules and abundantly distribute hydrogen atoms across the catalyst surface. Palladium catalysts have an acceptable activity, stability, and CO₂ conversion rate.

Nonetheless, it has poor properties when compared to other noble metals and when its cost is considered, it is taken out of competition for industrial applications [120], [124]. However, in a section below the effect of multimetallic catalysts will be analyzed where the synergistic action of palladium with other metals is noteworthy.

5.3.2 Non-noble metals

5.3.2.1 Nickel

The catalytic performance of this material combined with the low cost and the plentiful resources worldwide make it the protagonist of CO₂ methanation catalysts. Nickel catalysts have adequate methanation properties, with their main ability being the dissociation of H₂ molecules, which can be combined with a support material which effectively absorbs and activates CO₂ [124]. Wang et al. [127] bibliometric analysis has China as the leading nickel CO₂ methanation catalyst researcher, with 30.2% of the total papers published from Chinese institutes with Chinese Academy and International Journal of Hydrogen Energy intensely researching the catalysts properties. According to the abovementioned analysis, the benefits that nickel catalysts offer is the increase in catalyst specific area, formation of oxygen vacancies and moderately basic sites, which are accountable for improved CO₂ activation and adsorption. Additionally support materials monitor nickel particle size and dispersion, in order to avoid catalyst deactivation due to particle agglomeration while enhancing low temperature methanation yields. At last, resistance to oxidation is improved, leading to higher catalysts stability and higher material circulation. All in all, nickel-based catalysts will be able to industrialize carbon oxides methanation processes, once they can perform in a steady rate after many cycles and bare antioxidant properties without the need of precious metals.

5.3.2.2 Molybdenum

This transition metal has been studied as a complimentary element primarily to nickel and iron catalysts. The first studies classified the catalysts derived from this metal as negligible [128]. However, contemporary reports, have molybdenum as a part of complex structures which provide more than decent yields [129]. According to Hussain et al. [5] molybdenum has exhibited high sulfur tolerance during methanation process, finding hydrodesulfurization and hydrodenitrogenation applications. Additionally, the coexistence of Mo and Ni has reportedly promoted the carbon deposition tolerance of the catalysts, alongside with the prevention of Ni particles sintering [130]. However,

besides the poor performance of the metal by itself, it favors higher hydrocarbons production reducing methane yields [5].

5.3.2.3 Iron

Iron catalysts are another example of an active metal, exhibiting interesting results. Iron based catalysts can endure temperatures higher than 700°C, while it has lower price than the majority of the other metals used [5]. Catalysts solely based on iron as active metal have low reactivity and high methane selectivity, however the formation of alloys containing iron and other metals exhibit intriguing results, providing enhanced CO₂ conversion, CH₄ selectivity and catalyst tolerance over time [131]. On the contrary, iron catalysts are heavily influenced by the CO₂ feed, leading to various carbon species formation, without being capable to maintain their catalytic activity over time due to particle oxidation and surface sintering and coke formation [5], [132], [133].

5.3.2.4 Cobalt

Cobalt is a highly reactive transition metal, with similar or even higher activity than nickel with lower risk of deactivation [120]. The strong adsorption of CO₂ favors its catalytic activity, being better alternative than noble metals cost-wise, although it is more expensive than nickel, thus it is not that practical for large scale applications [116]. Literature extends to its combination with MOFs and organic acids as supports materials, with satisfactory results [120].

5.4 Bimetallic

As mentioned above, many metals showed improved catalytic activity for CO₂ methanation, with the presence of a complementary active metal in the catalyst. Metals such as Fe, Pt, MgO, Al, Co and other complementary metals, have been implied predominantly in already studied Ni catalysts, exhibiting better CO₂ conversion and CH₄ selectivity most of times. For instance, the formation of Ni₃Fe over γ -Al₂O₃ support, can achieve methanation in lower temperatures with higher activity compared to the Ni catalysts [134]. Moreover, cobalt can get integrated easily in the lattice of metallic nickel, while cobalt oxides can alter the electronic properties of Ni catalysts. High Co loading drastically improve the catalyst activity and potentially improve stability [135], [136].

5.5 Reactor design

Reactors are also another crucial part for carbon oxides methanation. The reaction conditions often require high temperatures, which combined with the exothermic nature of the CO₂ methanation can lead to excessive heat being released, thus the primary parameter of the reactor design is the adequate heat management and distribution among the reactor, which is responsible for the integrity of the reactor, to avert the deactivation of the catalyst, the uncontrolled shift of equilibrium or prevent side reactions from taking place. Over the years multiple designs have been developed, some of them capable of commercial applications, others still in the research and development phase. In this thesis, emphasis is given to fixed-bed, fluidized bed, three phase, microreactors, monolith, membrane and sorption enhanced reactors.

Fixed-bed reactors are the most common type of reactors applied to the methanation process. Overall, they bare sufficient exposure of the inlet gases to catalyst molecules even for long periods. There are two types of fixed bed reactors, the adiabatic and the polytropic.

In adiabatic fixed-bed reactors, the inlet gas reacts on the surface of a static catalytic bed. Usually, for high methanation efficiency, a series of adiabatic reactors or a recirculation system is used, with the outlet gas being exposed an intercooling system, feeding the outlet stream to a reactor for further hydrogenation. This process leads to high CO₂ conversion rates, with this type of reactors being considered an affordable solution, capable to manage a high gas hourly space velocity (GHSV) feed. Nonetheless, the formation of hot-spots and poor load management, alongside with the potential demand of multiple reactors in order to achieve satisfactory results are the main problems of this configuration [137].

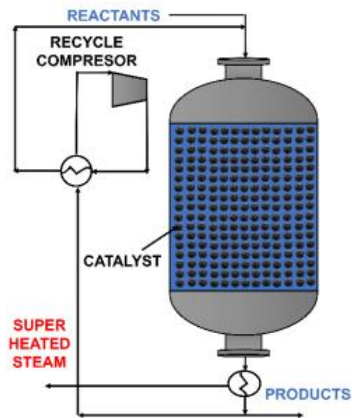


Figure 5.2 Fixed bed reactor [138]

Polytropic reactors on the other hand are based on cooled fixed-bed tubes, with the most common configuration being the multitubular fixed-bed exchanger reactor. This design consists of multiple catalyst carrying tubes, responsible for the hydrogenation of CO_2 , with the rest of the reactor being filled with a cooling medium, for instance oils, water, steam, or molten salts, which are responsible for the heat management. This configuration can carry out high temperature reactions without jeopardizing the integrity of the reactor. This ability, however, is limited to certain temperatures and pressure values, which vary with the medium used, depending on the available capital of the investment. Another limitation is the amount of inlet gas that can be processed, as the tube diameters are usually small. Compared to adiabatic reactors however, multitubular reactors have longer lifespan [138].

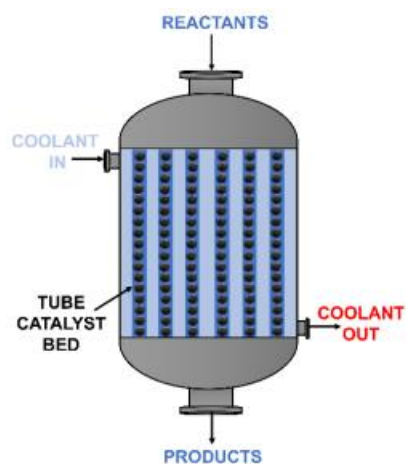


Figure 5.3 Multitubular fixed-bed reactor [138]

Fluidized bed reactor is roughly the reverse design of multitubular reactor. The steam of the reactants flows upwards, fluidizing the catalyst particles, with cooling mean, typically water, circulating inside a tube, extending inside the reactor. The surface of the catalyst practically is maximized, leading to improved efficiency heat exchange and

temperature control, compared to fixed bed reactors. This reactor is susceptible to degeneration due to high speeds of catalyst fluidization; thus, it has limited GHSV.

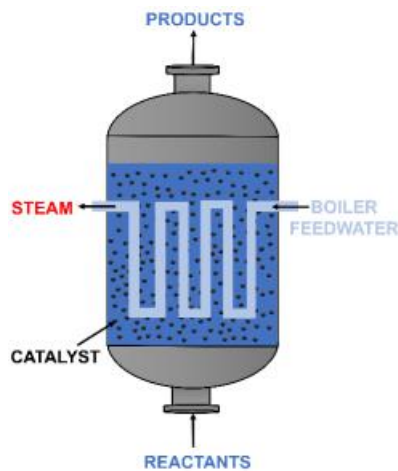


Figure 5.4 Fluidized bed reactor [138]

A reactor which still under development is the three-phase reactor. In this reactor, solid catalyst particles with diameter smaller than $100\mu\text{m}$ are suspended over liquid dibenzyltoluene, with the inert gas steam flowing upwards. The catalyst and the suspension medium are constantly renewed, ensuring the stable isothermal conditions of the reactor. This design is based on the fluidized bed principal, with a complimentary catalyst renewal system and a different fluidizing mean. This reactor, however, is prone to backmixing, dibenzyltoluene decomposition and evaporation, while a catalyst and liquid separation step is mandatory. This configuration favors CO_2 methanation over catalyst that quickly deactivates [138].

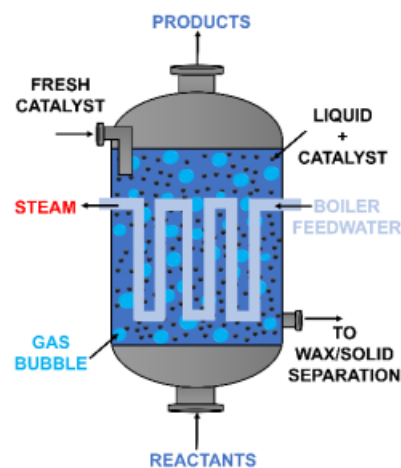


Figure 5.5 Three-phase reactor [138]

A revolutionary concept is the implementation of microreactors for CO_2 hydrogenation. The compact designed microreactors consist of microchannels coated or filled with catalyst, with diameter from $50\text{-}5000\mu\text{m}$. The architecture of this heat exchanger and reactor hybrid, offers a high catalyst to reactor volume ratio, with its

high heat transfer preventing catalyst deactivation. Nonetheless this reactor is costly, has single-use application and the catalyst removal is almost impossible [137], [138].

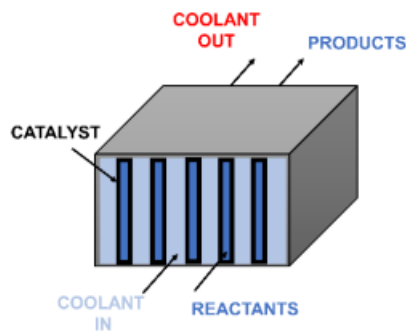


Figure 5.6 Microreactor [138]

A common reactor design, with a monolith catalyst, bares a large catalyst surface, adequate heat and pressure management and quick response time. The catalyst has holes giving it a honeycomb appearance, with the honeycomb walls with thickness from 0.05-0.3mm playing a significant role, as does hole density, in the catalyst activity. As the monoliths are primarily ceramic, they are characterized by poor mechanical properties and difficulty to be applied to large scale reactors. There is also the metallic option, which however has limited lifespan [137], [138].

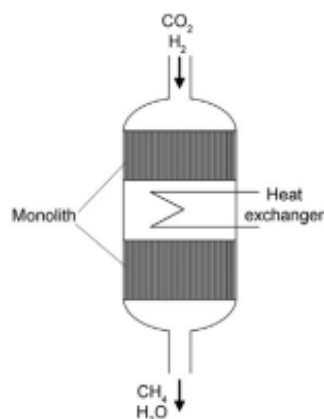


Figure 5.7 Monolith reactor [137]

Membrane reactors are based on a separate reactants feed. The hydrogen and the carbon dioxide are fed to different sides of H₂O selective membrane, which expels H₂O produced, forcing the methanation equilibrium to shift towards methane production. Membranes also exhibit the ability to distribute heat evenly among the reactor and producing a mixture of gases which requires less effort to be converted to SNG. On the other side of the coin, the short lifespan of the membrane, along with their cost should be further developed [137].

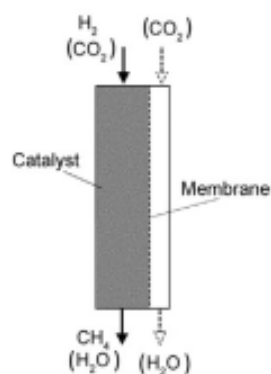


Figure 5.8 Membrane reactor [137]

Another reactor concept is sorption enhanced, which also follows Le Chatelier's principle as the membrane reactors. In this configuration, the catalyst is combined with an adsorbent which has high selectivity towards some reactants, pushing the equilibrium towards products formation in an outstanding rate. The adsorbent can regenerate through pressure or thermal swing adsorption, which however limits the reaction's operating time. Even though it is considered a complex reactor, studies report its ability to achieve up to 100% CO₂ conversion rate [137].

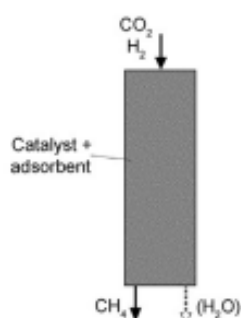


Figure 5.9 Sorption enhanced reactor [137]

5.6 Support materials

Support materials are a crucial part of the development of an effective catalyst. The primary objective of such materials is to enhance the active metal dispersion and complement its impact on the reaction. Support materials, often improve the reaction kinetics, reacting and forming anions or cations and stabilizing the active metal crystallites [120], [139].

The nature of the support material varies, from metal oxides to minerals and MOFs. The metal oxides like Al₂O₃, SiO₂, TiO₂, CeO₂, ZrO₂, have primarily been studied, with perovskites, zeolites, carbon materials and various novel support materials properties being examined [5].

5.6.1 Metal oxides

As mentioned above, metal oxides are the most common support materials reported. Among them, Al_2O_3 stands out, as the most studied support. The effect this oxide bears to the catalytic process is correlated with its crystallographic modifications ($\gamma, \kappa, \delta, \theta, \alpha$ phases). $\gamma\text{-Al}_2\text{O}_3$ exhibits the best properties among the other phases, with higher porosity, surface area, pore structure and satisfactory acid-base surface properties [5], [139].

More specifically, Jaffar et al. [140] investigated the differences between various active metals, supported by Al_2O_3 . According to this report, the alumina supported catalyst exhibited uniform dispersion of the active metal catalyst, as well as forming smaller particles. However various studies have reported a vulnerability to coke formation at high temperatures and particle agglomeration [5].

SiO_2 (silica) is another metal oxide that finds application as supporting material for CO_2 methanation. It is characterized by large pore size, high surface area significant thermal stability and inert properties [120]. Besides pure SiO_2 , structured catalyst supports based on this metal oxide, have also found applications on CO_2 methanation, showing interesting results. Such supports will be discussed in a later section.

Another metal oxide for similar application, is TiO_2 , which is one of the most effective Ni catalyst supports. Nickel can be absorbed by TiO_2 , forming oxide vacancies, which combines with the high hydrogen adsorption nature of Ni. Additionally, titanium oxides often achieve their high activity by supplying Ni with electrons, increasing the catalyst performance by improving the CO dissociation [139].

Cerium and zirconium oxides (CeO_2 , ZrO_2) influence catalysts is noteworthy. These oxides, have a redox property, which allows them to store and release oxygen, forming an environment which activates carbon oxides. This property, combined with an active component that attracts hydrogen can form a high-performance catalyst even in low temperatures [5], [139]. According to the examples of catalysts below, ZrO_2 and CeO_2 have excellent CH_4 selectivity, with catalysts achieving close to 100%, often demonstrating higher rates than other metal oxide supports, for the same active metal loadings.

5.6.2 Metal organic frameworks

Over the last years, the introduction of MOFs has revolutionized the catalytic studies, opening new diodes to carry out complex processes. These synthesized compounds are a result of organic ligands and metal cluster interaction. They are characterized by

high surface area (1,000-10,000 m²g⁻¹), stability, porosity, recyclability and multiple active centers. Besides that, MOFs bare the discrete ability of being modified, due to their structural flexibility, forming compounds with precise characteristics. Other aspects of these frameworks, is their high crystallinity, improving their CO₂ adsorption and the high surface porosity, leads to increased gas transfer along their structure, making these materials strong candidates for CO₂ methanation catalysts [141].

A perfect example of a MOF as support material is Pd/UiO-66 catalyst. UiO-66 is strongly basic, which lead to CO₂ to adhere, due to its mildly acidic nature. The material loading played a significant role to the process, with Pd 6wt% posing as the optimum active metal load, with higher loads leading to particle agglomeration and nonuniform particle dispersion. The UiO-66 support, was responsible for the decrease of byproducts concentrations [142].

5.6.3 Zeolites

Zeolites are hydrated aluminosilicate minerals, with interesting properties that can be tuned according to the reaction demands. Such minerals can be found in nature, but can also be manipulated, consisting of oxygen tetrahedra, which are surrounded by Si, Al, P, Be, Zn, Mg, Co, B and other metal cations. They are characterized by a large surface area, while considered a microporous material, capable of filtering ions [13], [143]. Additionally, zeolites have found industrial applications to NG “sweetening” from hydrogen sulfide, an ability that can benefit the methanation reaction, by avoiding product poisoning.

Chen et al [144] studied the properties of beta zeolite as a catalyst support, combined with Na cations, carrying Ni and La active metals. The sodium cations addition improved the CO₂ adsorption on the surface, where the addition of lanthanum significantly improved CO₂ conversion and CH₄ selectivity.

5.6.4 Carbon

Among the catalysts supports, multiple carbon materials have been implemented, providing different properties to the catalysts compared to the supports mentioned above. The effect of these supports in essence, is the enhanced hydrogen adsorption, primarily providing the reduced CO₂ with hydrogen atoms to form methane. More specifically, according to W.J Lee et al. [139], these supports provide high thermal conductivity, high hydrogen storage, easily manipulated surface properties, while avoiding coke formation.

Feng et al. [145] studied the effect of carbon nanotube (CNT) and Al_2O_3 supported nickel catalysts. According to this report, CNT support proved beneficial, improving the process overall outcome. The effects exhibited, are a result of CNT larger specific area, compared to Al_2O_3 support, which leads to higher Ni dispersion, combined with high hydrogen storage, providing enough hydrogen for the process.

5.7 Promoters

Multiple reports have examined the influence of adding compounds that complement or manipulate the catalyst in the methanation process. These compounds are referred in the literature as promoters, with alkali metals, alkaline earth metals, cerium oxide and rare earths being mostly examined.

According to literature, several studies observed that alkali metals can sometime obstruct the process, as a result of the alkali-carbonate formation, however, small quantities of alkalis were suggested to replace portion of costly active metals, decreasing the overall cost without reducing the activity of the catalyst [5]. More specifically, Panagiotopoulou et al [146] reported that alkali metal promotion favored the CO dissociation and carbon species hydrogenation on Ru/TiO_2 surface.

Alkaline earth metals have also showed great potential, as it improves active metal dispersion, increasing the amount of surface oxygen vacancies, enhancing catalytic performance. On the contrary, every promoter reacts differently with the catalyst, leading to different results for each combination or even activity decrease in $\text{Ni}/\text{Al}_2\text{O}_3$ and alkali earth metals case [5].

Cerium oxide (IV) besides its role as a support material, it is also added as a promoter, with noteworthy results. More specifically, the addition of CeO_2 in the 0.25wt% Ru-2.5wt% $\text{Fe}_3\text{O}_4/13\text{wt}\% \text{CeO}_x\text{-SiO}_2\text{-2}$ catalyst stabilized nanoparticle size throughout the process, improved the rate of product formation, due to the CO_2 absorbing and enhanced reduction ability, while improving the oxygen storage of mesoporous silica [147]. In $\text{Ni}/\text{Al}_2\text{O}_3$ case, CeO_2 promotion was responsible for increasing the number of active CO_2 and CH_4 sites, with higher loads of the promoter improving the CH_4 selectivity. Moreover, it was noticed that it prevented the disposition of carbon on the catalyst [148].

Other promoters include lanthanum oxide and lanthanide series. The effect of lanthanum oxide on a nickel catalyst supported by different types of zeolites, is characterized by an increase in the active sites along the catalysts surface, due to a decrease in Ni particle size, combined with an improved particle dispersion, thermal stability of the active metal and methane formation yields. Furthermore, an increase in La_2O_3 load contributes to higher CO_2 conversion, by aiding Ni to absorb more CO_2 at

higher rates [149]. Ahmad et al [150] studied the addition of lanthanide series elements, reporting that their addition promoted metal dispersion, maintained average particle size and stabilized support materials particles. It is worth noting that Praseodymium in particular increase the active sites of the catalyst.

5.8 Catalysts summary

This section contains Table 5.2, with multiple potential combinations of active metals, support materials and promoters, in different conditions and reactors. They are characterized by their reaction conditions, performance rates, reaction type, GHSV (Gas Hourly Space Velocity), which expresses the volume of gas entering the reactor per hour and promoters. Furthermore, the catalysts are classified based on the support material used.

Table 5.2 Overview of various methanation catalysts and their performance.

Catalyst	T (°C)	P(bar)	X _{CO2} (%)	S _{CH4} (%)	Reactor	GHSV (mL/g*h)	Promoters	Ref.
Metal oxide support								
2.5 wt% Ru/TiO ₂ (001)	325	1	>80	100	fixed-bed	-	-	[151]
Ru/CeO ₂	300		83	99	fixed-bed	7,640	-	[143]
0.25 wt%Ru-2.5 wt%Fe ₃ O ₄ /13 wt%CeO _x -SiO ₂ -2	300	20	82	32	fixed-bed	3,000	CeO _x	[147]
3.54wt% Ru/[Ca ₁₂ Al ₁₂ O ₃₃ :OH ⁻]	375	1	>80	>99	fixed-bed	-	-	[152]
Rh/Al ₂ O ₃	150	1	21	100	fixed-bed	-	-	[153]
0.5wt% Rh/TiO ₂	350	1	76-80	100	fixed-bed		-	[154]
1wt% Rh/ZrO ₂	300	1	61.8	98.3	tubular fixed-bed	-	-	[155]
0.5wt% Pd/TiO ₂	440	1	<10	~0	fixed-bed	-	-	[154]
5wt% Pd/γ-Al ₂ O ₃	240-300	1	-	22-40	tubular fixed-bed	45,000	-	[156]
Pd- MgO/SiO ₂	300	-	59	95	fixed-bed	-	MgO	[157]

10wt% Ni/Al ₂ O ₃	360	-	83	98	fixed-bed	6,000	-	[140]
27wt% Ni/MgO	325	1	91.2	99	fixed-bed	-	-	[158]
10wt% Ni/CeO ₂	350	1	~90	100	tubular fixed-bed	10,000	-	[159]
Ni/ZrO ₂	300	1	79.1	69.5	fixed-bed	60,000	-	[160]
Fe/Al ₂ O ₃	250		11.2	96.5	down-flow	-	-	
Ru-Mn-Ni/Al ₂ O ₃	400	1	99.74	72.36	microreactor	-	Ru-Mn	[5]
Ni-MgO/ZrO ₂	300	1	85.6	100	fixed-bed	-	MgO	
Co-Ni/ZrO ₂	250	5	93	90	fixed-bed	-	Co	
10wt% Ni-0.5wt% Pd/ Al ₂ O ₃	300	1	75	97	-	5,700	-	[138]
10wt% Ni-0.5wt% Pt/ Al ₂ O ₃	300	1	67	97	-	5,700	-	
Ni/Al ₂ O ₃	300	5	95	≥99	fixed-bed	-	La ₂ O ₃	[161]
17 wt % Ni ₃ Fe/ γ-Al ₂ O ₃	358	6	71	>98	microchannel packed bed	13,400	-	[134]
Mineral support								
Ru/ZSM-5	350	1	100	100	tubular microreactor	-	-	[162]
Zeolite 13X	320	1	79	100	fixed-bed	-	-	[5]
Ni-Ce/USY	305	1	78	99	fixed-bed	-	Cs+	
15Ni-20La/Na-BETA	400	-	84	97	fixed-bed	-	La	[144]
FS@SiO-BEA	~500	1	61	65	tubular fixed-bed	45,000	-	[13]
10Ni-10La ₂ O ₃ /Na-BETA	800		65	99	tubular fixed-bed	10,000	La ₂ O ₃	[149]
11.25 wt Ni/r-La _{0.5} Ce _{1.5} NiO ₄	350	-	78.9	99.3	tubular fixed-bed	10,000	-	[163]
50wt% Ni/AlCeO	200	1	83.2	99.5	fixed-bed	-	-	[164]

10wt% Ni- CaTiO ₃	325	1	80	100	fixed-bed	48,000	-	[165]
Carbon support								
2wt% Rh/PSAC	207	1	52.6	77.8	fixed-bed	-	-	[166]
0.8wt% Rh/ACZ	402	1	~50	~100	tubular fixed-bed	-	-	[167]
Fe/CNT	440	20	35	26	fixed-bed	-	K ⁺	[168]
Ni-Ca/AC	360	1	76	100	fixed-bed	-	Ca	[5]
MOFs support								
Ni- xCeO ₂ /M CM-41	380	1	85.6	99.8	fixed-bed	-	-	[5]
6wt% Pd/UiO- 66	340	40	56	97.3	fixed-bed	15,000	-	[169]
Ni ₂₀ - Al ₂ O ₃ /MI L-53	350	1	70-75	99	fixed-bed	1,435	-	[170]
Hydrotalcite support								
N-I-V2.0	300	1	74.7	100	quartz U- type tubular	12,000	V	[169]
Ni _{0.73} Zr _{0.0} ₃ Al _{0.24} -R	300	20	95	97.5	fixed-bed	-	-	[171]
0.25wt% Fe-Ni-Al O ₂ -HT	362	20	100	96.8	fixed-bed	-	Fe	[126]
Other support								
Ru/Ni NW	179	1	100	100	fixed-bed microrea ctor	-	-	[172]
Ni/F- SBA-15	400	1	99.7	98.2	tubular fixed-bed	24,900	-	[173]
Ni-Mg- Al/UH	300	-	82.3	99.8	U-shape quartz reactor	12,000	-	[174]
75wt% Ni-YSZ	300	9	>90	>99	Fixed- bed	15,700	-	[175]
15wt%Ni /Ce _{0.8} Zr _{0.2} O ₂	350	1	~81	~99.5	fixed-bed	12000	-	[176]
OMA- 1Co8Ni	400	1	79.9	97.5	tubular fixed-bed	15,000	-	[135]
6wt% Ni/MoO _x - La ₂ O ₃ /Si O ₃	362	1	96.8	100	fixed-bed	15,000	-	[129]

Co-Al-O-600	250	20	74	99	microreactor fixed-bed	5,000	-	[177]
8wt% Ni-2wt% Co	300	1	18	90	-	15,000	-	[138]

Table 5.2 shows the plethora of material combinations forming a catalyst. In this table multiple catalyst exhibit excellent performance in the methanation process. Even though Ru/ZSM-5 is the catalyst with the best catalytic performance, 27wt% Ni/MgO, 10wt% Ni/CeO₂, Ni/Al₂O₃, Ni/F-SBA-15, 6wt% Ni/MoO_x-La₂O₃/SiO₃ are catalyst that are better contenders overall, considering their performance to cost ratio, as Ni is far cheaper than Ru.

Practically, the assessment of the catalyst is vague, considering that their industrial implementation will be based on weights that will be assigned to various the performance capabilities of the plant, which will fluctuate in order to maximize the net profit of each plant. Thus, a precise catalyst classification will also depend on the expense to operate in the required conditions, the reactor cost, plants environmental impact and other parameters that demand specific structural, environmental and economic parameters to be taken into account. Some detailed techno-economic assessments will be studied in the following section.

Complimenting the table, Figure 5.10 and Figure 5.11 depict the effect of different catalysts in the same reaction. Both catalysts are characterized by high CH₄ selectivity and CO₂ conversion, however each catalyst follows different pathways to carry out the reaction. These examples highlight the importance of the effective combination of the catalyst materials.

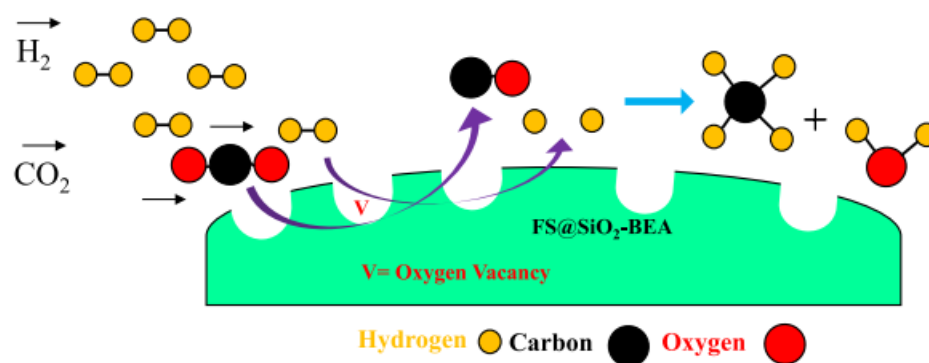


Figure 5.10 Silica Beta Zeolite catalyst setup and mechanism [13]

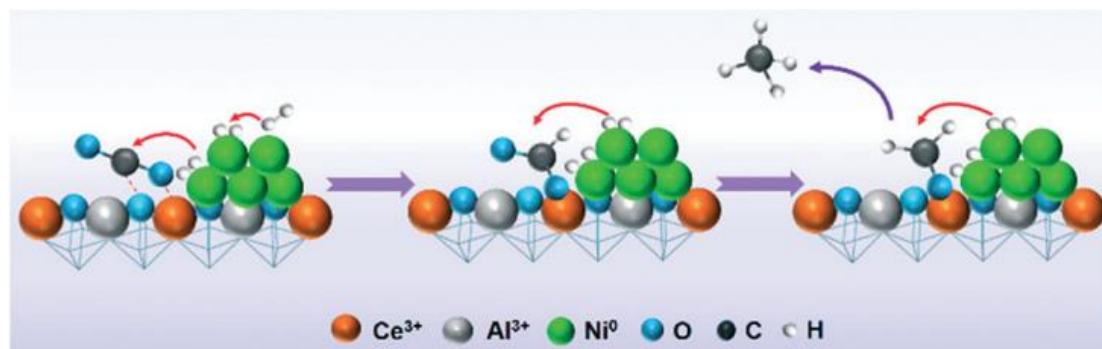


Figure 5.11 Nickel catalyst with $AlCeO_3$ support setup and mechanism [164].

5.9 Catalyst preparation methods

The combination of the active metal with the support material is vital for the catalyst activity. The catalyst preparations methods are responsible for the metal dispersion and loading on the catalyst surface, particle size and crystal structure.

The most simple and widespread method for heterogenous catalyst formation is the impregnation process. Impregnation can be achieved with two methods, with the first being wet impregnation and the second being dry or incipient wetness impregnation. The overall process starts with the diluting mean evaporation after a certain period, leading to an inactivated catalyst [178]. The difference between the two methods is the proportion of active solution to the pore volume of the support. In the first method, the solution is in abundance, contrary to dry impregnation, where the solution volume barely meets the pore volume. Each method has its defects, as the wet impregnation has active solution runoff, due to the high volume of the active solution. To minimize the active metal loss, a recycle and filtration step is required. The second method lacks the filtration of unwanted particles that may form, demanding a removal step if filtration is needed. Additionally, the simultaneous impregnation of a support by two metal solution is called co-impregnation [179].

Another popular preparation method is the sol-gel technology, where a metal salt or alkoxide is exposed to a solvent, forming a colloidal solution. This solution is then hydrolyzed and condensed, becoming liquid that surrounds a gel network. This method has drawn attention over the last years, due to its simplicity, allowing particle size and catalyst surface monitoring at low temperatures and the ability to adjust the properties of the catalyst [180].

Other preparation methods include the well-established method of microemulsion, which can form nanoparticle catalysts. In this technology, an aquatic solution of nanoparticles is dispersed over oil, forcing the particles to orientate and then integrate

with the support powder. This method forms catalysts with high thermal stability, metal dispersion, surface area and porosity [181]. Deposition precipitation process is a complex method, where metal salt is reduced and gets activated when it reacts with the support material, however this method forms catalysts with nonuniform particle dispersion [179].

5.10 Catalyst deactivation

Through the methanation process, catalysts are exposed to high temperatures and impurities that can decrease their impact through physical or chemical deactivation. More precisely, the most common issues that occur are catalyst fouling, sintering and poisoning. These phenomena can decrease the catalyst activity or even cause complete deactivation.

The fouling of a catalyst is the deposition of solids on its surface, interrupting the process. More specifically, in CO₂ methanation, carbon (also referred to as coke) deposition takes place during the Boudouard reaction, which blocks the pores and the active sites of the catalyst. However, this problem can be solved by increasing H₂ feed, or by adding steam in the reactor [5], [182], [183].

Catalyst poisoning is a big threat for the industrial carbon dioxide hydrogenation processes. Flue gases that can be fed to the reactor as CO₂ stream, often contain impurities as tars, NH₃, sulfur, zinc, chlorine and other compounds. Primarily, studies examine the addition of H₂S due to its high toxicity and concentration in flue gases. H₂S addition in the reaction deactivated the catalyst by getting absorbed by it [182]. The poisoning is considered almost permanent, with the conventional anti-poisoning methods aiming attacking the sulfur concentration before the CO₂ stream enters the reactor [5], or by adding Ce or Mo as promoters, which are elements with the ability to absorb sulfur [183]. A state-of-the-art solution has been developed by Bayer Material Science AG, capable of reviving Ru catalyst [182].

High temperatures in the reactor for certain periods can lead to metal particle fusion on the catalyst, leading to catalyst deactivation. This phenomenon is called sintering and is characterized by active surface decrease, due to metal particle agglomeration, while the occurrence of sintering can be found also in the support materials lattice [183]. The most significant parameter is the reactor type, as fixed bed reactors are prone to sintering. Additionally, sintering is prevented at operation temperatures around 30-40% of the active metal melting point [182].

Other mechanism that causes catalyst deactivation is the thermal stress of sudden temperature changes, damaging the catalyst. Moreover, in fluidized bed reactors, the

collision of the catalyst molecules with each other, or with the reactor walls, leads to deactivation, in a phenomenon called attrition [182].

To conclude, an effective PtG plant is strongly based on the catalyst chosen. The active metal combination with the support material plays the biggest role in the catalyst efficiency, while parameters like reactor type, preparation method and others, not only influence the effectiveness of the catalyst to convert CO_2 to CH_4 , but also the lifetime of the catalyst and its uniform activity throughout its surface.

6 Opportunities and challenges

Despite the ability to produce SNG from CO₂, PtG technology study has to extend to other dimensions. The study of the general effects, its potential and its limitations must be put under the microscope. Firstly, in this section, its environmental impacts reviewed, reporting the problems that its implementation may generate. Later, its financial feasibility is examined, as it directly correlates with its potential. Lastly, the process is studied from a sociopolitical standpoint, putting the humanitarian aspect into perspective.

6.1 Life cycle assessment

As environmental issues escalate, the need for a viable solution to the environmental crisis is bigger than ever. PtG processes are the most promising way to store renewable energy and excess energy produced from conventional means, while treating CO₂ as a valuable gas rather than a waste product. Nevertheless, CO₂ methanation demands energy supply not only for the main reaction but also for the acquisition of the reactants, with questions rising around its environmental sustainability.

Through various environmental assessment methodologies developed LCA is the most precise tool. The main principle of LCA is to examine most of the traces left from a product, taking into consideration the environmental impact of the raw materials production, up to the last stage of waste treatment. The whole methodology is based on the goal of the assessment, with the scope setting the limits for the detail that the life cycle will be studied. Afterwards, an inventory analysis step studies the energy and material flows, followed by an impact assessment, which determines the value of every category of environmental impact and concluding with the interpretation of life cycle, where the data are reviewed and presented [184]. Different variants of LCA exist, with the most known being cradle-to-grave, cradle-to-cradle and cradle-to-gate.

Many researchers have conducted LCA for Power-to-Methane (PtM), mostly assessing the environmental effects of different catalysts implemented in thermal methanation, with some also looking into the biological methanation alternative. In this thesis, the assessment of biological methanation will not be put into perspective.

Sayyah et al. [185] conducted LCA on CO₂ methanation, evaluating the environmental impact that different catalyst bares on this process. The process evaluated included a H₂ production unit (AEL), a CO₂ capture and purification unit (amine absorption), a catalyst synthesis unit and a CO₂ hydrogenation unit. The power plants studied produce energy with a combined cycle NG turbine and pulverized lignite coal (C) (400

MW and 800 MW produced respectively, without CO₂ sequestration), with the CO₂ capture process providing 95.6% molar purity of CO₂ while operating with 90% efficiency. Alongside with conventional energy production, wind turbines (WT) and 3 types of photovoltaics (PV), the amorphous silicon solar (SS) cell, copper indium selenide (CIS), CH₃NH₃SnI₃ perovskite (PS) are being considered.

The goal of the analysis is to assess 5 catalysts based on their lab scale reports and evaluate their total environmental impact. In this cradle to grave analysis the functional unit implemented in this is the production of 1 m³ of CH₄ in one hour, while the system boundaries expand until raw material extraction, energy acquisition, transportation and production.

Table 6.1 below contains the cases and the LCI reported. Case E is considered to have the biggest environmental impact, with the highest electricity usage, case D is responsible for the highest environmental toxicity, while case A is considered the greenest option, with the highest CO₂ conversion and CH₄ selectivity. Besides catalysts evaluation, Sayyah et al. [185] proceed to evaluate the overall impact of cases A, B, C for different power sources. Wind turbines are the most environmentally viable powering choices, while providing the following order of environmental friendliness of renewables and NG energy mixture.

$$WT + NG > CSI + NG > SS + NG > NG > PS + NG \quad (24)$$

Table 6.1 Environmental impact breakdown per catalyst [185]

Cases	Catalysts	Life cycle impact outline
A	20 wt% Ni/Al ₂ O ₃	<ul style="list-style-type: none"> Alumina preparation plays significant role in fossil depletion. H₂ production tetrachloromethane emissions make up most of ozone depletion. Nickel nitrate is responsible most of the impact of the rest of the categories.
B	15 wt% Ni/TiO ₂	<ul style="list-style-type: none"> TiO₂ carbon emissions for the catalyst production are responsible for 32% and 46% of total climate change and ozone depletion respectively. Conventional electricity production has significant influence in fossil depletion and terrestrial acidification.
C	10 wt% Ni/ZSM-5	<ul style="list-style-type: none"> High energy demands for catalyst production make CO₂ and energy production are the main contributors in the climate change category. N₂ substitution of Ar reduces overall impact almost 80%.
D	Rh@HZSM-5 core@shell	<ul style="list-style-type: none"> Production of Rh causes high levels of toxic elementary flow emissions into the environment (e.g. 97,650 kg CO₂, 0.0044 kg CFCs, and 2229 kg SO₂ per 1 kg of Rh).

		<ul style="list-style-type: none"> • Ar production has the second highest impact due to its use as an inert gas in catalyst reduction. • Catalyst synthesis and Ar production effects significantly outweigh H₂ and CO₂ acquisition.
E	Rh@KZSM-5 core@shell	<ul style="list-style-type: none"> • Worst scenario environmentally wise. • Requires more Rh and electricity to achieve the efficiency yields of other cases. • Significantly lower CO₂ conversion (55%) than other cases.

Another study [186] offers a simpler LCA, evaluating catalytic and biological from biogas methanation scenarios. The goal of this assessment is to quantify the environmental impact of Power-to-Methane (PtM) in a cradle to gate analysis, with the functional unit being 1 MWh worth of synthetic methane produced, based on the higher heating value (HHV). The data used are based on the Belgian NG grid, with EU and global data complementing any missing data. Additionally, only electricity produced from WT (1-3MW energy output) is considered in the system studied, no CO₂ sequestration, distribution or combustion is examined. It is assumed that the methanation is a continuous process without fluctuations nor halts in production of synthetic NG (SNG), with ideal production conditions (no leaks, heat losses, or pressure drops) and converting all CO₂ and H₂ isometrically. Finally, only operational consumption of raw materials is considered, while infrastructure is considered as a background process.

The overall global warming potential of catalytic CO₂ methanation is 26.93 kg CO₂-eq/MWh of SNG produced. Hydrogen production is 94.2% responsible for the total environmental impact of PtM, from which 98.8% is a result of WT energy consumption. Thus 1.58 kg CO₂-eq/KWh are produced from other parts of the process, most of which is due to the compressor, dryer and sulfur removal. Other impact categories were also assessed with total mineral resource depletion being calculated at 0.64 kgCu-eq/KWh mainly caused by the compressor and the electrolysis, the freshwater ecotoxicity is more than 0.45 kg 1.4-DCB-eq/MWh almost solely caused by sulfur removal and water consumption (0.7 m³water/MWh) is mainly generated by electrolysis and the water consumption in the background process, which is the water consumed for electricity and material production. Moreover, an interesting suggestion is the utilization of waste heat, which can save 156.5 kWh of electricity, with temperatures at 270 °C can be useful for industrial chemical activities, avoiding additional emissions, where upgrades on the process design can utilize the residual heat in different steps of the process, like CO₂ sequestration.

In a different approach, LCA is combined with JRC-EU-TIMES energy system model (ESM), offering a more holistic view on the PtM potential [187]. ESM offer an insight into the cost and feasibility of an energy system, with the specific model focusing on

analyzing energy systems in EU countries, UK and others, offering predictions about the technology performance, with the results also including the optimum investment portfolio [188]. ESM combination with LCA can be proven fruitful, as ESM takes into consideration the evolution of the process, materials and electricity mix, while integrates the financial aspect, by making assumptions about the market, leading to different energy mixes and impact. Lastly, ESM can predict the effect of policies and assess their consequences.

Despite the combination with ESM, LCA methodology remained the main, with the authors setting as a goal the assessment of 18 environmental impact categories for future methanation EU energy systems, from 1990-2050, primarily focusing on the assessment of PtM environmental impact and predict its effect. The functional unit is the satisfaction of all energy services demand, including residential, commercial, industrial, mobility and agriculture needs. Multiple CO₂ sources are considered, with a gradual dominance of air capture and biogenic technologies. In the scenarios the combustion emissions have not been calculated, a supply mix of liquid and gas fuels have been considered (with a gradual reform) and biofuels have been assigned neutral emissions. Furthermore, simplifications are made, as only processes with greater than ~1% contribution to total CO₂ emissions, only representative processes (e.g., 3/10 gas turbines), few heating and cooling methods and merge of value chains have been examined.

Six scenarios were studied in this LCA. The first two studied the reduction of total CO₂ by 80%, from 1990 to 2050, one with Carbon Capture and Storage (CCS) technologies and one without. The first is set as the lower limit for decarbonation, detecting trends and technologies, while the second has no CCS, examining the decarbonization feasibility if CCS meets sociopolitical barriers. The other four scenarios have 95% CO₂ reduction, with the first scenario evaluating the impact of a more intense decarbonization, the second without CCS, examining the effect of CCS for higher decarbonization demand, the third one is an optimum scenario, setting the higher bound for capacity and environmental impact, and the last scenario does not consider PtM, in order to evaluate the difference this process makes in the European decarbonization.

The results of this study are separated between the entire system impact and methanation impact. The indirect CO₂ emissions make up half of the emissions in 80% scenarios and two thirds in 95% scenarios. In the first case, 50% of these emissions are a result from upstream fossil fuel production, while on the second case the emissions are evenly distributed to manufacturing, power and industrial categories. In the 80% reduction scenario the total CO₂ emissions are 914 Mt CO₂eq, where in 2016 the average EU emissions from combustion and heat were 1000 Mt CO₂eq, with the supply sector being the most impactful sector. The power sector has the largest share

of overall impact, where 75% of electricity come from PV and WT. In general, the 80% CO₂ reduction scenarios have been found to have a higher toll for the environment, compared to 95% scenarios, terrestrial ecotoxicity impact is 50-80% higher in no CCS scenarios due to larger demand for electricity, marine and freshwater eutrophication impact increases, but all the other categories have a 5-10% impact reduction. Additionally, the most industry and transportation sectors cost the most to decarbonize.

Beside the main system impact results, PtM influence is the most notable outcome. The maximum allowable impact of PtM was estimated between 122.6-180.9 g CO₂eq/kWh, where its allowable electricity footprint should be between 3.8-62.2 g CO₂eq/kWh to be preferred over NG. Additionally, it has performed better than NG in 10 out of 18 categories, with the most energy consuming part being the electrolyzer. Methanation highest impact categories are metal and water depletion, ionizing radiation and lastly terrestrial, marine and human toxicity. In the model applied, PtM by 2050 was covering 75% of EU gas demands. Comparing the prediction with the technology available, with a prediction of not having this technology, climate change become approximately 4% worse and fossil depletion 9% worse.

In another literature review, Garcia-Garcia et al. [189] delve into the result of LCA studies in Power-to-X methods. The main findings of their research include that other than PEM electrolyzers, generate more greenhouse gas emissions than current NG production and electrolysis is beneficial for the environment only if it is powered by renewable energy sources (RES). Moreover, based on a research that analyzed Swiss data, they report that the upper bound for methanation emissions is 113 g CO₂eq/kWh without CCS and 73 g CO₂eq/kWh with CCS, while PtM powered by RES has higher impact than conventional NG production in human toxicity (cancer and non-cancer effects), freshwater ecotoxicity, mineral, fossil and renewable resource depletion, due to CO₂ capture and the wear and tear of the system.

6.2 Cost estimations and Techno-economic analyses

In recent years, the need for sustainable energy, processes and materials has been developed into a necessity. Beside the environmental aspect of sustainability, which shows the direction in which modern society must move towards, the economic aspects define the paths available. Especially in the energy sector, companies have already integrated RES energy development, expanding their interests in energy transition. However, the options that will prevail are the ones that are financially viable. Consequently, for PtM processes, the economical perspective has to be studied in order to evaluate their viability as a CCU option.

Baier et al. [190], studied the cost of CO₂ methanation plant in 2017, capturing CO₂ directly from Swiss cement industry flue gases, with the SNG produced reused on site. The reason that the Swiss cement industry is specifically studied, is its high energy consumption and CO₂ emissions. More specifically, in 2015, it was accountable for 5% of total energy consumption and for 36% of the total CO₂ industrial emissions [191]. Additionally, another reason for applying CO₂ methanation in this industry in Switzerland, is that its centralized and continuous activity, leading to a steady production of flue gases, while making the collection of the majority of carbon oxides emissions from this sector feasible. Moreover, the high calcination temperature can provide the heat required for the SNG production.

Beside the characteristics of the industry, additional parameters have to be noted in order to understand the depth of the analysis. Firstly, this analysis aims to convert 2.5 million tons of CO₂, alongside with 0.46 million tons of H₂ (ratio of H₂/ CO₂ is 4:1), producing 2.04 million tons of H₂O and 0.9 million tons of CH₄ per year, for 30 years. For the Sabatier reaction to achieve the conversion of 2.5 million tons of CO₂, 503 GWh annually are required, while H₂ demand is covered by AEL (efficiency is set to 64%), requiring 4.1 million tons of fresh H₂O and 23,900 GWh per year, with approximately 3.6 million tons of O₂ as a byproduct. The entire plant is powered by photovoltaics, assumed to have 16% efficiency, with 20% output loss and 5% losses of the inverter system. Thus, the power production system is designed to produce 27,604 GWh annually to offset the system losses.

After defining the parameters, the authors proceeded to estimate the cost of such an installation, using net present value (NPV) formula with interest rate of 3% and a 10% discount to PV and AEL installation due their large size. The results of the capital expenditures (CapEx) and operational expenses (OpEx) are reported in the Table 6.2 below.

Table 6.2 Costs per infrastructure in detail [190]

Infrastructure	Expenditure	Value
Photovoltaics installation	Investment cost (million CHF)	20,703
	Investment cost/power (CHF/kW)	900
	Operational cost (million CHF/year)	1,982
	Cost/energy consumption (CHF/kWh)	0.09
Alkaline Electrolysis plant	Investment cost (million CHF)	13,471
	Investment cost/power (CHF/kW)	636
	Operational cost (million CHF/year)	1,397
	Cost/energy consumption (CHF/kWh)	0.11
Methanation plant	Investment cost (million CHF)	4,405
	Investment cost/power (CHF/kW)	208

	Operational cost (million CHF/year)	457
	Cost/energy consumption (CHF/kWh)	0.04
Overall plant	Investment cost (million CHF)	38,579
	Investment cost/power (CHF/kW)	900
	Operational cost (million CHF/year)	3,836
	Cost/energy consumption (CHF/kWh)	0.24

According to the findings of the abovementioned report, PV installation has the highest CapEx and OpEx, being responsible for the 53.66% of the total investment cost and 51.67% of the total annual operational expenses. On the other hand, the methanation plant makes up 11.41% of total investment cost and 11.91% of the total annual operational expenses, being the least expensive both operational and investment wise. It worths noting that there is no SNG and H₂ transportation and storage cost taken into consideration. Additionally, the SNG produced translates to one third of the Swiss annual NG consumption, which was evaluated 3.6 times more expensive than conventional NG, projected to generate 1.059 billion CHF per year if consumed concluding to a feasible investment.

Another interesting techno-economic assessment [192] was conducted in 2021, evaluating PtM plant feasibility in Greece, capturing CO₂ from cement plant flue gases with MEA scrubbing combined with AEL H₂ production powered by PV and WT. The system that they studied was defined by the capture of the entirety of the cement industry flue gases, the H₂ production was fixed for ratio of H₂/ CO₂ of 4, the methanation was carried out by the most efficient catalyst, the existence of heat management alongside with pressure drops, heat loses and other equipment not having optimum efficiency (e.g for pumps and compressors efficiency is approximately 75-80%). Lastly, the useful life of the plant was expected to be 25 years, the discount rate was set at 4% and the regional tax rate on the net profit is 24%.

The system studied has also defined infrastructure parameters. The MEA unit was assumed to have 88% efficiency, capturing flue gases containing 13.7 v/v% CO₂. The renewable powered 2200 MW AEL is expected to produce 32.4 t/h, is powered annually by 7043 GWh and 2032 GWh power produced by PV and WT respectively, with 303 GWh/yr of surplus power being stored in lead acid batteries. The efficiency of the AEL was expected to be 75%, producing also O₂ of more than 99% purity at 10 bar, which is sold. For the CO₂ methanation, CO₂ is compressed to 10 bar, and heated with H₂ to 300°C, producing SNG of 90.5% purity, with H₂ making up most of the byproducts. The catalyst consists of nickel, supported by ceria nanorods, with CO₂

conversion of 93% and ~92% CH₄ yield. The projected expenses for the entire plant and the market value for the products are presented in the Table 6.3 below.

Table 6.3 Cost breakdown [192]

Type of value	Value
Total Utilities Cost (€/yr)	28,734,500
Total Fixed Capital Investment (€)	9,707,703,950
Total Annual Production Cost (€/yr)	145,479,100
Produced Oxygen Value (€/yr)	156,409,600
Produced SNG Value (€/yr)	239,191,800
Electricity Surplus Value (€/yr)	12,400,000

Cost breakdown is the most significant aspect of the cost analysis. The costs take into perspective all the systems used, with Total Fixed Capital Investment and Total Annual Production Costs also considering the support systems. The AEL plant powered by renewables is accountable for the majority of the Total Fixed Capital Investment and the Total Utilities Cost, as it comprises 93.33% and 54.26% of the costs respectively. Additionally, the 75% of H₂ production plant investment cost is made up by the renewables and 23% of the AEL unit. The Total Annual Cost is more evenly distributed as the CO₂ sequestration plant is responsible for the biggest portion of the cost (34.61%). In general, CO₂ methanation plant has the less significant cost among all categories, besides the Total Annual Production cost where the support system costs the least. Taking the products value into perspective, the produced SNG produces the most revenue with the electricity surplus producing the least significant revenue.

To study the feasibility of the assessed plant, three scenarios were developed. The first scenario (scenario A) is the base case scenario, considering 25 €/t carbon penalty, without SNG redirected in the cement industry, the second scenario (scenario B) explores the recycle of 200tn/h of SNG in the cement industry (equivalent to 30-35% of this industry energy needs), partial financing of the renewables for H₂ production and the effect of different CO₂ penalty costs. The last scenario (scenario C) assumed that the AEL plant is powered by the grid and the SNG is recycled in the industry. Table 6.4 below, puts the main findings into perspective.

Table 6.4 Results per scenario [192]

Scenario A	Scenario B	Scenario C
<ul style="list-style-type: none"> Non-feasible scenario (NPV<0) SNG adapted price to break-even is 1500 €/t (SNG assumed cost is 500 €/t). 	<ul style="list-style-type: none"> SNG recycle reduces SNG and O₂ price to achieve break even, by 31% and 35% respectively. The CO₂ penalty increase to 100 €/t has the most 	<ul style="list-style-type: none"> Price per kWh is set at 0.02€ where market value ranges between 0.04€ to 0.06€ per kWh.

<ul style="list-style-type: none"> • O₂ adapted price to break even is 366 €/t (O₂ assumed cost is 80 €/t). 	<p>significant effect to break effect prices (38.5% for SNG and 54.3% for O₂).</p> <ul style="list-style-type: none"> • For 25€/t of CO₂ penalty, 10% and 30% of renewables capital reduction, translates to 41.1% and 61.7% break even SNG price reduction respectively. • For 25€/t of CO₂ penalty, 36% of renewables capital reduction, leads to SNG and O₂ market values. • For 50€/t of CO₂ penalty, 28% of renewables capital reduction, leads to SNG and O₂ market values. • For 100€/t of CO₂ penalty, 13% of renewables capital reduction, leads to SNG and O₂ market values. 	<ul style="list-style-type: none"> • SNG break even prices is 1079€/t for 25€/t of CO₂ penalty, 954€/t for 50€/t of CO₂ penalty, 711€/t for 100€/t of CO₂ penalty. • O₂ break even prices is 237€/t for 25€/t of CO₂ penalty, 204€/t for 50€/t of CO₂ penalty, 138€/t for 100€/t of CO₂ penalty.
--	--	---

Such endeavors, however, cannot find the same application in every country across the globe, due to geological and legal limitations. Morimoto et al. [193] studied the ways that PtM could be implemented in Japan and the prospect of cooperation with another country. This study aims to evaluate the carbon footprint of Japan and economic feasibility of a methanation plant powered by various energy sources and partner with trading countries. Five different scenarios were examined, with the first (scenario A) assuming SNG was imported, CO₂ and H₂ without any CO₂ captured in Japan, the second scenario (scenario B) studies CO₂ capture in Japan combined with H₂ and CH₄ production overseas, the next scenario (scenario C) studies CO₂ capture and CH₄ production in Japan transported with pipelines, with H₂ produced overseas, scenario D is the same as C with LNG transport instead of pipelines and lastly, scenario E examines the whole process in Japan.

In order to review this study, the system studied has to be defined. CO₂ sources examined where flue gases of coal fired exhaust gases, from LNG powered plants and

from blast furnace gas from steel plants, which are absorbed by MEA with 90% efficiency. CO₂ catalytic hydrogenation was carried out by an adiabatic reactor at 649.7°C and 13.5 bar. Heat produced from the methanation reaction can power the electrolysis and methanation pumps and compressors, while steam produced from the reaction can generate 2.95 MWh/t CH₄ which is sufficient for MEA regeneration. When the methanation plant is not adjacent to CO₂ sequestration plant the MEA regeneration is conducted with LNG. The runoff heat is utilized only in scenarios A, C, D, E. The life cycle of CO₂ examined 3 different powered sources, uses CO₂/t CH₄ as the function unit and did not include the construction phase in the assessment. Six different overseas locations were studied (UAE, Indonesia, Australia, Malaysia, Qatar, Russia)

The outcome of this study classifies scenario B for Indonesia and scenario 5 as the best options. Firstly, life cycle of CO₂ results suggests that SNG is environmentally viable over imported LNG, only when H₂ production is powered by renewables for the scenarios A and B, while for the rest of scenarios the whole process must be powered by renewables. The main comparison for the scenarios was done assuming coal plants as the CO₂ source. Scenario A was found to be the cheapest PtM option when paired with Indonesia (420,5 USD/t CO₂), where scenario E costs 510,9 USD/t CO₂. The low cost of scenario A was a result of the lack of liquefaction process, combined with the low renewable energy cost in Indonesia and the close distance between Indonesia and Japan. On the other side of the coin, scenario A is not preferred for CO₂ reduction, as it does not consume Japan's CO₂. The CO₂ reduction optimal scenario was scenario E. Moreover, comparison between scenario B and C suggests that importing H₂ is less profitable than exporting CO₂, while comparison of scenario C and D found that pipeline transportation is the cheapest option.

The report proceeded to examine further scenario B and E, with the assessment of CO₂ sources, showing that the lowest CO₂ reduction value occurred for coal produced CO₂ in scenario B (473.3 USD/t CO₂), blast furnace produced CO₂ in scenario E (511.8 USD/t CO₂) and LNG produced CO₂ in scenario E (471.5 USD/t CO₂). The option with the highest cost to potential was found to be scenario E utilizing LNG produced CO₂, which has the potential of converting 143.9 Mt CO₂/yr with 3.0-5.1 billion USD/yr total annual cost. However, this number is far from reality, as it assumes that all the renewable power available in the island would power the PtM process.

6.3 Existing plants

Theoretical studies of scenarios, no matter how detailed they are, usually lack some aspects that may play a role in reality. Thus, studying existing PtM plants offers a complete view of the plant operations, accompanied with the preferred technologies

in the field, market development and leading countries experimenting with this technology on industrial level.

Thema et al. [194] analyzed data collected from 153 CO₂ methanation plants and their H₂ production technologies. The data collected are from completed, current and planned plants, some dating back to 1988, considering the plant size, shares and amount of H₂ and SNG produced, plant allocation and plant power development. Results from this publication are separated to H₂ production and PtM, using CapEx data for H₂ and PtM obtained from literature, paired with data collected from experts through a survey conducted in 2017.

Putting H₂ production under the microscope, Thema et al. [194] forecasted H₂ technologies prices through exponential approximation. AEL cost is expected to decrease from 1300 €/kW in 2017 to 700 €/kW in 2030 and 500 €/kW by 2050, PEM cost is expected to decrease from 1900 €/kW in 2017 to 600 €/kW by 2030 and 500 €/kW by 2050 and SOEC price is projected to drop from 3570 €/kW to 535 €/kW. These prices projections are susceptible to policies and legislations that may be enforced in the future.

Regarding CO₂ hydrogenation to CH₄, most aspects of the study cover the technologies used and the growth of PtM. Firstly, only 57% of the studied plants cover H₂ production, while when the electrolysis technologies preferred were AEL and PEM, approximately in a 50/50 ratio, where SOEC and combination of electrolysis technologies were rarely tested. The number of biological and catalytic methanation plants was evenly distributed, with the majority located in Central Europe with Germany, Denmark and The Netherlands being the frontrunners. Their potential is directly correlated with the electrical power of their installed electrolyzers, with the first having 40 MW, the second 20 MW and The Netherlands was looking to set at 12 MW. The most common type of reactor is fixed bed, followed by fluidized bed, while roughly 45% of the produced SNG was injected in the grid, probably due to standard limitations. Furthermore, the number of plants soared between 2012 and 2015, with the average plant increasing from 118 kW to 390 kW in the same timeframe.

On top of the reported results, other interesting results include plant characteristics. Mean hydrogen and methanation unit size is estimated to be 0.7 MW, where mean methanation unit power is estimated to be 1.56 MW and mean H₂ plant size is 0.45 MW due to small projects. Mean efficiency of methanation plants is 41% and H₂ plant is 77%. Additionally, only 10% of plants manages heat produced from the reaction. Considering plants lifespan, projects that were reported between 1998 and 2018 has one to three years of life, taking usually up to 1.5 year to be constructed. Lastly, mean cost of powering CO₂ methanation costs 800 €/kW in 2017, decreasing to 500 €/kW in 2030 and ranging between 130-440 €/kW in 2050, with methanation and electrolysis cost aligning with the progression of the years.

Some plants stand out from others due to their size, or innovation in CH₄ synthesis. Bailera et al. [195] reviewed the objectives and future plans for some plants in 2017. The plants reviewed were converting CO₂ either catalytically or biologically. As this thesis studies catalytic methanation, most of the plants reported will regard catalytic methanation, as one biological plant will be analyzed in order to provide a more complete view in the alternative PtM processes and market. The main outlook of the plants is given in Table 6.5 below.

Table 6.5 Detailed review of existing PtG plants [195]

Plant	Details
ETOGAS - Audi e-gas plant Location: Wertle, Germany	<ul style="list-style-type: none"> • Longest plant in the world, with three 2 MW EAL, powered by offshore WT park in the North Sea. • Catalytic methanation of pure H₂ and CO₂ (obtained from biogas with amine scrubbing) in a single isothermal fixed bed reactor. • The project is funded primarily by AUDI AD and the local power company. • Runs on 54% efficiency and lacks heat management system. • Produces approximately 1000t of SNG and consumes 4,000 hours of renewable power annually. • Mature plant, which has steadily expanded, experimenting with various reactor types, CO₂ sources and product refinement methods. • Main goal is to produce SNG with 80% efficiency, while expanding to commercialized PtM systems of approximately 20 MW.
Sunfire – HELMETH Location: Karlsruhe, Germany	<ul style="list-style-type: none"> • PtM system with 85% efficiency, paired with 15 kW SOEC operating at 800°C and 15 bar. • Two methanation reactors in series, operating at 300°C and 30 bar with intermediate water removal methanation. • Total project funds are 3.8 million €, with 2.5 million funded by EU, with Karlsruhe Institute of Technology, Sunfire and other institutes and universities.
Haldor Topsoe – El-Opgraderet Biogas Location: Foulum, Denmark	<ul style="list-style-type: none"> • Demonstration plant, which upgrades biogas through CO₂ methanation, with H₂ produced from a 40 kW SOEC.

	<ul style="list-style-type: none"> • Total budget is 5.3 million €, with 3.5 million € funded by EU • Haldor Topsoe leads the project, partnered with Aarhus University which received a fund covering 70% of the construction expenses. Other institutes, power and NG companies also participate
<p>Aarhus University - MeGa store Location: Lemvig, Denmark</p>	<ul style="list-style-type: none"> • Two step biogas upgrade, with biogas purification and methanation in an air cooled reactor, using bottle H₂. • Launched in 2013 with a lifespan of two years, produced SNG with methane content higher than 97% at 270°C and 8 bar
<p>Enagas – RENOVAGAS Location: Spain</p>	<ul style="list-style-type: none"> • First methanation plant in Spain, launched in 104 and with the first phase ending in 2017, upgrading biogas to SNG capable of being injected into the existing gas network. • H₂ produced from a 15 kW AEL unit, with the CO₂ conversion taking place in a multichannel reactor with a Ni or Ru catalyst based on Al₂O₃, oil-based cooling, operating at 25 bar, 275-300°C and GHSV of 2000-20000 per hour. • The goal is to build a 5MW commercial scale plant.
<p>DNV GL – Power to Gas in Rozenburg Location: Rozenburg, Netherlands</p>	<ul style="list-style-type: none"> • Basic objective is to produce SNG capable of being injected in the existing gas network. • Operates since 2014, providing SNG to 30 nearby apartments. • The unit consists of a 7 kW PEM electrolyzer, a four reactor methanation system, 2 CO₂ tanks and 4 solar panels on the container roof combined with power from the grid, cover the energy demands. • The reactors use different reaction of Ni, with the first two being 11%w, the third 37%w and the last 54%w, exhibiting optimum results at 377°C and 8 bar.
<p>Hitachi Zosen – CO₂ Conversion to Methane project Location: Rayong, Thailand</p>	<ul style="list-style-type: none"> • CO₂ conversion project based on Hashimoto [7] studies, with multiple universities and institutes being recruited to develop the technology.

	<ul style="list-style-type: none"> • A CO₂ conversion plant, collecting CO₂ from NG extraction sites. • 5 meters long tubular reactors, baring Ni supported by zirconia-samarium catalyst. • H₂ produced from AEL. • A consortium of Hitachi Zosen corporation and other technology and petroleum companies.
<p>EMPA – catalytic methanation of industrially-derived CO₂ Location: Switzerland</p>	<ul style="list-style-type: none"> • Experimental sorption enhanced CO₂ methanation reactor, with high CO₂ conversion, while absorbing water through a Ni, supported by a zeolite, catalyst. • This plant has 3 different projects carried out, one for catalyst development, one for biogas upgrade and one for CO₂ methanation. • Experiments are performed at 1.2 bar GHSV is 1000 per hour, with an output of 1 kW. • Research is focused on renewable fuels, photo-electrolysis of water, utilization CO₂ from cement plant flue gases and sulfur poisoning.
<p>Tauron – CO₂ – SNG Location: Poland</p>	<ul style="list-style-type: none"> • Launched in 2014, aiming to produce SNG in order to store power surplus. • CO₂ is collected from Tauron coal power plant. • Tauron has partnered up with Atomic Energy, Alternative Energy commission and Atmosstat, which developed a reactor with 95% CO₂ conversion rate. • AGH University has developed and tested and tested the catalyst. • The plant potential is still examined.
<p>Electrochaea – BioCat Location: Avedøre, Denmark</p>	<ul style="list-style-type: none"> • Biological PtM plant, which aims to be the biggest biomethnation plant globally, producing SNG at 4 bar which gets injected in the gas grid. • It operates in dynamic mode, capable to store Danish energy surplus, converting CO₂ from an anaerobic digester (60% CH₄, 40% CO₂), or pure CO₂ from a conventional biogas upgrading system.

-
- H₂ is produced by a 1MW AEL unit, powered by excess wind power, with O₂ and heat produced reused at wastewater treatment.
 - Methanation is carried out by methanogenic archaea, single-celled microorganisms, evolved by Electrochaea GmbH, metabolizing H₂ and CO₂ to CH₄, with 98.6% CO₂ conversion at 60-65°C.
 - The microorganisms exhibit tolerance to H₂S, NH₃, nitrogen oxides and other particles.
 - The overall budget is 6.7 million €, with the plant managed by the danish energy supply company Energinet.dk, in cooperation with multiple other companies.
-

6.4 Sociopolitical aspect

Sociopolitical acceptance is key requirement towards a successful PtM technologies implementation. As every technology available to date however, it is not perfect, as it is clear through LCA that has an environmental impact, regarding fossil depletion, human health and freshwater ecotoxicity. Consequently, introducing a new, groundbreaking technology, with certain risks for the local ecosystem, has to be examined in terms of social acceptance and the way its benefits and risks can be communicated.

Public opinion, especially in EU does not stand with similar technologies. As H₂ production and occasionally CO₂ conversion is examined to be paired with renewable energy, it may face social backlash, as renewables have not been totally accepted, as many regions still disagree with their application. Additionally, CCU is often confused for CCS by the public, while CCS technologies have met resistance from stakeholders and the public in multiple European countries, CCU may be more easily accepted, as it can be regarded as waste recycling [196]. The same study assessed Power-to-X (PtX) technologies, with PtG being the method with the highest social acceptance.

Other studies suggest that CCU technologies should differentiate their approach to the general public and the local communities that they will find applications, as the first will emphasize on the benefits of their implementation and the latter will focus on the environmental risk lurking. As a matter of fact, a survey between France and Spain public opinion of CCU and CCS technologies, in regional and national level are

noteworthy. In general, CCU was approximately 10-15% more acceptable than CCS technologies, while the French were more open-minded in regional level compared to nation-wide, in contrast with Spanish where the opposite occurred [197]. Detailed graph of the result is presented in Figure 6.1.

The perspective of the public is momentous for a successful technology industrial development. Understanding the criteria in which the technologies will be assessed by the public is mandatory, as psychological, cultural and technological perception aspects are crucial for a successful implementation strategy [198]. A study conducted in 2015 in UK, suggested that stakeholders, policymakers, media and politicians are the means that are responsible for setting the tone for the social acceptance of such technologies [199].

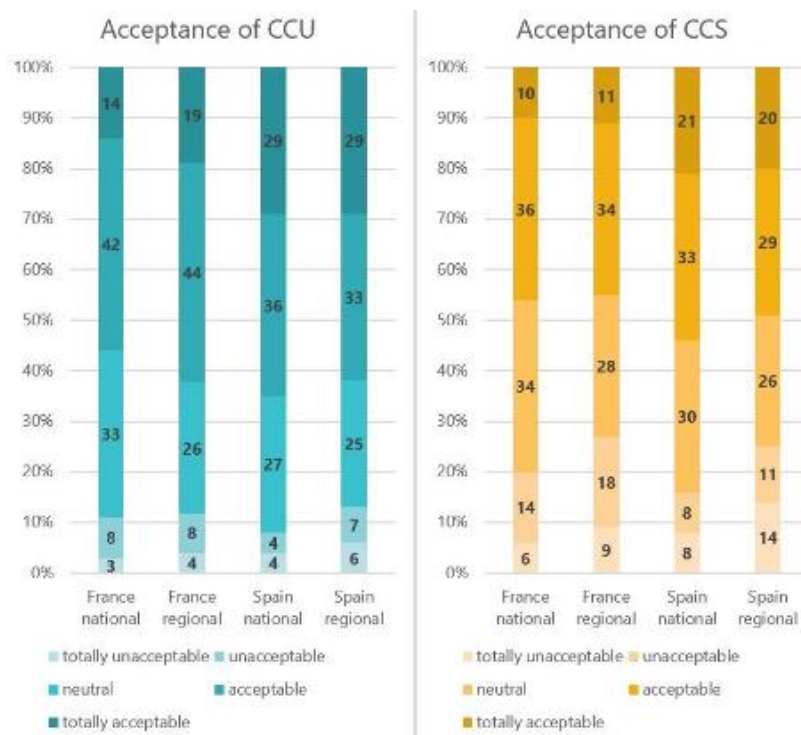


Figure 6.1 Survey regarding CCU social acceptance in France and Spain [197]

7 Conclusions

The purpose of this thesis was to review the catalytic CO₂ methanation status and potential, as a mean to restrict GHG effects, while producing an alternative fuel, capable to cover a portion of human energy demands.

CO₂ concentration in the atmosphere of the earth is increasing annually, with its effects being more noticeable than ever. At the same time, human activities are mostly based on fossil fuel consumption, a depleting resource which has to be substituted, while renewable sources are not capable of providing energy consistently. In this framework, significant research has been conducted on alternative energy sources, especially alternative fuels, produced by renewable sources and potentially storing their surplus. One of the most promising alternatives is SNG production as it has high calorific value and there is already existing infrastructure for its exploitation.

In this context, the present thesis studies the processes surrounding CO₂ methanation, followed by an analysis of their opportunities. Firstly, there is a thermodynamic analysis of the reaction, followed by a review of the CO₂ sequestration and separation methods, an examination of literature around the alternative hydrogen production methods and their energy sources, alongside with a detailed analysis of the CO₂ methanation processes, the importance of the catalysts and the details in the infrastructure and the report of current breakthroughs. Regarding the future of the technology, its environmental impact, financial viability and socio-political acceptance are reviewed in depth.

Notable findings mostly revolve around H₂ production, CO₂ methanation. H₂ produced globally, is almost solely powered from fossil fuels, due to the reduced cost compared to renewable powered production. However, utilizing H₂ produced with fossil fuels in order to convert CO₂ is sisyphism. Additionally, mostly electrolysis is mostly studied as an alternative hydrogen production method, due to its maturity and ability to be paired with renewable sources. However, for this specific process thermochemical H₂ production may have an effective contribution on CO₂ methanation, utilizing its excess heat produced. Beside H₂ production, the most promising catalyst for CO₂ hydrogenation to CH₄, is Ni based on Al₂O₃, due to its low cost, exceptional performance and according to LCA limited environmental impact.

The above sections, suggest that CO₂ catalytic methanation is a promising technology, capable to produce SNG relatively close to NG prices in certain occasions. However, there are plentiful obstacles that this process has to overcome, mostly regarding the immense cost of investment if the process is paired with water electrolysis and the impact of human health, caused by the catalyst.

References

- [1] <https://www.climate.gov/news-features/understanding-climate/climate-change-atmospheric-carbon-dioxide>, “Climate Change: Atmospheric Carbon Dioxide.”
- [2] <https://www.iea.org/news/global-co2-emissions-rose-less-than-initially-feared-in-2022-as-clean-energy-growth-offset-much-of-the-impact-of-greater-coal-and-oil-use>, “Global CO₂ emissions rose less than initially feared in 2022 as clean energy growth offset much of the impact of greater coal and oil use”.
- [3] <https://www.eia.gov/todayinenergy/detail.php?id=41433>, “EIA projects nearly 50% increase in world energy usage by 2050, led by growth in Asia”.
- [4] <https://world-nuclear.org/information-library/facts-and-figures/heat-values-of-various-fuels.aspx>, “Heat Values of Various Fuels.”
- [5] I. Hussain, A. A. Jalil, N. S. Hassan, and M. Y. S. Hamid, “Recent advances in catalytic systems for CO₂ conversion to substitute natural gas (SNG): Perspective and challenges,” *Journal of Energy Chemistry*, vol. 62, pp. 377–407, Nov. 2021, doi: 10.1016/J.JECHEM.2021.03.040.
- [6] S. Rönsch *et al.*, “Review on methanation – From fundamentals to current projects,” *Fuel*, vol. 166, pp. 276–296, Feb. 2016, doi: 10.1016/j.fuel.2015.10.111.
- [7] K. Hashimoto *et al.*, “Global CO₂ recycling—novel materials and prospect for prevention of global warming and abundant energy supply,” *Materials Science and Engineering: A*, vol. 267, no. 2, pp. 200–206, Jul. 1999, doi: 10.1016/S0921-5093(99)00092-1.
- [8] C. Vogt, M. Monai, G. J. Kramer, and B. M. Weckhuysen, “The renaissance of the Sabatier reaction and its applications on Earth and in space,” *Nat Catal*, vol. 2, no. 3, pp. 188–197, Mar. 2019, doi: 10.1038/s41929-019-0244-4.
- [9] O. Korotkikh and R. Farrauto, “Selective catalytic oxidation of CO in H₂: fuel cell applications,” *Catal Today*, vol. 62, no. 2–3, pp. 249–254, Nov. 2000, doi: 10.1016/S0920-5861(00)00426-0.
- [10] L. Jürgensen, E. A. Ehimen, J. Born, and J. B. Holm-Nielsen, “Dynamic biogas upgrading based on the Sabatier process: Thermodynamic and dynamic process simulation,” *Bioresour Technol*, vol. 178, pp. 323–329, Feb. 2015, doi: 10.1016/J.BIORTECH.2014.10.069.
- [11] W. Ahmad, A. Al-Matar, R. Shawabkeh, and A. Rana, “An experimental and thermodynamic study for conversion of CO₂ to CO and methane over Cu-K/Al₂O₃,” *J Environ Chem Eng*, vol. 4, no. 3, pp. 2725–2735, Sep. 2016, doi: 10.1016/J.JECE.2016.05.019.

- [12] C. V. Miguel, M. A. Soria, A. Mendes, and L. M. Madeira, "Direct CO₂ hydrogenation to methane or methanol from post-combustion exhaust streams – A thermodynamic study," *J Nat Gas Sci Eng*, vol. 22, pp. 1–8, Jan. 2015, doi: 10.1016/J.JNGSE.2014.11.010.
- [13] I. Hussain *et al.*, "Thermodynamic and experimental explorations of CO₂ methanation over highly active metal-free fibrous silica-beta zeolite (FS@SiO₂-BEA) of innovative morphology," *Chem Eng Sci*, vol. 229, p. 116015, Jan. 2021, doi: 10.1016/J.CES.2020.116015.
- [14] R. B. Anderson, C.-B. Lee, and J. C. Machiels, "The thermodynamics of the hydrogenation of oxides of carbon," *Can J Chem Eng*, vol. 54, no. 6, pp. 590–594, Dec. 1976, doi: 10.1002/cjce.5450540619.
- [15] C. v. Miguel, A. Mendes, and L. M. Madeira, "Intrinsic kinetics of CO₂ methanation over an industrial nickel-based catalyst," *Journal of CO₂ Utilization*, vol. 25, pp. 128–136, May 2018, doi: 10.1016/J.JCOU.2018.03.011.
- [16] F. Meng, X. Li, X. Lv, and Z. Li, "CO hydrogenation combined with water-gas-shift reaction for synthetic natural gas production: a thermodynamic and experimental study," *Int J Coal Sci Technol*, vol. 5, no. 4, pp. 439–451, Dec. 2018, doi: 10.1007/s40789-017-0177-y.
- [17] S. Vaz, A. P. Rodrigues de Souza, and B. E. Lobo Baeta, "Technologies for carbon dioxide capture: A review applied to energy sectors," *Clean Eng Technol*, vol. 8, p. 100456, Jun. 2022, doi: 10.1016/j.clet.2022.100456.
- [18] E. Blomen, C. Hendriks, and F. Neele, "Capture technologies: Improvements and promising developments," *Energy Procedia*, vol. 1, no. 1, pp. 1505–1512, Feb. 2009, doi: 10.1016/J.EGYPRO.2009.01.197.
- [19] M. Kanniche, R. Gros-Bonnivard, P. Jaud, J. Valle-Marcos, J. M. Amann, and C. Bouallou, "Pre-combustion, post-combustion and oxy-combustion in thermal power plant for CO₂ capture," *Appl Therm Eng*, vol. 30, no. 1, pp. 53–62, Jan. 2010, doi: 10.1016/J.APPLTHERMALENG.2009.05.005.
- [20] D. Y. C. Leung, G. Caramanna, and M. M. Maroto-Valer, "An overview of current status of carbon dioxide capture and storage technologies," *Renewable and Sustainable Energy Reviews*, vol. 39, pp. 426–443, Nov. 2014, doi: 10.1016/J.RSER.2014.07.093.
- [21] A. A. Olajire, "CO₂ capture and separation technologies for end-of-pipe applications – A review," *Energy*, vol. 35, no. 6, pp. 2610–2628, Jun. 2010, doi: 10.1016/J.ENERGY.2010.02.030.
- [22] I. Sreedhar, T. Nahar, A. Venugopal, and B. Srinivas, "Carbon capture by absorption – Path covered and ahead," *Renewable and Sustainable Energy Reviews*, vol. 76, pp. 1080–1107, Sep. 2017, doi: 10.1016/J.RSER.2017.03.109.

- [23] D. Aaron and C. Tsouris, "Separation of CO₂ from Flue Gas: A Review," *Sep Sci Technol*, vol. 40, no. 1–3, pp. 321–348, Feb. 2005, doi: 10.1081/SS-200042244.
- [24] B. Petrovic, M. Gorbounov, and S. Masoudi Soltani, "Influence of surface modification on selective CO₂ adsorption: A technical review on mechanisms and methods," *Microporous and Mesoporous Materials*, vol. 312, p. 110751, Jan. 2021, doi: 10.1016/J.MICROMESO.2020.110751.
- [25] J. Bonjour, J.-B. Chalfen, and F. Meunier, "Temperature Swing Adsorption Process with Indirect Cooling and Heating," *Ind Eng Chem Res*, vol. 41, no. 23, pp. 5802–5811, Nov. 2002, doi: 10.1021/ie011011j.
- [26] R. Ben-Mansour and N. A. A. Qasem, "An efficient temperature swing adsorption (TSA) process for separating CO₂ from CO₂/N₂ mixture using Mg-MOF-74," *Energy Convers Manag*, vol. 156, pp. 10–24, Jan. 2018, doi: 10.1016/j.enconman.2017.11.010.
- [27] C. A. Grande, R. P. L. Ribeiro, E. L. G. Oliveira, and A. E. Rodrigues, "Electric swing adsorption as emerging CO₂ capture technique," *Energy Procedia*, vol. 1, no. 1, pp. 1219–1225, Feb. 2009, doi: 10.1016/J.EGYPRO.2009.01.160.
- [28] G. Xu, F. Liang, Y. Yang, Y. Hu, K. Zhang, and W. Liu, "An Improved CO₂ Separation and Purification System Based on Cryogenic Separation and Distillation Theory," *Energies (Basel)*, vol. 7, no. 5, pp. 3484–3502, May 2014, doi: 10.3390/en7053484.
- [29] C. Font-Palma, D. Cann, and C. Udemu, "Review of Cryogenic Carbon Capture Innovations and Their Potential Applications," *C (Basel)*, vol. 7, no. 3, p. 58, Jul. 2021, doi: 10.3390/c7030058.
- [30] Y. Han and W. S. W. Ho, "Polymeric membranes for CO₂ separation and capture," *J Memb Sci*, vol. 628, p. 119244, Jun. 2021, doi: 10.1016/J.MEMSCI.2021.119244.
- [31] C. Ma, M. Wang, Z. Wang, M. Gao, and J. Wang, "Recent progress on thin film composite membranes for CO₂ separation," *Journal of CO₂ Utilization*, vol. 42, p. 101296, Dec. 2020, doi: 10.1016/J.JCOU.2020.101296.
- [32] J. M. S. Henis and M. K. Tripodi, "Composite hollow fiber membranes for gas separation: the resistance model approach," *J Memb Sci*, vol. 8, no. 3, pp. 233–246, Jan. 1981, doi: 10.1016/S0376-7388(00)82312-1.
- [33] H. Dashti, L. Zhehao Yew, and X. Lou, "Recent advances in gas hydrate-based CO₂ capture," *J Nat Gas Sci Eng*, vol. 23, pp. 195–207, Mar. 2015, doi: 10.1016/J.JNGSE.2015.01.033.
- [34] R. Pruscek, G. Oeljeklaus, G. Haupt, G. Zimmermann, D. Jansen, and J. S. Ribberink, "The role of IGCC in CO₂ abatement," *Energy Convers Manag*, vol. 38, no. SUPPL. 1, pp. S153–S158, Jan. 1997, doi: 10.1016/S0196-8904(96)00262-2.

- [35] S. Li, S. Fan, J. Wang, X. Lang, and Y. Wang, "Clathrate Hydrate Capture of CO₂ from Simulated Flue Gas with Cyclopentane/Water Emulsion," *Chin J Chem Eng*, vol. 18, no. 2, pp. 202–206, Apr. 2010, doi: 10.1016/S1004-9541(08)60343-2.
- [36] H. Tajima, A. Yamasaki, and F. Kiyono, "Energy consumption estimation for greenhouse gas separation processes by clathrate hydrate formation," *Energy*, vol. 29, no. 11, pp. 1713–1729, Sep. 2004, doi: 10.1016/J.ENERGY.2004.03.003.
- [37] H. A. Alalwan and A. H. Alminshid, "CO₂ capturing methods: Chemical looping combustion (CLC) as a promising technique," *Science of The Total Environment*, vol. 788, p. 147850, Sep. 2021, doi: 10.1016/J.SCITOTENV.2021.147850.
- [38] J. Adanez, A. Abad, F. Garcia-Labiano, P. Gayan, and L. F. de Diego, "Progress in Chemical-Looping Combustion and Reforming technologies," *Prog Energy Combust Sci*, vol. 38, no. 2, pp. 215–282, Apr. 2012, doi: 10.1016/J.PECS.2011.09.001.
- [39] A. Buttler and H. Spliethoff, "Current status of water electrolysis for energy storage, grid balancing and sector coupling via power-to-gas and power-to-liquids: A review," *Renewable and Sustainable Energy Reviews*, vol. 82, pp. 2440–2454, Feb. 2018, doi: 10.1016/J.RSER.2017.09.003.
- [40] H. Lu, X. Ma, K. Huang, L. Fu, and M. Azimi, "Carbon dioxide transport via pipelines: A systematic review," *J Clean Prod*, vol. 266, p. 121994, Sep. 2020, doi: 10.1016/J.JCLEPRO.2020.121994.
- [41] Z. X. Zhang, G. X. Wang, P. Massarotto, and V. Rudolph, "Optimization of pipeline transport for CO₂ sequestration," *Energy Convers Manag*, vol. 47, no. 6, pp. 702–715, Apr. 2006, doi: 10.1016/J.ENCONMAN.2005.06.001.
- [42] K. Johnsen, K. Helle, S. Rønneid, and H. Holt, "DNV recommended practice: Design and operation of CO₂ pipelines," *Energy Procedia*, vol. 4, pp. 3032–3039, Jan. 2011, doi: 10.1016/J.EGYPRO.2011.02.214.
- [43] G. Pantoleontos, N. I. Tsongidis, E. Daskalos, and A. G. Konstandopoulos, "Development of transportation cost functions and optimization of transportation networks for solar-aided utilization of CO₂," *International Journal of Greenhouse Gas Control*, vol. 112, p. 103528, Dec. 2021, doi: 10.1016/J.IJGGC.2021.103528.
- [44] H. al Baroudi, A. Awoyomi, K. Patchigolla, K. Jonnalagadda, and E. J. Anthony, "A review of large-scale CO₂ shipping and marine emissions management for carbon capture, utilisation and storage," *Appl Energy*, vol. 287, p. 116510, Apr. 2021, doi: 10.1016/J.APENERGY.2021.116510.
- [45] A. Ajanovic, M. Sayer, and R. Haas, "The economics and the environmental benignity of different colors of hydrogen," *Int J Hydrogen Energy*, vol. 47, no. 57, pp. 24136–24154, Jul. 2022, doi: 10.1016/J.IJHYDENE.2022.02.094.

- [46] M. Yu, K. Wang, and H. Vredenburg, "Insights into low-carbon hydrogen production methods: Green, blue and aqua hydrogen," *Int J Hydrogen Energy*, vol. 46, no. 41, pp. 21261–21273, Jun. 2021, doi: 10.1016/J.IJHYDENE.2021.04.016.
- [47] P. R. Kapadia, J. (Jacky) Wang, M. S. Kallos, and I. D. Gates, "Practical process design for in situ gasification of bitumen," *Appl Energy*, vol. 107, pp. 281–296, Jul. 2013, doi: 10.1016/J.APENERGY.2013.02.035.
- [48] Grant D. STREM, Ian D. GATES, and Jingyi WANG, "IN - SITU PROCESS TO PRODUCE SYNTHESIS GAS FROM UNDERGROUND HYDROCARBON RESERVOIRS ," 2021
- [49] W. Liu, H. Zuo, J. Wang, Q. Xue, B. Ren, and F. Yang, "The production and application of hydrogen in steel industry," *Int J Hydrogen Energy*, vol. 46, no. 17, pp. 10548–10569, Mar. 2021, doi: 10.1016/J.IJHYDENE.2020.12.123.
- [50] M. Yue, H. Lambert, E. Pahon, R. Roche, S. Jemei, and D. Hissel, "Hydrogen energy systems: A critical review of technologies, applications, trends and challenges," *Renewable and Sustainable Energy Reviews*, vol. 146, p. 111180, Aug. 2021, doi: 10.1016/J.RSER.2021.111180.
- [51] T. Jiang and W. Chen, "Nickel hydrogen gas batteries: From aerospace to grid-scale energy storage applications," *Curr Opin Electrochem*, vol. 30, p. 100859, Dec. 2021, doi: 10.1016/J.COEELEC.2021.100859.
- [52] K. Scott, "Introduction to Hydrogen, Electrolyzers and Fuel Cells Science and Technology," *Comprehensive Renewable Energy*, pp. 1–28, Jan. 2022, doi: 10.1016/B978-0-12-819727-1.00142-4.
- [53] A. Banu and Y. Bicer, "Review on CO_x-free hydrogen from methane cracking: Catalysts, solar energy integration and applications," *Energy Conversion and Management: X*, vol. 12, p. 100117, Dec. 2021, doi: 10.1016/J.ECMX.2021.100117.
- [54] Hannah Ritchie, Max Roser, and Pablo Rosado, "Energy," *Our World in Data*, 2022.
- [55] W. J. Martinez-Burgos *et al.*, "Hydrogen: Current advances and patented technologies of its renewable production," *J Clean Prod*, vol. 286, p. 124970, Mar. 2021, doi: 10.1016/J.JCLEPRO.2020.124970.
- [56] J. Milewski, G. Guandalini, and S. Campanari, "Modeling an alkaline electrolysis cell through reduced-order and loss-estimate approaches," *J Power Sources*, vol. 269, pp. 203–211, Dec. 2014, doi: 10.1016/J.JPOWSOUR.2014.06.138.
- [57] A. Ursua, L. M. Gandia, and P. Sanchis, "Hydrogen Production From Water Electrolysis: Current Status and Future Trends," *Proceedings of the IEEE*, vol. 100, no. 2, pp. 410–426, Feb. 2012, doi: 10.1109/JPROC.2011.2156750.
- [58] W. Kreuter and H. Hofmann, "Electrolysis: The important energy transformer in a world of sustainable energy," *Int J Hydrogen Energy*, vol. 23, no. 8, pp. 661–666, Aug. 1998, doi: 10.1016/S0360-3199(97)00109-2.

- [59] R. GILLIAM, J. GRAYDON, D. KIRK, and S. THORPE, "A review of specific conductivities of potassium hydroxide solutions for various concentrations and temperatures," *Int J Hydrogen Energy*, vol. 32, no. 3, pp. 359–364, Mar. 2007, doi: 10.1016/j.ijhydene.2006.10.062.
- [60] C. A. Schug, "Operational characteristics of high-pressure, high-efficiency water-hydrogen-electrolysis," *Int J Hydrogen Energy*, vol. 23, no. 12, pp. 1113–1120, Dec. 1998, doi: 10.1016/S0360-3199(97)00139-0.
- [61] K. Zeng and D. Zhang, "Recent progress in alkaline water electrolysis for hydrogen production and applications," *Prog Energy Combust Sci*, vol. 36, no. 3, pp. 307–326, Jun. 2010, doi: 10.1016/J.PECS.2009.11.002.
- [62] Z. D. Wei *et al.*, "Water electrolysis on carbon electrodes enhanced by surfactant," *Electrochim Acta*, vol. 52, no. 9, pp. 3323–3329, Feb. 2007, doi: 10.1016/J.ELECTACTA.2006.10.011.
- [63] "Water Facts - Worldwide Water Supply," <https://www.usbr.gov/mp/arwec/water-facts-ww-water-sup.html>, 2020.
- [64] W. T. Grubb and L. W. Niedrach, "Batteries with Solid Ion-Exchange Membrane Electrolytes," *J Electrochem Soc*, 1960.
- [65] "<https://www.nafion.com/en>."
- [66] P. Millet *et al.*, "PEM water electrolyzers: From electrocatalysis to stack development," *Int J Hydrogen Energy*, vol. 35, no. 10, pp. 5043–5052, May 2010, doi: 10.1016/J.IJHYDENE.2009.09.015.
- [67] K. Ayers, "The potential of proton exchange membrane-based electrolysis technology," *Curr Opin Electrochem*, vol. 18, pp. 9–15, Dec. 2019, doi: 10.1016/J.COEELEC.2019.08.008.
- [68] F. Scheepers *et al.*, "Temperature optimization for improving polymer electrolyte membrane-water electrolysis system efficiency," *Appl Energy*, vol. 283, p. 116270, Feb. 2021, doi: 10.1016/J.APENERGY.2020.116270.
- [69] B. Yodwong, D. Guilbert, M. Phattanasak, W. Kaewmanee, M. Hinaje, and G. Vitale, "AC-DC Converters for Electrolyzer Applications: State of the Art and Future Challenges," *Electronics (Basel)*, vol. 9, no. 6, p. 912, May 2020, doi: 10.3390/electronics9060912.
- [70] J. B. Hansen, "Solid oxide electrolysis – a key enabling technology for sustainable energy scenarios," *Faraday Discuss*, vol. 182, pp. 9–48, 2015, doi: 10.1039/C5FD90071A.
- [71] A. Nechache and S. Hody, "Alternative and innovative solid oxide electrolysis cell materials: A short review," *Renewable and Sustainable Energy Reviews*, vol. 149, p. 111322, Oct. 2021, doi: 10.1016/J.RSER.2021.111322.

- [72] T. Chen *et al.*, "High performance solid oxide electrolysis cell with impregnated electrodes," *Electrochem commun*, vol. 54, pp. 23–27, May 2015, doi: 10.1016/J.ELECOM.2015.02.015.
- [73] N. Gao, C. Quiroz-Arita, L. A. Diaz, and T. E. Lister, "Intensified co-electrolysis process for syngas production from captured CO₂," *Journal of CO₂ Utilization*, vol. 43, p. 101365, Jan. 2021, doi: 10.1016/J.JCOU.2020.101365.
- [74] L. Bi, S. Boulfrad, and E. Traversa, "Steam electrolysis by solid oxide electrolysis cells (SOECs) with proton-conducting oxides," *Chem. Soc. Rev.*, vol. 43, no. 24, pp. 8255–8270, Aug. 2014, doi: 10.1039/C4CS00194J.
- [75] M. Carmo, D. L. Fritz, J. Mergel, and D. Stolten, "A comprehensive review on PEM water electrolysis," *Int J Hydrogen Energy*, vol. 38, no. 12, pp. 4901–4934, Apr. 2013, doi: 10.1016/J.IJHYDENE.2013.01.151.
- [76] J. Chi and H. Yu, "Water electrolysis based on renewable energy for hydrogen production," *Chinese Journal of Catalysis*, vol. 39, no. 3, pp. 390–394, Mar. 2018, doi: 10.1016/S1872-2067(17)62949-8.
- [77] M. C. Tucker, "Progress in metal-supported solid oxide electrolysis cells: A review," *Int J Hydrogen Energy*, vol. 45, no. 46, pp. 24203–24218, Sep. 2020, doi: 10.1016/J.IJHYDENE.2020.06.300.
- [78] N. Gerloff, "Comparative Life-Cycle-Assessment analysis of three major water electrolysis technologies while applying various energy scenarios for a greener hydrogen production," *J Energy Storage*, vol. 43, p. 102759, Nov. 2021, doi: 10.1016/J.EST.2021.102759.
- [79] Craig A. Grimes, Oomman K. Varghese, and Sudhir Ranjan, *Light, Water, Hydrogen*. 2008.
- [80] S. Z. Baykara, "Hydrogen: A brief overview on its sources, production and environmental impact," *Int J Hydrogen Energy*, vol. 43, no. 23, pp. 10605–10614, Jun. 2018, doi: 10.1016/J.IJHYDENE.2018.02.022.
- [81] P. Nikolaidis and A. Poullikkas, "A comparative overview of hydrogen production processes," *Renewable and Sustainable Energy Reviews*, vol. 67, pp. 597–611, Jan. 2017, doi: 10.1016/J.RSER.2016.09.044.
- [82] M. Ji and J. Wang, "Review and comparison of various hydrogen production methods based on costs and life cycle impact assessment indicators," *Int J Hydrogen Energy*, vol. 46, no. 78, pp. 38612–38635, Nov. 2021, doi: 10.1016/J.IJHYDENE.2021.09.142.
- [83] M. Mehrpooya and R. Habibi, "A review on hydrogen production thermochemical water-splitting cycles," *J Clean Prod*, vol. 275, p. 123836, Dec. 2020, doi: 10.1016/J.JCLEPRO.2020.123836.

- [84] L. C. Juárez-Martínez, G. Espinosa-Paredes, A. Vázquez-Rodríguez, and H. Romero-Paredes, "Energy optimization of a Sulfur–Iodine thermochemical nuclear hydrogen production cycle," *Nuclear Engineering and Technology*, vol. 53, no. 6, pp. 2066–2073, Jun. 2021, doi: 10.1016/J.NET.2020.12.014.
- [85] K. Onuki, S. Kubo, A. Terada, N. Sakaba, and R. Hino, "Thermochemical water-splitting cycle using iodine and sulfur," *Energy Environ Sci*, vol. 2, no. 5, p. 491, 2009, doi: 10.1039/b821113m.
- [86] Y. Zhang, P. Peng, J. Zhou, Z. Wang, J. Liu, and K. Cen, "Thermal efficiency evaluation of a ZnSI thermochemical cycle for CO₂ conversion and H₂ production – Complete system," *Int J Hydrogen Energy*, vol. 40, no. 18, pp. 6004–6012, May 2015, doi: 10.1016/J.IJHYDENE.2015.03.008.
- [87] V. Immanuel and A. Shukla, "Effect of operating variables on performance of membrane electrolysis cell for carrying out Bunsen reaction of I–S cycle," *Int J Hydrogen Energy*, vol. 37, no. 6, pp. 4829–4842, Mar. 2012, doi: 10.1016/J.IJHYDENE.2011.12.102.
- [88] H. Ishaq, I. Dincer, and G. F. Naterer, "Industrial heat recovery from a steel furnace for the cogeneration of electricity and hydrogen with the copper-chlorine cycle," *Energy Convers Manag*, vol. 171, pp. 384–397, Sep. 2018, doi: 10.1016/J.ENCONMAN.2018.05.039.
- [89] H. Ozcan and I. Dincer, "Performance investigation of magnesium–chloride hybrid thermochemical cycle for hydrogen production," *Int J Hydrogen Energy*, vol. 39, no. 1, pp. 76–85, Jan. 2014, doi: 10.1016/J.IJHYDENE.2013.10.088.
- [90] M. F. Simpson, S. D. Herrmann, and B. D. Boyle, "A hybrid thermochemical electrolytic process for hydrogen production based on the reverse Deacon reaction," *Int J Hydrogen Energy*, vol. 31, no. 9, pp. 1241–1246, Aug. 2006, doi: 10.1016/J.IJHYDENE.2005.08.014.
- [91] R. Kothari, D. Buddhi, and R. L. Sawhney, "Comparison of environmental and economic aspects of various hydrogen production methods," *Renewable and Sustainable Energy Reviews*, vol. 12, no. 2, pp. 553–563, Feb. 2008, doi: 10.1016/J.RSER.2006.07.012.
- [92] M. Ni, D. Y. C. Leung, M. K. H. Leung, and K. Sumathy, "An overview of hydrogen production from biomass," *Fuel Processing Technology*, vol. 87, no. 5, pp. 461–472, May 2006, doi: 10.1016/J.FUPROC.2005.11.003.
- [93] Y. Kalinci, A. Hepbasli, and I. Dincer, "Biomass-based hydrogen production: A review and analysis," *Int J Hydrogen Energy*, vol. 34, no. 21, pp. 8799–8817, Nov. 2009, doi: 10.1016/J.IJHYDENE.2009.08.078.

- [94] J. D. Holladay, J. Hu, D. L. King, and Y. Wang, "An overview of hydrogen production technologies," *Catal Today*, vol. 139, no. 4, pp. 244–260, Jan. 2009, doi: 10.1016/J.CATTOD.2008.08.039.
- [95] N. Akhlaghi and G. Najafpour-Darzi, "A comprehensive review on biological hydrogen production," *Int J Hydrogen Energy*, vol. 45, no. 43, pp. 22492–22512, Sep. 2020, doi: 10.1016/J.IJHYDENE.2020.06.182.
- [96] L. Singh and Z. A. Wahid, "Methods for enhancing bio-hydrogen production from biological process: A review," *Journal of Industrial and Engineering Chemistry*, vol. 21, pp. 70–80, Jan. 2015, doi: 10.1016/J.JIEC.2014.05.035.
- [97] H. Argun and F. Kargi, "Bio-hydrogen production by different operational modes of dark and photo-fermentation: An overview," *Int J Hydrogen Energy*, vol. 36, no. 13, pp. 7443–7459, Jul. 2011, doi: 10.1016/J.IJHYDENE.2011.03.116.
- [98] P. K. Rai and S. P. Singh, "Integrated dark- and photo-fermentation: Recent advances and provisions for improvement," *Int J Hydrogen Energy*, vol. 41, no. 44, pp. 19957–19971, Nov. 2016, doi: 10.1016/J.IJHYDENE.2016.08.084.
- [99] R. Łukajtis *et al.*, "Hydrogen production from biomass using dark fermentation," *Renewable and Sustainable Energy Reviews*, vol. 91, pp. 665–694, Aug. 2018, doi: 10.1016/J.RSER.2018.04.043.
- [100] J. Riley, C. Atallah, R. Siriwardane, and R. Stevens, "Technoeconomic analysis for hydrogen and carbon Co-Production via catalytic pyrolysis of methane," *Int J Hydrogen Energy*, vol. 46, no. 39, pp. 20338–20358, Jun. 2021, doi: 10.1016/J.IJHYDENE.2021.03.151.
- [101] M. Younas, S. Shafique, A. Hafeez, F. Javed, and F. Rehman, "An Overview of Hydrogen Production: Current Status, Potential, and Challenges," *Fuel*, vol. 316, p. 123317, May 2022, doi: 10.1016/J.FUEL.2022.123317.
- [102] M. Onozaki, K. Watanabe, T. Hashimoto, H. Saegusa, and Y. Katayama, "Hydrogen production by the partial oxidation and steam reforming of tar from hot coke oven gas," *Fuel*, vol. 85, no. 2, pp. 143–149, Jan. 2006, doi: 10.1016/J.FUEL.2005.02.028.
- [103] M. Ozturk and I. Dincer, "A comprehensive review on power-to-gas with hydrogen options for cleaner applications," *Int J Hydrogen Energy*, vol. 46, no. 62, pp. 31511–31522, Sep. 2021, doi: 10.1016/J.IJHYDENE.2021.07.066.
- [104] M. F. Orhan, I. Dincer, M. A. Rosen, and M. Kanoglu, "Integrated hydrogen production options based on renewable and nuclear energy sources," *Renewable and Sustainable Energy Reviews*, vol. 16, no. 8, pp. 6059–6082, Oct. 2012, doi: 10.1016/J.RSER.2012.06.008.
- [105] "[https://www.iberdrola.com/sustainability/green-hydrogen.](https://www.iberdrola.com/sustainability/green-hydrogen)"

- [106] Dr. Thomas Vahlenkamp and Dr. Peter Feldhaus, *Transformation of Europe's power system until 2050*. McKinsey & Company, Inc, 2010.
- [107] M. C. Romano *et al.*, "Comment on 'How green is blue hydrogen?,'" *Energy Sci Eng*, vol. 10, no. 7, pp. 1944–1954, Jul. 2022, doi: 10.1002/ese3.1126.
- [108] R. Pinsky, P. Sabharwall, J. Hartvigsen, and J. O'Brien, "Comparative review of hydrogen production technologies for nuclear hybrid energy systems," *Progress in Nuclear Energy*, vol. 123, p. 103317, May 2020, doi: 10.1016/J.PNUCENE.2020.103317.
- [109] C. Jørgensen and S. Ropenus, "Production price of hydrogen from grid connected electrolysis in a power market with high wind penetration.," *Int J Hydrogen Energy*, vol. 33, no. 20, pp. 5335–5344, Oct. 2008, doi: 10.1016/J.IJHYDENE.2008.06.037.
- [110] H. Barthelemy, M. Weber, and F. Barbier, "Hydrogen storage: Recent improvements and industrial perspectives," *Int J Hydrogen Energy*, vol. 42, no. 11, pp. 7254–7262, Mar. 2017, doi: 10.1016/J.IJHYDENE.2016.03.178.
- [111] R. Moradi and K. M. Groth, "Hydrogen storage and delivery: Review of the state of the art technologies and risk and reliability analysis," *Int J Hydrogen Energy*, vol. 44, no. 23, pp. 12254–12269, May 2019, doi: 10.1016/J.IJHYDENE.2019.03.041.
- [112] A. M. Abdalla, S. Hossain, O. B. Nisfindy, A. T. Azad, M. Dawood, and A. K. Azad, "Hydrogen production, storage, transportation and key challenges with applications: A review," *Energy Convers Manag*, vol. 165, pp. 602–627, Jun. 2018, doi: 10.1016/J.ENCONMAN.2018.03.088.
- [113] O. Faye, J. Szpunar, and U. Eduok, "A critical review on the current technologies for the generation, storage, and transportation of hydrogen," *Int J Hydrogen Energy*, vol. 47, no. 29, pp. 13771–13802, Apr. 2022, doi: 10.1016/J.IJHYDENE.2022.02.112.
- [114] Y. Ma, X. R. Wang, T. Li, J. Zhang, J. Gao, and Z. Y. Sun, "Hydrogen and ethanol: Production, storage, and transportation," *Int J Hydrogen Energy*, vol. 46, no. 54, pp. 27330–27348, Aug. 2021, doi: 10.1016/J.IJHYDENE.2021.06.027.
- [115] G. Giacomazzi, "Prospects for intercontinental seaborne transportation of hydrogen," *Int J Hydrogen Energy*, vol. 14, no. 8, pp. 603–616, Jan. 1989, doi: 10.1016/0360-3199(89)90120-1.
- [116] N. Ali, M. Bilal, M. S. Nazir, A. Khan, F. Ali, and H. M. N. Iqbal, "Thermochemical and electrochemical aspects of carbon dioxide methanation: A sustainable approach to generate fuel via waste to energy theme," *Science of The Total Environment*, vol. 712, p. 136482, Apr. 2020, doi: 10.1016/J.SCITOTENV.2019.136482.
- [117] A. Galadima and O. Muraza, "Catalytic thermal conversion of CO₂ into fuels: Perspective and challenges," *Renewable and Sustainable Energy Reviews*, vol. 115, p. 109333, Nov. 2019, doi: 10.1016/J.RSER.2019.109333.

- [118] S. S. Tan, L. Zou, and E. Hu, "Photosynthesis of hydrogen and methane as key components for clean energy system," *Sci Technol Adv Mater*, vol. 8, no. 1–2, pp. 89–92, Jan. 2007, doi: 10.1016/j.stam.2006.11.004.
- [119] M. Watanabe, "Photosynthesis of methanol and methane from CO₂ and H₂O molecules on a ZnO surface," *Surface Science Letters*, vol. 279, no. 3, pp. L236–L242, Dec. 1992, doi: 10.1016/0167-2584(92)90227-V.
- [120] W. K. Fan and M. Tahir, "Recent trends in developments of active metals and heterogenous materials for catalytic CO₂ hydrogenation to renewable methane: A review," *J Environ Chem Eng*, vol. 9, no. 4, p. 105460, Aug. 2021, doi: 10.1016/J.JECE.2021.105460.
- [121] B. Zhang, Y. Jiang, M. Gao, T. Ma, W. Sun, and H. Pan, "Recent progress on hybrid electrocatalysts for efficient electrochemical CO₂ reduction," *Nano Energy*, vol. 80, p. 105504, Feb. 2021, doi: 10.1016/J.NANOEN.2020.105504.
- [122] A. Alitalo, M. Niskanen, and E. Aura, "Biocatalytic methanation of hydrogen and carbon dioxide in a fixed bed bioreactor," *Bioresour Technol*, vol. 196, pp. 600–605, Nov. 2015, doi: 10.1016/J.BIORTECH.2015.08.021.
- [123] I. Kuznecova and J. Gusca, "Property based ranking of CO and CO₂ methanation catalysts," *Energy Procedia*, vol. 128, pp. 255–260, Sep. 2017, doi: 10.1016/J.EGYPRO.2017.09.068.
- [124] J. Ashok, S. Pati, P. Hongmanorom, Z. Tianxi, C. Junmei, and S. Kawi, "A review of recent catalyst advances in CO₂ methanation processes," *Catal Today*, vol. 356, pp. 471–489, Oct. 2020, doi: 10.1016/J.CATTOD.2020.07.023.
- [125] L. Falbo, M. Martinelli, C. G. Visconti, L. Lietti, C. Bassano, and P. Deiana, "Kinetics of CO₂ methanation on a Ru-based catalyst at process conditions relevant for Power-to-Gas applications," *Appl Catal B*, vol. 225, pp. 354–363, Jun. 2018, doi: 10.1016/J.APCATB.2017.11.066.
- [126] S. Sharifian and N. Asasian-Kolur, "Studies on CO_x hydrogenation to methane over Rh-based catalysts," *Inorg Chem Commun*, vol. 118, p. 108021, Aug. 2020, doi: 10.1016/J.INOCHE.2020.108021.
- [127] Z. Wang, L. Wang, Y. Cui, Y. Xing, and W. Su, "Research on nickel-based catalysts for carbon dioxide methanation combined with literature measurement," *Journal of CO₂ Utilization*, vol. 63, p. 102117, Sep. 2022, doi: 10.1016/J.JCOU.2022.102117.
- [128] M. Saito and R. B. Anderson, "The activity of several molybdenum compounds for the methanation of CO₂," *J Catal*, vol. 67, no. 2, pp. 296–302, Feb. 1981, doi: 10.1016/0021-9517(81)90289-X.
- [129] S. Li, S. Guo, D. Gong, N. Kang, K. G. Fang, and Y. Liu, "Nano composite composed of MoO_x-La₂O₃Ni on SiO₂ for storing hydrogen into CH₄ via CO₂ methanation," *Int J*

- Hydrogen Energy*, vol. 44, no. 3, pp. 1597–1609, Jan. 2019, doi: 10.1016/J.IJHYDENE.2018.11.130.
- [130] Z. Bian, X. Meng, M. Tao, Y. H. Lv, and Z. Xin, “Effect of MoO₃ on catalytic performance and stability of the SBA-16 supported Ni-catalyst for CO methanation,” *Fuel*, vol. 179, pp. 193–201, Sep. 2016, doi: 10.1016/J.FUEL.2016.03.091.
- [131] J. Kirchner, Z. Baysal, and S. Kureti, “Activity and Structural Changes of Fe-based Catalysts during CO₂ Hydrogenation towards CH₄ – A Mini Review,” *ChemCatChem*, vol. 12, no. 4, pp. 981–988, Feb. 2020, doi: 10.1002/cctc.201901956.
- [132] J. Kirchner, C. Zambrzycki, S. Kureti, and R. Güttel, “CO₂ Methanation on Fe Catalysts Using Different Structural Concepts,” *Chemie Ingenieur Technik*, vol. 92, no. 5, pp. 603–607, May 2020, doi: 10.1002/cite.201900157.
- [133] J. Kirchner, J. K. Anolleck, H. Lösch, and S. Kureti, “Methanation of CO₂ on iron based catalysts,” *Appl Catal B*, vol. 223, pp. 47–59, Apr. 2018, doi: 10.1016/J.APCATB.2017.06.025.
- [134] B. Mutz *et al.*, “Potential of an Alumina-Supported Ni₃Fe Catalyst in the Methanation of CO₂: Impact of Alloy Formation on Activity and Stability,” *ACS Catal*, vol. 7, no. 10, pp. 6802–6814, Oct. 2017, doi: 10.1021/acscatal.7b01896.
- [135] L. Xu *et al.*, “CO₂ methanation over CoNi bimetal-doped ordered mesoporous Al₂O₃ catalysts with enhanced low-temperature activities,” *Int J Hydrogen Energy*, vol. 43, no. 36, pp. 17172–17184, Sep. 2018, doi: 10.1016/J.IJHYDENE.2018.07.106.
- [136] A. I. Tsiotsias, N. D. Charisiou, I. v. Yentekakis, and M. A. Goula, “Bimetallic Ni-Based Catalysts for CO₂ Methanation: A Review,” *Nanomaterials*, vol. 11, no. 1, p. 28, Dec. 2020, doi: 10.3390/nano11010028.
- [137] K. Ghaib and F. Z. Ben-Fares, “Power-to-Methane: A state-of-the-art review,” *Renewable and Sustainable Energy Reviews*, vol. 81, pp. 433–446, Jan. 2018, doi: 10.1016/J.RSER.2017.08.004.
- [138] Andreina Alexandra Alarcón Avellán, “Catalyst and reactor design for carbon dioxide methanation,” Universitat de Barcelona, Barcelona, 2021.
- [139] W. J. Lee *et al.*, “Recent trend in thermal catalytic low temperature CO₂ methanation: A critical review,” *Catal Today*, vol. 368, pp. 2–19, May 2021, doi: 10.1016/J.CATTOD.2020.02.017.
- [140] M. M. Jaffar, M. A. Nahil, and P. T. Williams, “Parametric Study of CO₂ Methanation for Synthetic Natural Gas Production,” *Energy Technology*, vol. 7, no. 11, p. 1900795, Nov. 2019, doi: 10.1002/ente.201900795.
- [141] S. Gulati *et al.*, “Recent advances in the application of metal-organic frameworks (MOFs)-based nanocatalysts for direct conversion of carbon dioxide (CO₂) to value-

- added chemicals," *Coord Chem Rev*, vol. 474, p. 214853, Jan. 2023, doi: 10.1016/J.CCR.2022.214853.
- [142] H. Jiang, Q. Gao, S. Wang, Y. Chen, and M. Zhang, "The synergistic effect of Pd NPs and UiO-66 for enhanced activity of carbon dioxide methanation," *Journal of CO2 Utilization*, vol. 31, pp. 167–172, May 2019, doi: 10.1016/J.JCOU.2019.03.011.
- [143] J. A. H. Dreyer *et al.*, "Influence of the oxide support reducibility on the CO2 methanation over Ru-based catalysts," *Appl Catal B*, vol. 219, pp. 715–726, Dec. 2017, doi: 10.1016/J.APCATB.2017.08.011.
- [144] H. Chen *et al.*, "Coupling non-thermal plasma with Ni catalysts supported on BETA zeolite for catalytic CO₂ methanation," *Catal Sci Technol*, vol. 9, no. 15, pp. 4135–4145, 2019, doi: 10.1039/C9CY00590K.
- [145] Y. Feng, W. Yang, S. Chen, and W. Chu, "Cerium Promoted Nano Nickel Catalysts Ni-Ce/CNTs and Ni-Ce/Al₂O₃ for CO₂ Methanation," *Integrated Ferroelectrics*, vol. 151, no. 1, pp. 116–125, Feb. 2014, doi: 10.1080/10584587.2014.901141.
- [146] P. Panagiotopoulou, D. I. Kondarides, and X. E. Verykios, "Selective methanation of CO over supported Ru catalysts," *Appl Catal B*, vol. 88, no. 3–4, pp. 470–478, May 2009, doi: 10.1016/J.APCATB.2008.10.012.
- [147] S. Roy *et al.*, "Selective CO₂ reduction to methane catalyzed by mesoporous Ru-Fe₃O₄/CeO_x-SiO₂ in a fixed bed flow reactor," *Molecular Catalysis*, vol. 528, p. 112486, Aug. 2022, doi: 10.1016/J.MCAT.2022.112486.
- [148] R. Daroughegi, F. Meshkani, and M. Rezaei, "Enhanced low-temperature activity of CO₂ methanation over ceria-promoted Ni-Al₂O₃ nanocatalyst," *Chem Eng Sci*, vol. 230, p. 116194, Feb. 2021, doi: 10.1016/J.CES.2020.116194.
- [149] A. Quindimil, U. De-La-Torre, B. Pereda-Ayo, J. A. González-Marcos, and J. R. González-Velasco, "Ni catalysts with La as promoter supported over Y- and BETA-zeolites for CO₂ methanation," *Appl Catal B*, vol. 238, pp. 393–403, Dec. 2018, doi: 10.1016/J.APCATB.2018.07.034.
- [150] W. Ahmad, M. N. Younis, R. Shawabkeh, and S. Ahmed, "Synthesis of lanthanide series (La, Ce, Pr, Eu & Gd) promoted Ni/ γ -Al₂O₃ catalysts for methanation of CO₂ at low temperature under atmospheric pressure," *Catal Commun*, vol. 100, pp. 121–126, Sep. 2017, doi: 10.1016/J.CATCOM.2017.06.044.
- [151] S. Chai *et al.*, "Boosting CO₂ methanation activity on Ru/TiO₂ catalysts by exposing (001) facets of anatase TiO₂," *Journal of CO2 Utilization*, vol. 33, pp. 242–252, Oct. 2019, doi: 10.1016/J.JCOU.2019.05.031.
- [152] H. Wu *et al.*, "CO₂ methanation over Ru/12CaO·7Al₂O₃ catalysts: Effect of encaged anions on catalytic mechanism," *Appl Catal A Gen*, vol. 595, p. 117474, Apr. 2020, doi: 10.1016/J.APCATA.2020.117474.

- [153] M. Jacquemin, A. Beuls, and P. Ruiz, "Catalytic production of methane from CO₂ and H₂ at low temperature: Insight on the reaction mechanism," *Catal Today*, vol. 157, no. 1–4, pp. 462–466, Nov. 2010, doi: 10.1016/J.CATTOD.2010.06.016.
- [154] P. Panagiotopoulou, "Hydrogenation of CO₂ over supported noble metal catalysts," *Appl Catal A Gen*, vol. 542, pp. 63–70, Jul. 2017, doi: 10.1016/J.APCATA.2017.05.026.
- [155] T. Kai, Y. Yamasaki, T. Takahashi, T. Masumoto, and H. Kimura, "Increase in the thermal stability during the methanation of CO₂ over a Rh catalyst prepared from an amorphous alloy," *Can J Chem Eng*, vol. 76, no. 2, pp. 331–335, Apr. 1998, doi: 10.1002/cjce.5450760223.
- [156] X. Wang, H. Shi, J. H. Kwak, and J. Szanyi, "Mechanism of CO₂ Hydrogenation on Pd/Al₂O₃ Catalysts: Kinetics and Transient DRIFTS-MS Studies," *ACS Catal*, vol. 5, no. 11, pp. 6337–6349, Nov. 2015, doi: 10.1021/acscatal.5b01464.
- [157] H. Y. Kim, H. M. Lee, and J.-N. Park, "Bifunctional Mechanism of CO₂ Methanation on Pd-MgO/SiO₂ Catalyst: Independent Roles of MgO and Pd on CO₂ Methanation," *The Journal of Physical Chemistry C*, vol. 114, no. 15, pp. 7128–7131, Apr. 2010, doi: 10.1021/jp100938v.
- [158] A. Loder, M. Siebenhofer, and S. Lux, "The reaction kinetics of CO₂ methanation on a bifunctional Ni/MgO catalyst," *Journal of Industrial and Engineering Chemistry*, vol. 85, pp. 196–207, May 2020, doi: 10.1016/J.JIEC.2020.02.001.
- [159] S. Tada, T. Shimizu, H. Kameyama, T. Haneda, and R. Kikuchi, "Ni/CeO₂ catalysts with high CO₂ methanation activity and high CH₄ selectivity at low temperatures," *Int J Hydrogen Energy*, vol. 37, no. 7, pp. 5527–5531, Apr. 2012, doi: 10.1016/J.IJHYDENE.2011.12.122.
- [160] X. Jia, X. Zhang, N. Rui, X. Hu, and C. jun Liu, "Structural effect of Ni/ZrO₂ catalyst on CO₂ methanation with enhanced activity," *Appl Catal B*, vol. 244, pp. 159–169, May 2019, doi: 10.1016/J.APCATB.2018.11.024.
- [161] J. Guilera, J. del Valle, A. Alarcón, J. A. Díaz, and T. Andreu, "Metal-oxide promoted Ni/Al₂O₃ as CO₂ methanation micro-size catalysts," *Journal of CO₂ Utilization*, vol. 30, pp. 11–17, Mar. 2019, doi: 10.1016/J.JCOU.2019.01.003.
- [162] S. Scirè, C. Crisafulli, R. Maggiore, S. Minicò, and S. Galvagno, "Influence of the support on CO₂ methanation over Ru catalysts: an FT-IR study," *Catal Letters*, vol. 51, no. 1/2, pp. 41–45, 1998, doi: 10.1023/A:1019028816154.
- [163] J. Ren *et al.*, "Enhanced CO₂ methanation activity over La_{2-x}Ce_xNiO₄ perovskite-derived catalysts: Understanding the structure-performance relationships," *Chemical Engineering Journal*, vol. 426, p. 131760, Dec. 2021, doi: 10.1016/J.CEJ.2021.131760.
- [164] J. Zhang, B. Ren, G. Fan, L. Yang, and F. Li, "Exceptional low-temperature activity of a perovskite-type AlCeO₃ solid solution-supported Ni-based nanocatalyst towards CO₂

- methanation," *Catal Sci Technol*, vol. 11, no. 11, pp. 3894–3904, 2021, doi: 10.1039/D1CY00340B.
- [165] A. Blanco *et al.*, "CO₂ methanation activity of Ni-doped perovskites," *Fuel*, vol. 320, p. 123954, Jul. 2022, doi: 10.1016/J.FUEL.2022.123954.
- [166] M. Younas, S. Sethupathi, L. L. Kong, and A. R. Mohamed, "CO₂ methanation over Ni and Rh based catalysts: Process optimization at moderate temperature," *Int J Energy Res*, vol. 42, no. 10, pp. 3289–3302, Aug. 2018, doi: 10.1002/er.4082.
- [167] G. Botzolaki *et al.*, "CO₂ Methanation on Supported Rh Nanoparticles: The combined Effect of Support Oxygen Storage Capacity and Rh Particle Size," *Catalysts*, vol. 10, no. 8, p. 944, Aug. 2020, doi: 10.3390/catal10080944.
- [168] J. Wang, Z. You, Q. Zhang, W. Deng, and Y. Wang, "Synthesis of lower olefins by hydrogenation of carbon dioxide over supported iron catalysts," *Catal Today*, vol. 215, pp. 186–193, Oct. 2013, doi: 10.1016/J.CATTOD.2013.03.031.
- [169] K. Świrk, P. Summa, D. Wierzbicki, M. Motak, and P. da Costa, "Vanadium promoted Ni(Mg,Al)O hydrotalcite-derived catalysts for CO₂ methanation," *Int J Hydrogen Energy*, vol. 46, no. 34, pp. 17776–17783, May 2021, doi: 10.1016/J.IJHYDENE.2021.02.172.
- [170] L. Karam *et al.*, "Mesoporous nickel-alumina catalysts derived from MIL-53(Al) metal-organic framework: A new promising path for synthesizing CO₂ methanation catalysts," *Journal of CO₂ Utilization*, vol. 51, p. 101651, Sep. 2021, doi: 10.1016/J.JCOU.2021.101651.
- [171] F. He *et al.*, "Ni-based catalysts derived from Ni-Zr-Al ternary hydrotalcites show outstanding catalytic properties for low-temperature CO₂ methanation," *Appl Catal B*, vol. 293, p. 120218, Sep. 2021, doi: 10.1016/J.APCATB.2021.120218.
- [172] T. Siudyga *et al.*, "Nano-Ru Supported on Ni Nanowires for Low-Temperature Carbon Dioxide Methanation," *Catalysts*, vol. 10, no. 5, p. 513, May 2020, doi: 10.3390/catal10050513.
- [173] S. N. Bukhari, C. C. Chong, H. D. Setiabudi, Y. W. Cheng, L. P. Teh, and A. A. Jalil, "Ni/Fibrous type SBA-15: Highly active and coke resistant catalyst for CO₂ methanation," *Chem Eng Sci*, vol. 229, p. 116141, Jan. 2021, doi: 10.1016/J.CES.2020.116141.
- [174] M. Nguyen-Quang, F. Azzolina-Jury, B. Samojeden, M. Motak, and P. da Costa, "On the influence of the preparation routes of NiMgAl-mixed oxides derived from hydrotalcite on their CO₂ methanation catalytic activities," *Int J Hydrogen Energy*, vol. 47, no. 89, pp. 37783–37791, Nov. 2022, doi: 10.1016/J.IJHYDENE.2022.08.278.
- [175] F. Kosaka *et al.*, "Effect of Ni content on CO₂ methanation performance with tubular-structured Ni-YSZ catalysts and optimization of catalytic activity for temperature

- management in the reactor," *Int J Hydrogen Energy*, vol. 45, no. 23, pp. 12911–12920, Apr. 2020, doi: 10.1016/J.IJHYDENE.2020.02.221.
- [176] B. Chen, J. Qiu, L. Xu, and Y. Cui, "Ni-based mesoporous Ce_{0.8}Zr_{0.2}O₂ catalyst with enhanced low-temperature performance for CO₂ methanation," *Catal Commun*, vol. 171, p. 106515, Nov. 2022, doi: 10.1016/J.CATCOM.2022.106515.
- [177] Z. Liu, X. Gao, B. Liu, Q. Ma, T. sheng Zhao, and J. Zhang, "Recent advances in thermal catalytic CO₂ methanation on hydrotalcite-derived catalysts," *Fuel*, vol. 321, p. 124115, Aug. 2022, doi: 10.1016/J.FUEL.2022.124115.
- [178] S.-Y. Lee and R. Aris, "The Distribution of Active ingredients in Supported Catalysts Prepared by Impregnation," *Catalysis Reviews*, vol. 27, no. 2, pp. 207–340, Jun. 1985, doi: 10.1080/01614948508064737.
- [179] B. A. T. Mehrabadi, S. Eskandari, U. Khan, R. D. White, and J. R. Regalbuto, "A Review of Preparation Methods for Supported Metal Catalysts," *Advances in Catalysis*, vol. 61, pp. 1–35, Jan. 2017, doi: 10.1016/BS.ACAT.2017.10.001.
- [180] P. A. K. Nair, W. L. Vasconcelos, K. Paine, and J. Calabria-Holley, "A review on applications of sol-gel science in cement," *Constr Build Mater*, vol. 291, p. 123065, Jul. 2021, doi: 10.1016/J.CONBUILDMAT.2021.123065.
- [181] S. Eriksson, U. Nylén, S. Rojas, and M. Boutonnet, "Preparation of catalysts from microemulsions and their applications in heterogeneous catalysis," *Appl Catal A Gen*, vol. 265, no. 2, pp. 207–219, Jul. 2004, doi: 10.1016/J.APCATA.2004.01.014.
- [182] C. Mebrahtu, F. Krebs, S. Abate, S. Perathoner, G. Centi, and R. Palkovits, "CO₂ Methanation: Principles and Challenges," *Stud Surf Sci Catal*, vol. 178, pp. 85–103, Jan. 2019, doi: 10.1016/B978-0-444-64127-4.00005-7.
- [183] P. Strucks, L. Failing, and S. Kaluza, "A Short Review on Ni-Catalyzed Methanation of CO₂: Reaction Mechanism, Catalyst Deactivation, Dynamic Operation," *Chemie Ingenieur Technik*, vol. 93, no. 10, pp. 1526–1536, Oct. 2021, doi: 10.1002/cite.202100049.
- [184] I. V. Muralikrishna and V. Manickam, "Life Cycle Assessment," *Environ Manage*, pp. 57–75, Jan. 2017, doi: 10.1016/B978-0-12-811989-1.00005-1.
- [185] A. Sayyah *et al.*, "Environmental assessment of carbon dioxide methanation process using mixed metal oxide and zeolite-supported catalysts by life cycle assessment methodology," *J Clean Prod*, vol. 362, p. 132529, Aug. 2022, doi: 10.1016/J.JCLEPRO.2022.132529.
- [186] F. Goffart De Roeck, A. Buchmayr, J. Gripekoven, J. Mertens, and J. Dewulf, "Comparative life cycle assessment of power-to-methane pathways: Process simulation of biological and catalytic biogas methanation," *J Clean Prod*, vol. 380, p. 135033, Dec. 2022, doi: 10.1016/J.JCLEPRO.2022.135033.

- [187] H. Blanco, V. Codina, A. Laurent, W. Nijs, F. Maréchal, and A. Faaij, "Life cycle assessment integration into energy system models: An application for Power-to-Methane in the EU," *Appl Energy*, vol. 259, p. 114160, Feb. 2020, doi: 10.1016/J.APENERGY.2019.114160.
- [188] <https://data.jrc.ec.europa.eu/collection/id-00287>, "The JRC European TIMES Energy System Model."
- [189] G. Garcia-Garcia, M. C. Fernandez, K. Armstrong, S. Woolass, and P. Styring, "Analytical Review of Life-Cycle Environmental Impacts of Carbon Capture and Utilization Technologies," *ChemSusChem*, vol. 14, no. 4, pp. 995–1015, Feb. 2021, doi: 10.1002/cssc.202002126.
- [190] J. Baier, G. Schneider, and A. Heel, "A Cost Estimation for CO₂ Reduction and Reuse by Methanation from Cement Industry Sources in Switzerland," *Front Energy Res*, vol. 6, Feb. 2018, doi: 10.3389/fenrg.2018.00005.
- [191] M. D. Obrist, R. Kannan, T. J. Schmidt, and T. Kober, "Decarbonization pathways of the Swiss cement industry towards net zero emissions," *J Clean Prod*, vol. 288, p. 125413, Mar. 2021, doi: 10.1016/J.JCLEPRO.2020.125413.
- [192] D. Ipsakis, G. Varvoutis, A. Lampropoulos, S. Papaefthimiou, G. E. Marnellos, and M. Konsolakis, "Techno-economic assessment of industrially-captured CO₂ upgrade to synthetic natural gas by means of renewable hydrogen," *Renew Energy*, vol. 179, pp. 1884–1896, Dec. 2021, doi: 10.1016/J.RENENE.2021.07.109.
- [193] S. Morimoto, N. Kitagawa, N. Thuy, A. Ozawa, R. A. Rustandi, and S. Kataoka, "Scenario assessment of implementing methanation considering economic feasibility and regional characteristics," *Journal of CO₂ Utilization*, vol. 58, p. 101935, Apr. 2022, doi: 10.1016/J.JCOU.2022.101935.
- [194] M. Thema, F. Bauer, and M. Sterner, "Power-to-Gas: Electrolysis and methanation status review," *Renewable and Sustainable Energy Reviews*, vol. 112, pp. 775–787, Sep. 2019, doi: 10.1016/J.RSER.2019.06.030.
- [195] M. Bailera, P. Lisbona, L. M. Romeo, and S. Espatolero, "Power to Gas projects review: Lab, pilot and demo plants for storing renewable energy and CO₂," *Renewable and Sustainable Energy Reviews*, vol. 69, pp. 292–312, Mar. 2017, doi: 10.1016/J.RSER.2016.11.130.
- [196] R. Chauvy and G. De Weireld, "CO₂ Utilization Technologies in Europe: A Short Review," *Energy Technology*, vol. 8, no. 12, p. 2000627, Dec. 2020, doi: 10.1002/ente.202000627.
- [197] <https://www.strategyccus.eu/news-and-events/news/experiences-surveys-social-acceptance-ccus-general-public>, "Experiences from surveys: Social acceptance of CCUS by the general public."

- [198] K. Arning, J. Offermann-van Heek, A. Sternberg, A. Bardow, and M. Ziefle, "Risk-benefit perceptions and public acceptance of Carbon Capture and Utilization," *Environ Innov Soc Transit*, vol. 35, pp. 292–308, Jun. 2020, doi: 10.1016/J.EIST.2019.05.003.
- [199] C. R. Jones, B. Olfe-Kräutlein, H. Naims, and K. Armstrong, "The Social Acceptance of Carbon Dioxide Utilisation: A Review and Research Agenda," *Front Energy Res*, vol. 5, Jun. 2017, doi: 10.3389/fenrg.2017.00011.

